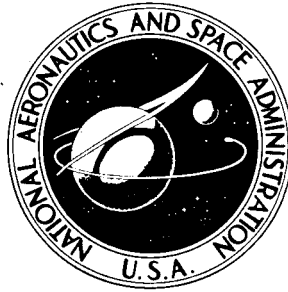


**NASA CONTRACTOR
REPORT**



NASA CR-2835

NASA CR-2835

**CASE FILE
COPY**

**ANALYSIS AND COMPILATION
OF MISSILE AERODYNAMIC DATA
Volume I - Data Presentation and Analysis**

James O. Nichols

Prepared by

AUBURN UNIVERSITY

Auburn, Ala. 36830

for Langley Research Center

NATIONAL AERONAUTICS AND SPACE ADMINISTRATION • WASHINGTON, D. C. • MAY 1977

1. Report No. NASA CR-2835	2. Government Accession No.	3. Recipient's Catalog No.	
4. Title and Subtitle ANALYSIS AND COMPILATION OF MISSILE AERODYNAMIC DATA - VOLUME I DATA PRESENTATION AND ANALYSIS		5. Report Date May 1977	6. Performing Organization Code
		8. Performing Organization Report No.	
7. Author(s) James O. Nichols		10. Work Unit No.	
9. Performing Organization Name and Address Aerospace Engineering Department Auburn University Auburn, Alabama 36830		11. Contract or Grant No. NSG 1002	
		13. Type of Report and Period Covered Contractor Report	
12. Sponsoring Agency Name and Address National Aeronautics and Space Administration Langley Research Center Hampton, VA 23365		14. Sponsoring Agency Code	
		15. Supplementary Notes Langley Technical Monitor: M. Leroy Spearman Volume I of Final Report	
16. Abstract This summary document was prepared in order to facilitate dissemination of a large amount of missile aerodynamic data which has recently been declassified. Only summary data are presented in this report, but a list of reference documents provides sources of detailed data. Most of the configurations considered are suitable for highly maneuverable air-to-air or surface-to-air missiles; however, data for a few air-to-surface, cruise missile, and one projectile configuration are also presented. The Mach number range of the data is from about 0.2 to 4.63; however, data for most configurations cover only a portion of this range. The following aerodynamic characteristics at various Mach numbers and zero angle of attack are presented: a) Base drag coefficient, $C_{D,b}$. b) Drag coefficient, $C_{D,o}$. c) Lift-curve slope, $C_{L\alpha}$. d) Aerodynamic-center location, X_{ac}/ℓ . e) Slideslip derivatives, $C_{n\beta}$, $C_{l\beta}$, and $C_{Y\beta}$. f) Control effectiveness, $C_{m\delta}$, $C_{n\delta}$, $C_{l\delta}$, and $C_{Y\delta}$. The maximum lift-drag ratio is also presented for some configurations.			
17. Key Words (Suggested by Author(s)) Missiles Missile Configurations Missile Performance		18. Distribution Statement Unclassified - Unlimited Subject Category 02	
19. Security Classif. (of this report) Unclassified	20. Security Classif. (of this page) Unclassified	21. No. of Pages 124	22. Price* \$5.50

FOREWORD

The declassification of a number of technical documents which contain missile aerodynamic data and the need to facilitate the dissemination of this data to potential users prompted the work reported herein.

It was felt that the task could have educational benefits to senior level aerospace engineering students and could be incorporated into their regular academic work. Those students who participated received academic credit for Aeronautical Problems 1 and 2; Aerospace Design 1 and 2; and Missile Aerodynamics. Participation was on a volunteer basis since the Problems and Design courses are individual effort type laboratory courses and Missile Aerodynamics is a senior level technical elective. Altogether some 15 to 20 students have been involved.

A grant from the National Aeronautics and Space Administration provided the necessary funds for class materials, field trips, and for preparation and publication of the report. Mr. Leroy Spearman of NASA's Langley Research Center has served as Technical Officer for this grant and provided the documents which were used.

This final report, Analysis and Compilation of Missile Aerodynamic Data, is presented in two volumes. Volume I contains the analysis and compilation of data and Volume II, which will be compiled by Dr. John E. Burkhalter, will contain the results of some performance analyses based on the data.

An interim report was submitted December 31, 1974, which contained a compilation of the longitudinal data. The interim report has received

some distribution, thus some errors that exist in that report and in the original technical documents will be pointed out here. These errors have been corrected in this final report.

- 1) A typographical error in the ABSTRACT of the Interim Report lists the pitch control effectiveness as C_{m_α} . It should be C_{m_δ} .
- 2) The model drawing from TM X-3070 shown in the Interim Report shows the distance from the nose to the canard hinge line to be 12.60 centimeters. It should be 15.60 centimeters.
- 3) The plot of C_{m_δ} for TM X-3070 is incorrect in both the Interim Report and TM X-3070. The data shown bases the pitching moment coefficient on body length instead of body diameter as stated in SYMBOLS. The plot of C_{m_δ} in this final report has been corrected to use body diameter as the reference length.
- 4) The aerodynamic-center locations, X_{ac}/l , were shown as percentages for the configurations in TM X-1839, TM X-2289, and TM X-2491 in the Interim Report.
- 5) The summary plot of longitudinal parameters in TM X-1332 and the Interim Report incorrectly show C_{m_δ} to be negative.
- 6) The conversion of reference area and length were inadvertently omitted for C_{m_δ} in the summary plot of data from RM L58C19 in the Interim Report.
- 7) The decimal point was omitted in the base axial-force coefficient data in TM X-2367.

The summary data have been checked a number of times in order to reduce the number of errors which will appear in this final report.

Finally, I want to express my appreciation to Mrs. Marjorie McGee, secretary in the Aerospace Engineering Department, Auburn University, for typing this report.

Auburn, Alabama

James O. Nichols

SUMMARY

This summary document was prepared in order to facilitate dissemination of a large amount of missile aerodynamic data which has recently been declassified. Only summary data are presented in this report, but a list of reference documents provides sources of detailed data.

Most of the configurations considered are suitable for highly maneuverable air-to-air or surface-to-air missiles; however, data for a few air-to-surface, cruise missile, and one projectile configuration are also presented.

The Mach number range of the data is from about 0.2 to 4.63; however, data for most configurations cover only a portion of this range. The following aerodynamic characteristics at various Mach numbers and zero angle of attack are presented:

- a) Base drag coefficient, $C_{D,b}$.
- b) Drag coefficient, $C_{D,o}$.
- c) Lift-curve slope, C_{L_α} .
- d) Aerodynamic-center location, X_{ac}/λ .
- e) Sideslip derivatives, C_{n_β} , C_{ℓ_β} , and C_{Y_β} .
- f) Control effectiveness, C_{m_δ} , C_{n_δ} , C_{ℓ_δ} , and C_{Y_δ} .

The maximum lift-drag ratio is also presented for some configurations.

TABLE OF CONTENTS

FOREWORD iii

SUMMARY vi

SYMBOLS. ix

INTRODUCTION 1

APPARATUS AND TESTS 2

METHOD OF DATA PRESENTATION 3

DATA ANALYSIS. 6

SUMMARY OF CONFIGURATIONS. 9

DATA SUMMARIES 16

LIST OF DOCUMENTS SUMMARIZED 105

SYMBOLS

A	body maximum cross-sectional area, $\pi d^2/4$
C_A	axial-force coefficient, $\frac{\text{Axial force}}{qA}$
C_D	drag coefficient, $\frac{\text{Drag}}{qA}$
$C_{D,b}$	base drag coefficient at $\alpha=0^\circ$, $\frac{\text{Base drag at } \alpha=0^\circ}{qA}$
$C_{D,o}$	drag coefficient at $\alpha=0^\circ$
C_L	lift coefficient, $\frac{\text{Lift}}{qA}$
$C_{L\alpha}$	lift-curve slope at $\alpha=0^\circ$, per deg.
C_λ	rolling-moment coefficient, $\frac{\text{Rolling moment}}{qAd}$
$C_{\lambda\beta}$	effective-dihedral parameter, per deg.
$C_{\lambda\delta}$	lateral (roll) control effectiveness, per deg.
C_m	pitching-moment coefficient, $\frac{\text{Pitching moment}}{qAd}$
$C_{m\alpha}$	slope of pitching-moment curve at $\alpha=0^\circ$, per deg.
$C_{m\delta}$	pitch control effectiveness at $\alpha=0^\circ$, per deg.
C_N	normal-force coefficient, $\frac{\text{Normal force}}{qA}$
$C_{N\alpha}$	normal-force-curve slope at $\alpha=0^\circ$, per deg.
$C_{N\delta}$	variation of normal-force coefficient with pitch control surface deflection at $\alpha=0^\circ$, per deg.
C_n	yawing-moment coefficient, $\frac{\text{Yawing moment}}{qAd}$
$C_{n\beta}$	directional stability parameter, per deg.
$C_{n\delta}$	directional control effectiveness, per deg.
C_Y	side-force coefficient, $\frac{\text{Side force}}{qA}$

$C_{Y\beta}$	side-force parameter, per deg.
$C_{Y\delta}$	variation of side-force coefficient with directional control surface deflection, per deg.
d	maximum body diameter
$(L/D)_{\max}$	maximum lift-drag ratio
l	body length
M	free-stream Mach number
m/m_{∞}	mass-flow ratio
q	free-stream dynamic pressure
x,y,z	orthogonal set of body axes
x_s, y_s, z_s	orthogonal set of stability axes
X_{ac}/l	aerodynamic-center of lift location referenced to body length, positive aft from the nose
X_{mc}/l	moment center location referenced to body length, positive aft from the nose
α	angle of attack, deg.
β	sideslip angle, deg.
δ	angle of control surface deflection, positive trailing edge down or to left looking upstream, deg.
ϕ	angle of roll, deg.

Subscripts:

a	aileron
c	canard
F	flap
roll	indicates deflection of lateral control surfaces
w	wing
yaw	indicates deflection of directional control surfaces

Subscripts are used when there may be some confusion about which control surface is being deflected.

INTRODUCTION

Recently a number of technical documents containing missile aerodynamic data published by the Langley Research Center of the National Aeronautics and Space Administration have been declassified. In order to facilitate dissemination of the data contained in these documents, this summary report was prepared. It was not intended that all of the original data be included, only summary plots of curve slopes and data suitable for comparison of the relative merits of the various configurations considered. A list of the reference documents is included to provide a source of more detailed data for configurations of interest.

Some of the documents summarized were not previously classified but were included to give a more complete coverage of the configurations that have been tested at Langley. In all, thirty documents have been summarized. Some of these were themselves compilations of data that had been reported previously. Data from one of the documents, TM X-348, has not been included herein because of its limited scope, and because of the difficulty in presenting summary data for the numerous configurations tested. It is primarily a report of a parametric study of the static stability characteristics of a series of cone-cylinder bodies with various afterbody configurations-flares, fins, and boattails.

Most of the configurations reported herein are suitable for highly maneuverable air-to-air or surface-to-air missiles; however, data for a few air-to-surface, cruise missile, and one projectile configuration are

also presented. The Mach number range of the data is generally from about 1.5 to 4.63; however, data for some configurations extend to subsonic Mach numbers.

APPARATUS AND TESTS

The data summarized in this report were obtained originally in the Langley 8-foot transonic pressure tunnel and the Langley Unitary Plan wind tunnel. These tunnels are variable-pressure, continuous flow facilities. The 8-foot tunnel has a slotted test section which is about 2.44 meters square and has a Mach number range from about 0.20 to 1.30.

The Unitary Plan wind tunnel has two test sections, each about 1.22 meters square and about 2.13 meters long. The nozzle leading to each test section is of the asymmetric sliding block type which permits a continuous variation in Mach number from about 1.47 to 2.86 in the low Mach number test section and from 2.3 to 4.7 in the high Mach number test section.

The Reynolds number at which the tests were conducted varied from about 6.56×10^6 per meter to 9.84×10^6 per meter. Boundary-layer transition strips were used on the models.

Aerodynamic forces and moments were measured by means of a six-component electrical strain-gage balance located within the model and, in turn, rigidly fastened to a sting-support system. Angles of attack were corrected for sting and balance deflection due to aerodynamic loads and for tunnel airflow misalignment. The results have been adjusted to correspond to free-stream static pressure acting over the model base.

Since cruciform configurations may fly with wings in the vertical and horizontal planes or with wings in 45° planes, data at both $\phi = 0^\circ$ and $\phi = 45^\circ$ are presented for many of these configurations. The longitudinal aerodynamic characteristics were similar in both attitudes except for increased pitch control effectiveness at $\phi = 45^\circ$ due to deflection of four surfaces instead of two.

METHOD OF DATA PRESENTATION

The following aerodynamic characteristics at various Mach numbers and zero angle of attack are presented in this report:

- a) Base drag coefficient, $C_{D,b}$.
- b) Drag coefficient, $C_{D,o}$.
- c) Lift-curve slope, C_{L_α} .
- d) Aerodynamic-center location, X_{ac}/ℓ .
- e) Sideslip derivatives, C_{n_β} , C_{l_β} , and C_{Y_β} .
- f) Control effectiveness, C_{m_δ} , C_{n_δ} , C_{l_δ} , and C_{Y_δ} .

Cross coupling effects at zero angle of attack are presented for a few cases where they were not negligible. Maximum lift-drag ratios are also shown for some configurations.

Maximum body cross-sectional area and maximum body diameter are used as reference area and length, respectively, for the aerodynamic coefficients in this report. In one case (TM X-1538) where the body was not a body of revolution, the maximum frontal area and an equivalent maximum body diameter are used. Care should be exercised when comparing the data in this report with that in the original documents since conversion of some data was necessary because different reference areas and lengths were used.

The longitudinal aerodynamic characteristics are presented relative to a stability-axis system while directional and lateral characteristics are relative to a body-axis system. Figure 1 shows the axes systems. In one case (TM X-846) there was insufficient data to convert to the stability-axis system. In that one case, the longitudinal data are also presented relative to the body-axis system. The moment reference center is shown on each model drawing included in the Data Summary. Drawings of model configurations were generally duplicated directly from the original reports; thus, not all model dimensions are given in the International System of Units (SI). In some cases where new drawings were necessary, model dimensions were converted to the SI system.

The aerodynamic-center location, X_{ac}/ℓ , is referenced to body length and measured positive aft from the nose. It was calculated with the following equation when it was not included in the original reports

$$X_{ac}/\ell = - (C_{m_{\alpha}}/C_{L_{\alpha}})(d/\ell) + (X_{mc}/\ell)$$

where X_{mc} is the distance from the nose to the moment center, d is maximum body diameter, and ℓ is body length.

The data are shown in the Data Summary plotted against Mach number except in cases where data for only one or two Mach numbers were available. In those cases the data are presented in tabular form. Each data summary contains a reference to the original report from which the data were taken. A complete list of the reports summarized is given in the last section of this report.

The order in which the data are presented for each configuration is as follows. A model drawing is followed by the longitudinal characteristics, C_{m_δ} , $C_{D,o}$, $C_{D,b}$, C_{L_α} , $(L/D)_{\max}$, and X_{ac}/ℓ . All of these characteristics are evaluated at zero angle of attack except $(L/D)_{\max}$. Variation of sideslip derivatives C_{n_β} , C_{ℓ_β} , and C_{Y_β} are shown next for those configurations for which these data are available. Table 1 is a listing of the original reports which contain directional and lateral data. Finally, directional and lateral control effectiveness parameters are presented. Cross coupling is generally negligible at zero angle of attack but is shown for those cases where it is not negligible.

The method of calculating C_{ℓ_δ} varies widely among the original reports and care must be exercised when comparing various configurations. In some cases the roll control deflection is the algebraic difference (absolute sum) of the surface deflections, while others use the average of the deflections. In this report all the control data have been presented in terms of the average of the surface deflections. Since, for roll, the control surfaces are deflected differentially but equally in magnitude, the average deflection is equal to the magnitude of deflection of the individual control surface. The sign convention also varies but in this report positive deflection gives positive rolling moment.

Unless indicated otherwise, C_{n_δ} means the change in yawing moment coefficient per degree of deflection of the directional (yaw) control surfaces. C_{ℓ_δ} is the change in rolling moment coefficient per degree of deflection of the lateral (roll) control surfaces, and C_{Y_δ} indicates the change in side force coefficient per degree deflection of the

directional control surfaces. Cross coupling is usually indicated by a subscript; e.g., $C_{l\delta_{yaw}}$, which means the change in rolling moment coefficient per degree of deflection of the directional (yaw) control surfaces. In some of the data tables the subscripts are omitted and the column headings indicate the appropriate control surface. Subscripts are used also to indicate the control surface used to produce a control moment when there may be more than one set of control surfaces which could be used for pitch and roll. A pitching control effectiveness $C_{m\delta_c}$ or $C_{m\delta_f}$ would indicate the change in pitching moment coefficient per degree deflection of the canards or wing flap, respectively. Rolling moment effectiveness $C_{l\delta_c}$ or $C_{l\delta_a}$ would indicate the change in rolling moment coefficients per degree deflection of the canards or ailerons, respectively.

DATA ANALYSIS

Linearity of data - The range at angle of attack for which the data can be assumed to be linear varies from $\pm 2^\circ$ for some configurations to $\pm 12^\circ$ for others. The lift-curve slopes tend to increase with angle of attack while they decrease with increasing Mach number at supersonic speeds. The slope of the pitching-moment curve in some cases increases with angle of attack, while in others it decreases. In all cases $C_{m\alpha}$ decreases with increasing Mach number.

The nonlinearity of the data makes the use of curve slopes to calculate missile performance questionable when used over a complete trajectory. Missile performance calculations would be more accurate if equations representing the aerodynamic characteristics as functions of Mach number and angle of attack were used. The nonlinearity of the data

contained in the original reports is such that it should not be difficult to formulate equations to fit the data.

Effects of wing planform shape, size, and location - Some of the original documents were reports of design studies in which various configuration parameters were investigated. For example, TM X-1839 reports the results of an investigation of the effects of wing planform shape, size, and location. The planform shapes tested were delta, rectangular, and cranked. The sizes were classified as small, mid, and large; however, only the midsized cranked wing was tested. The location of the rectangular wing was also varied. The summary included in this report contains only the data for the three mid-sized wings.

Canards and tail control surfaces - Two of the original documents compared canard and tail control surfaces. TM X-1834 reports the results of an investigation of the effects of various longitudinal positions of canard control surfaces and tail control surfaces on the same wing-body combination. Also included in the report are the effects of the various components on the aerodynamic characteristics. In this summary report only the data for one canard configuration and one tail configuration from TM X-1834 are included. In TM X-2780, the body is the same for the canard configuration and the tail configuration but the wings are different. The effect of a blunt or conical forebody is also reported. It was found that differentially deflected canard controls were not effective as roll control devices because a control reversal resulted at low angles of attack. The tail control surfaces were effective as roll control devices; however, some adverse yawing moments did result.

Various tail control configurations - An investigation of various tail-control surface configurations was reported in TM X-71984. The tail-control configurations investigated were the cruciform inclined 45° to the horizontal and vertical planes, the conventional airplane type with an upper vertical fin and the inverted type with lower vertical fin. The cruciform tail configuration exhibits the greatest pitch-control effectiveness; however, relatively large nonlinear pitching moment characteristics are experienced due to the effects of the wing wake. The lower vertical fin shows a substantial increase in control effectiveness as angle of attack is increased, whereas the configuration with the upper vertical fin exhibits a small decrease.

A summary of the configurations considered in the original documents is given in the next section. Not all the configurations are shown, only typical examples. These examples were chosen on the basis of various configuration classification such as:

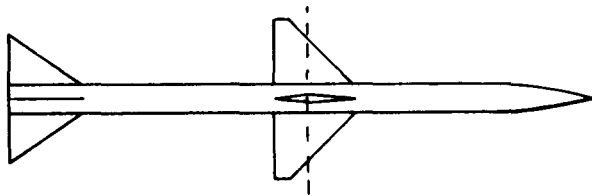
- a) Wing planform shape.
- b) Wing arrangement - cruciform or monoplane.
- c) Control surfaces - wing, tail, or canard. Hinge lines are shown as dashed lines.
- d) Surface arrangement - in-line or interdigitated.

With each configuration the reference documents which contain data for that configuration and the page numbers of this report where the summary data is presented are listed.

These configurations are grouped according to the missions for which they were originally designed. Arrangement of Data Summary follows the same plan as the Summary of Configurations.

SUMMARY OF CONFIGURATIONS

AIR-TO-AIR



REFERENCE
DOCUMENT

SUMMARY IN THIS
REPORT ON PAGES

TM X-846

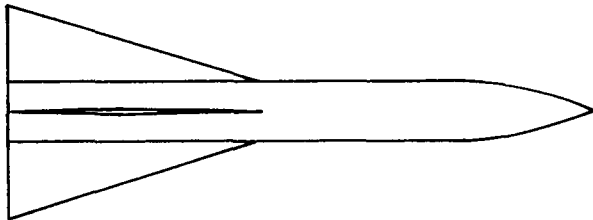
16-17



TM X-3070

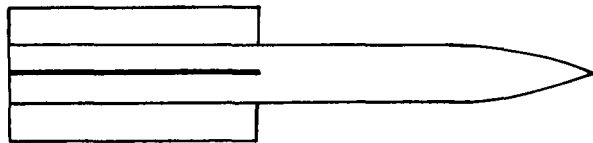
18-20

SURFACE-TO-AIR OR AIR-TO-AIR



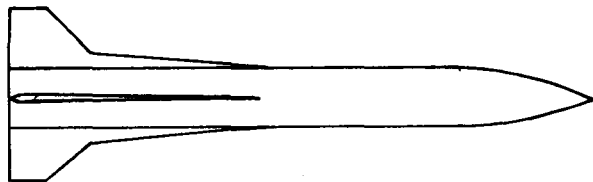
TM X-1839, TM X-2289

21-28



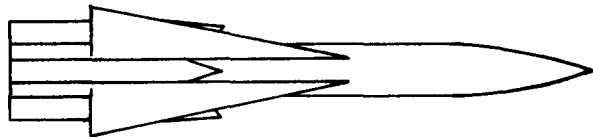
TM X-1839

21-23



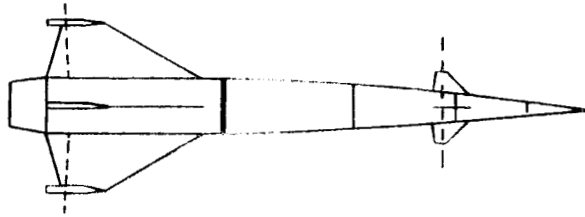
TM X-1839

21-23



TM X-2491

29-31

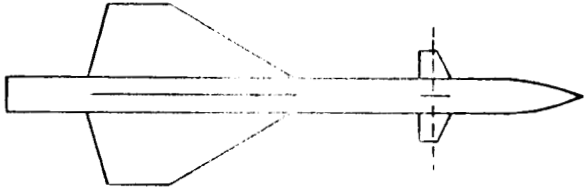


REFERENCE

PAGES

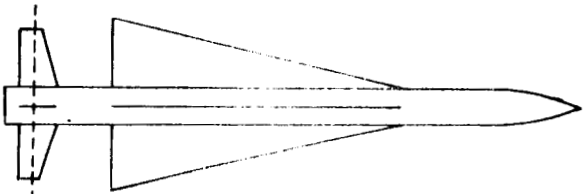
TM X-1309, TM X-1352,
TM X-2367

32-37



TM X-2780, TM X-1834

38-45



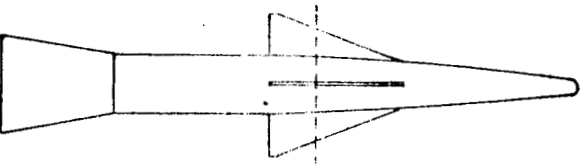
TM X-1834, TM X-2780

38-45



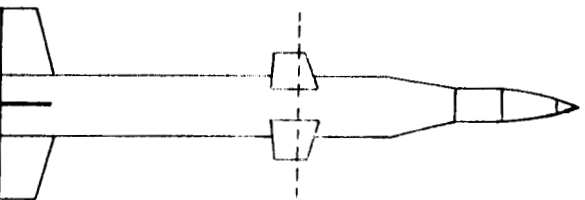
TM X-187

46-47



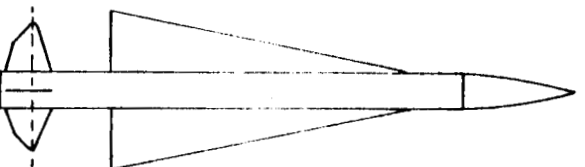
TM X-187

46-47



TM X-1184, TM X-1332

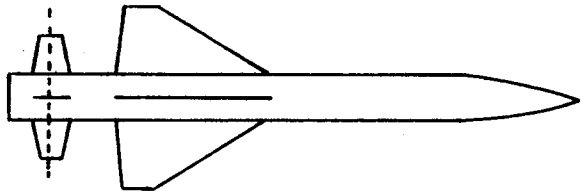
48-51



TM X-71984

52-55

SURFACE-TO-AIR

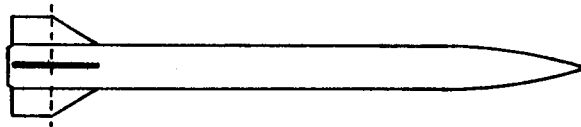


REFERENCE

TM X-1025, TM X-1416,
TM X-1751

PAGES

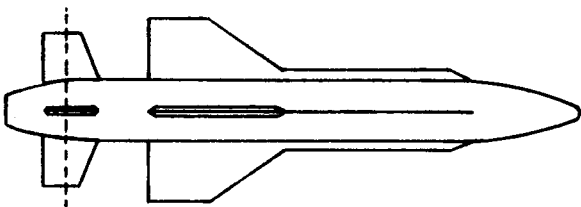
56-64



TM X-2774

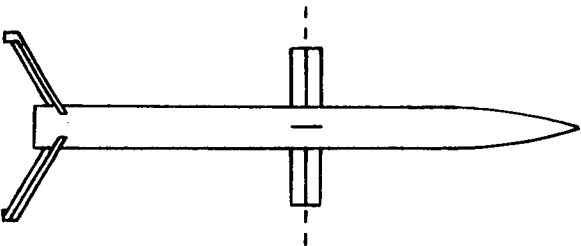
65-67

AIR-TO-SURFACE



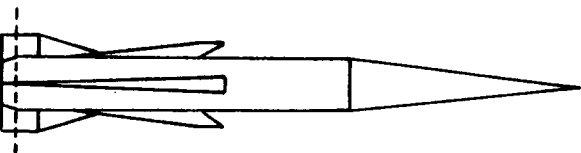
TM X-1112

68-71



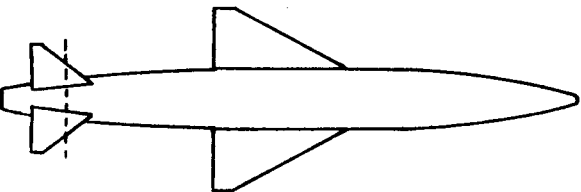
TM X-1491

72-73



TM X-1492

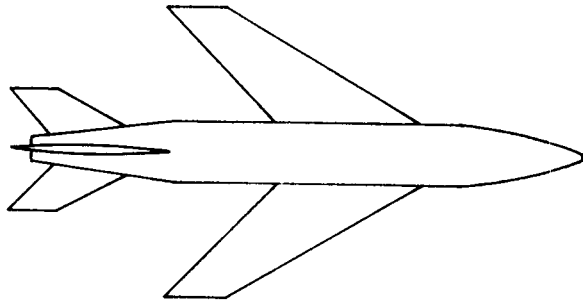
74-77



RM L58C19

78-79

CRUISE, TARGET DRONE

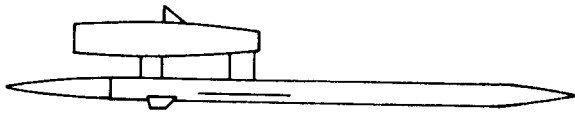


REFERENCE

PAGES

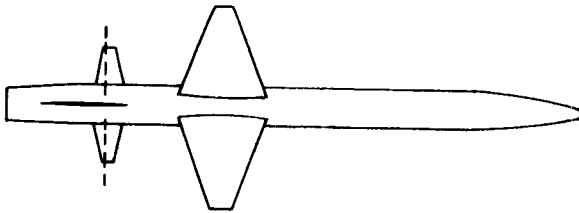
TN D-7069

80-82



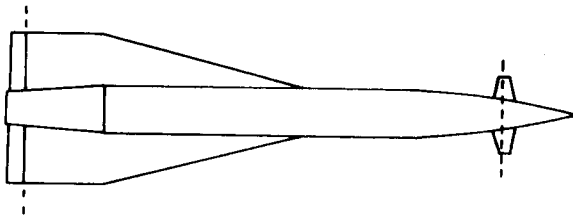
TM X-1304

83-87



TM X-1538

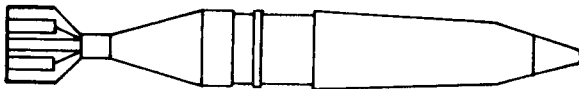
88-91



TM SX-1531, TM SX-1961,
TM SX-2299

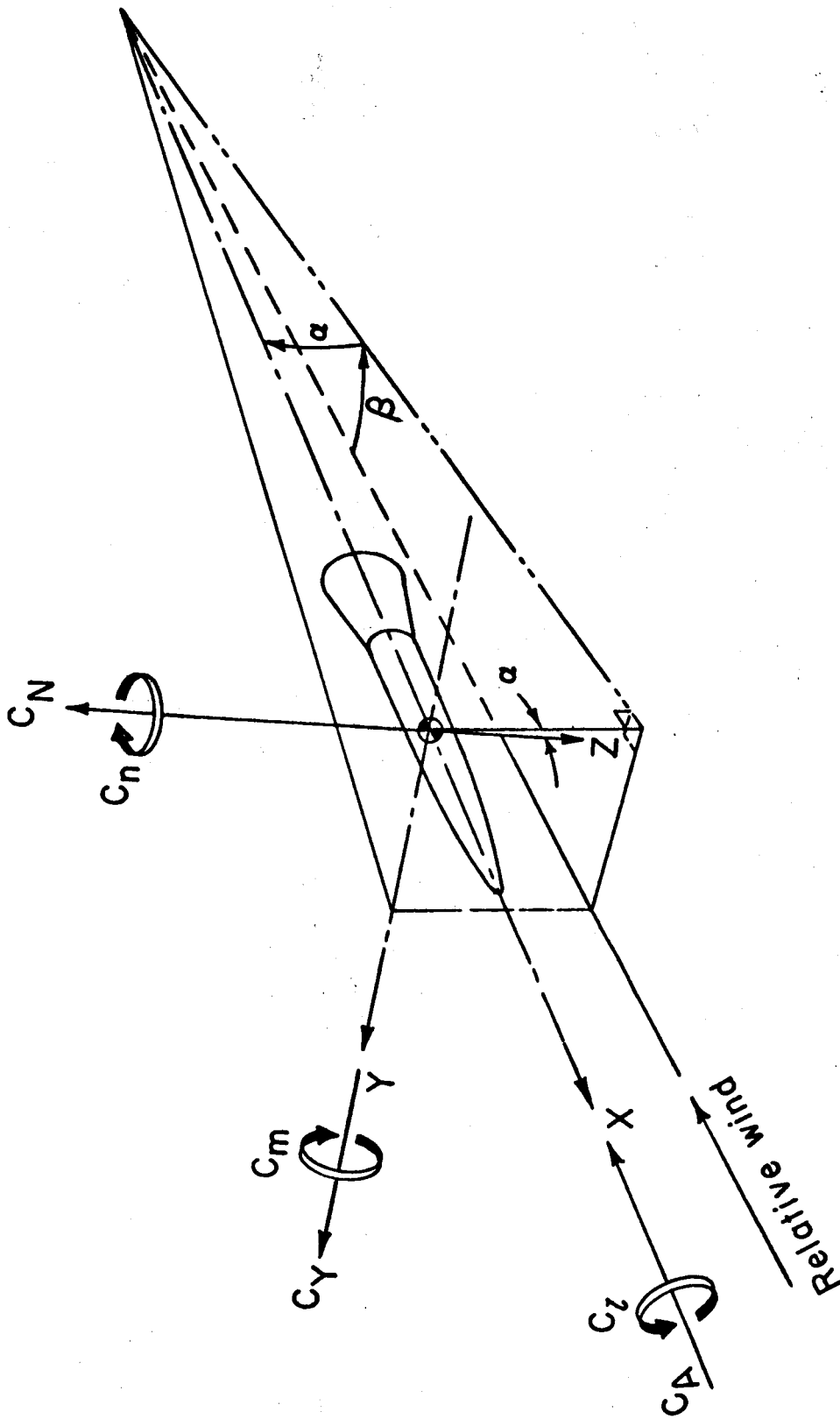
92-102

PROJECTILE



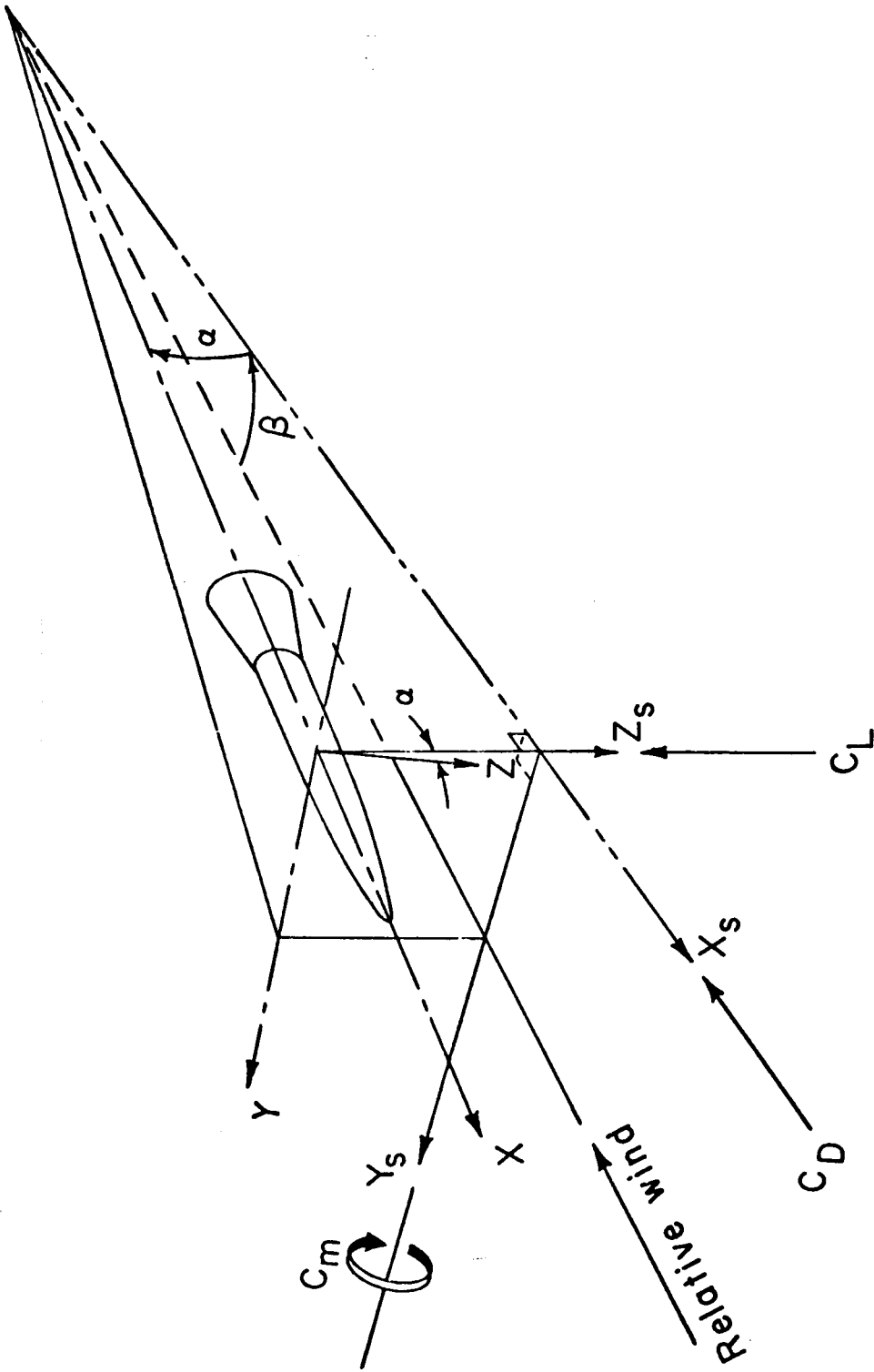
TM X-2831

103-104



(a) Body axes.

Figure 1. - Systems of axes. Arrows indicate directions of positive forces, moments, and angles.



(b) Stability axes.

Figure 1. - Concluded.

TABLE 1. DIRECTIONAL AND LATERAL STABILITY AND CONTROL DATA
CONTAINED IN REFERENCE REPORTS

REPORT NO.	SIDESLIP			YAW CONTROL			ROLL CONTROL			REMARKS
	C_{n_β}	C_{l_β}	C_{Y_β}	C_{n_δ}	C_{l_δ}	C_{Y_δ}	C_{n_δ}	C_{l_δ}	C_{Y_δ}	
RM L58C19	✓		✓							1
TM X-187	✓	✓	✓	✓	✓	✓	✓	✓	✓	2,3
TM X-1025	✓	✓	✓	✓	✓	✓				4
TM X-1112	✓	✓	✓	✓	✓	✓	✓	✓	✓	3,5,6
TM X-1184	✓	✓	✓	✓	✓	✓	✓	✓	✓	3,7,8
TM X-1304	✓	✓	✓	✓	✓	✓	✓	✓	✓	5,9
TM X-1309	✓	✓	✓	✓	✓	✓	✓	✓	✓	3,10
TM X-1332	✓	✓	✓	✓	✓	✓	✓	✓	✓	3,7,8
TM X-1352	✓	✓	✓	✓	✓	✓	✓	✓	✓	3,10
TM X-1416	✓	✓	✓				✓	✓	✓	3,11
TM X-1491				✓	✓	✓				12
TM X-1492	✓	✓	✓				✓	✓	✓	2,3
TM SX-1531	✓	✓	✓				✓	✓	✓	10
TM X-1538	✓	✓	✓	✓	✓	✓	✓	✓	✓	3
TM X-1834	✓	✓	✓							
TM X-1839	✓	✓	✓							
TM SX-1961	✓	✓	✓				✓	✓	✓	3,5,10
TM X-2289	✓	✓	✓							
TM SX-2299	✓	✓	✓				✓	✓	✓	3,5,10
TM X-2780				✓	✓	✓	✓	✓	✓	3,5
TM X-3070				✓	✓	✓	✓	✓	✓	3
TM X-71984	✓	✓	✓	✓	✓	✓	✓	✓	✓	13
TN D-7069	✓	✓	✓							

1. Data for one Mach number only, not included in this report.
2. Data for one Mach number only, table included in this report.
3. Cross coupling negligible at $\alpha=0^\circ$.
4. Vertical-tail surfaces were deflected in combination with horizontal-tail deflection.
5. Measurements of control surface hinge moments included in Reference.
6. Lateral and directional control provided by movement of the two vertical tail surfaces.
7. Lateral control provided by deflection of all four wings.
8. Cross coupling adverse at angle of attack.
9. Reference report also shows effect of mass flow rate through nacelle.
10. Lateral control provided by differential deflection of wing flaps.
11. Differential deflection of all four tails used to produce roll.
12. Control wings effective in providing increments in normal force and side force with essentially no effect on yawing or pitching moments.
13. Cross coupling in roll negligible.

DATA SUMMARIES

AIR-TO-AIR MISSILES (AAM)

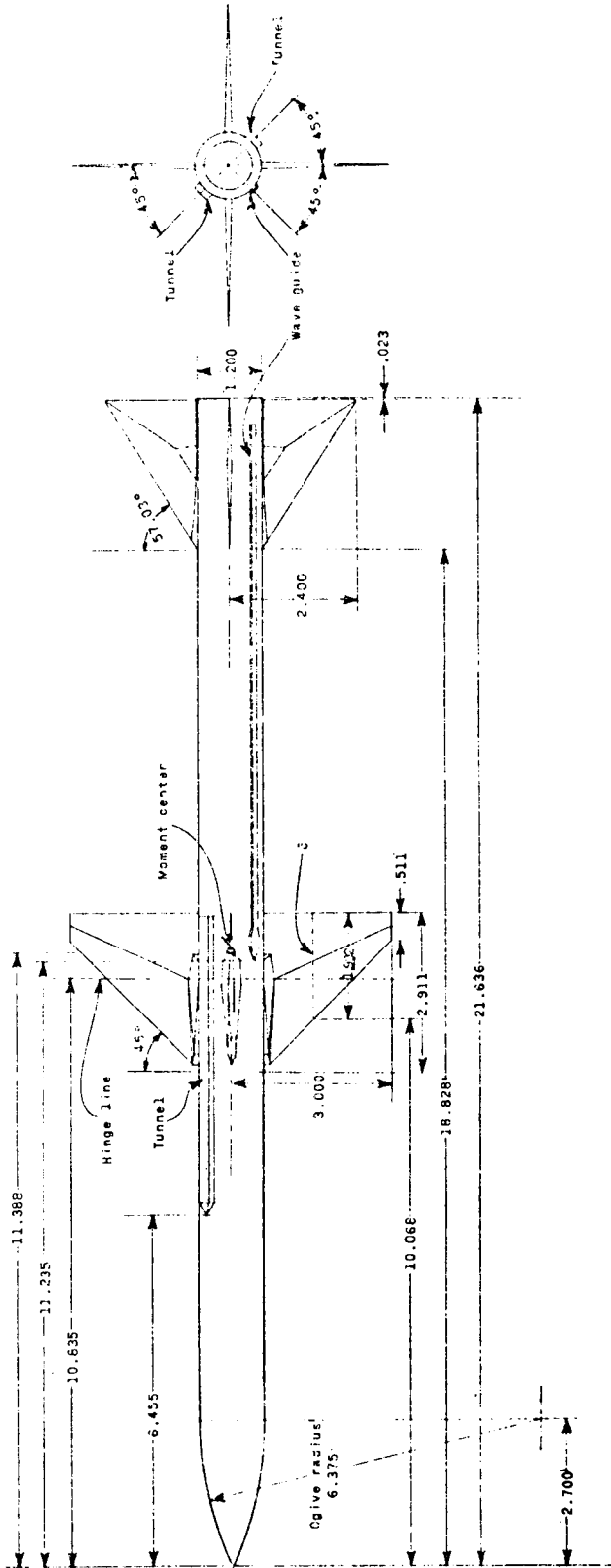


Figure 2. - Configuration with diamond airfoil sections.

Model details. Dimensions are in inches unless otherwise noted.

TABLE 2. - LONGITUDINAL PARAMETERS; $\alpha=0^\circ$.

DIAMOND AIRFOIL				
	M = 2.30		M = 4.60	
	$\phi=0^\circ$	$\phi=45^\circ$	$\phi=0^\circ$	$\phi=45^\circ$
$C_{N\alpha}$	0.592	0.568	0.454	0.373
$C_{m\alpha}$	-0.643	-0.440	-0.421	-0.146
$\frac{X_{ac}}{l}$	0.586	0.569	0.577	0.547
$C_{m\delta}$	0.267	0.427	0.026	0.090
$C_{N\delta}$	0.208	0.294	0.117	0.166

WEDGE AIRFOIL				
	M = 2.30		M = 4.60	
	$\phi=0^\circ$	$\phi=45^\circ$	$\phi=0^\circ$	$\phi=45^\circ$
$C_{N\alpha}$	0.568	0.547	0.424	0.374
$C_{m\alpha}$	-0.589	-0.507	-0.626	-0.345
$\frac{X_{ac}}{l}$	0.584	0.577	0.608	0.577
$C_{m\delta}$	0.361	0.463	0.030	0.066
$C_{N\delta}$	0.199	0.304	0.145	0.210

Ref. TM X-846

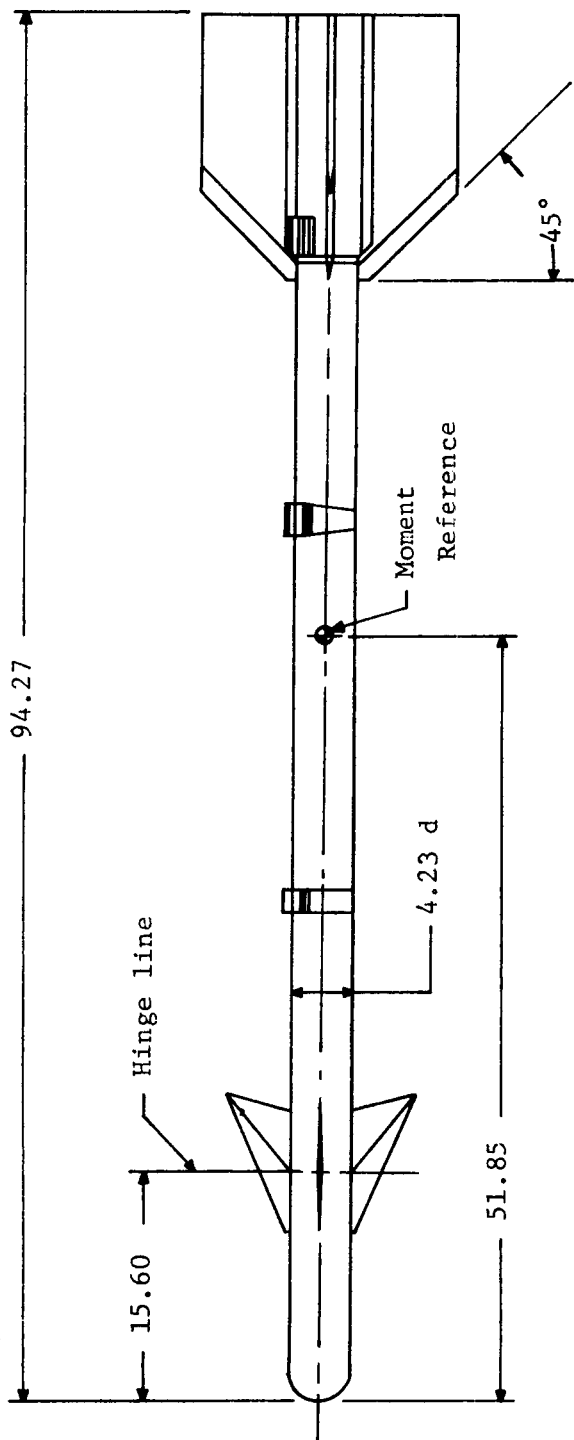


Figure 3. - Model drawing. $\phi = -90^\circ$. (All dimensions are in centimeters.)

Ref. TM X-3070

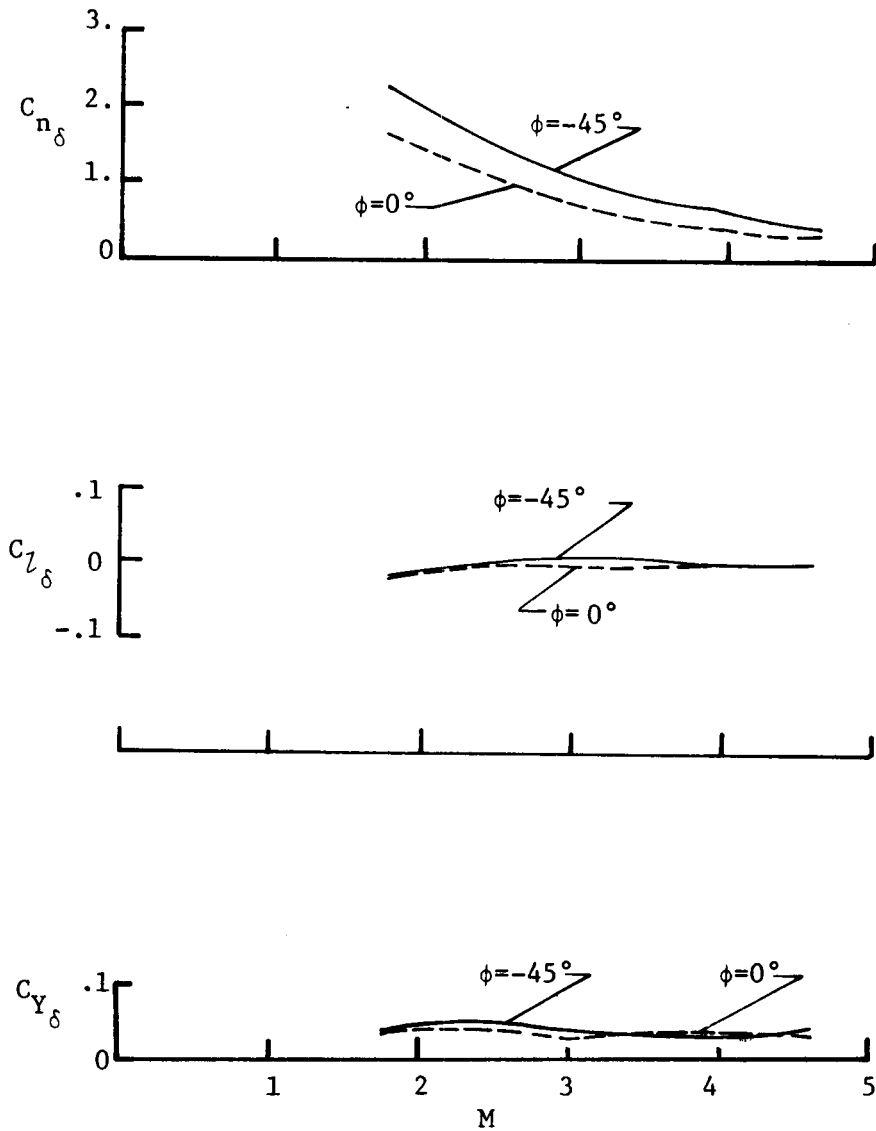
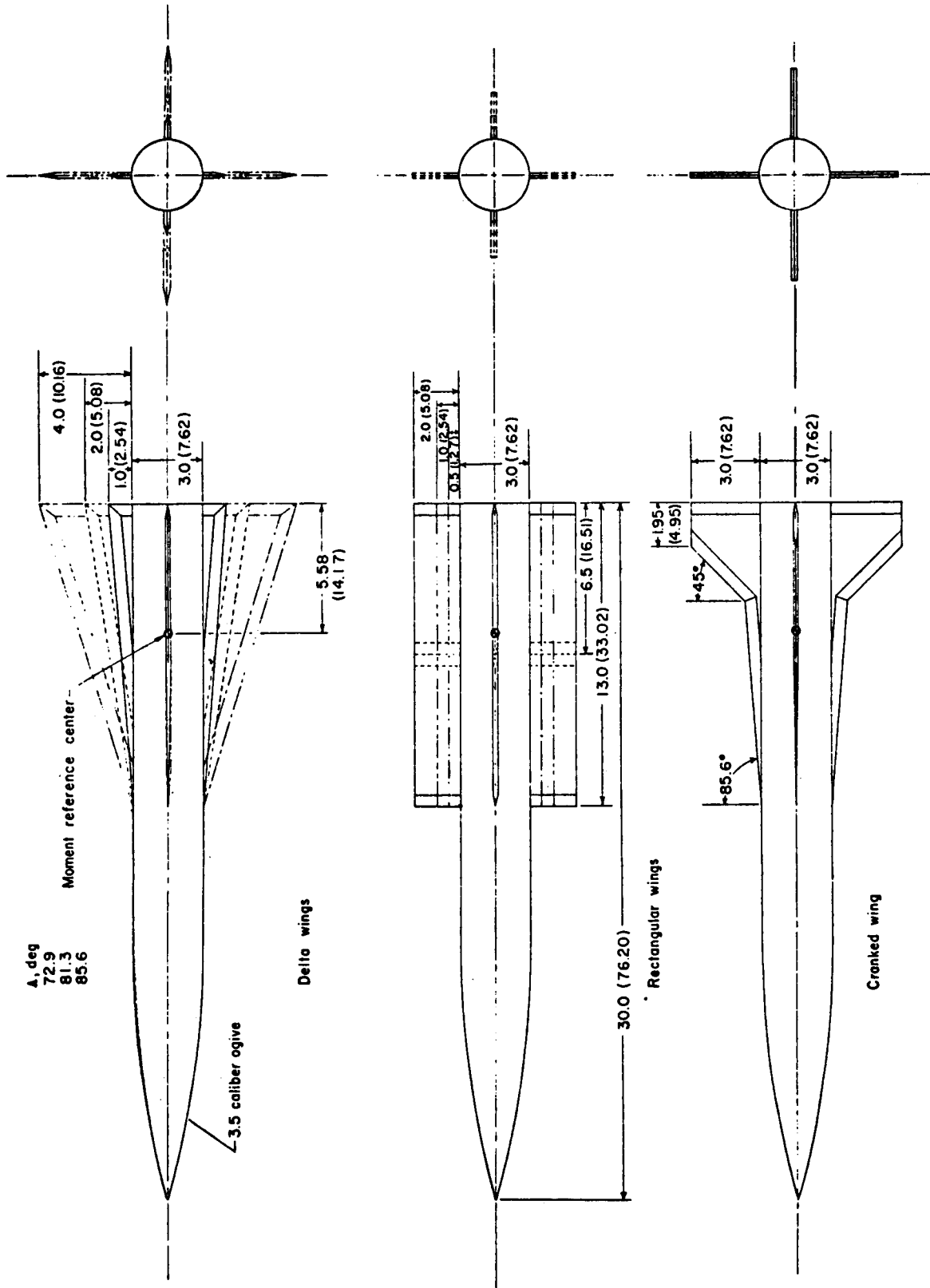


Figure 5. - Directional and lateral control effectiveness; $\alpha=0^\circ$.

SURFACE-TO-AIR MISSILES (SAM)

OR

AIR-TO-AIR MISSILES (AAM)



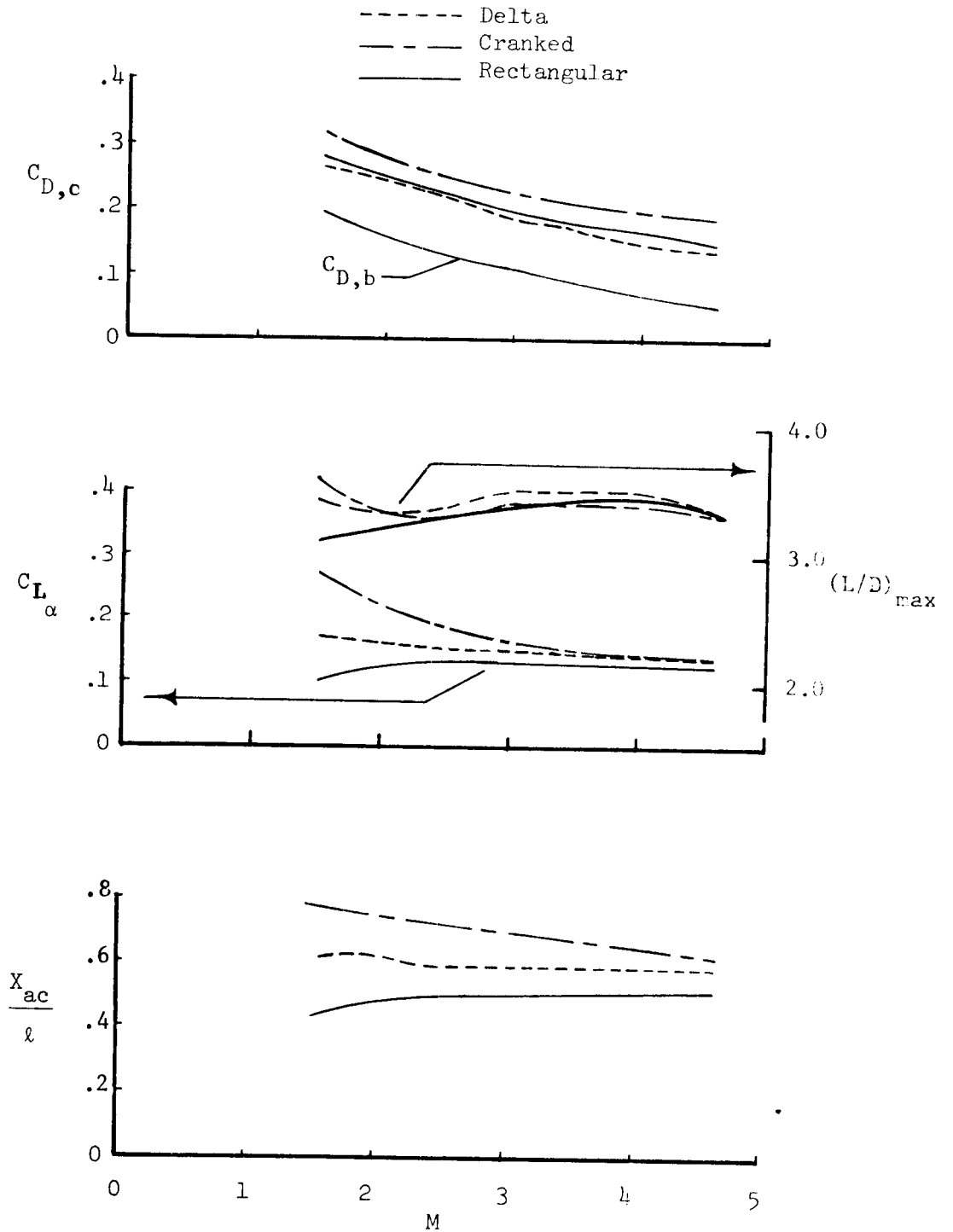


Figure 7. - Variation of longitudinal parameters with Mach number; $\alpha=0$, $\phi=0$, mid-sized wings.

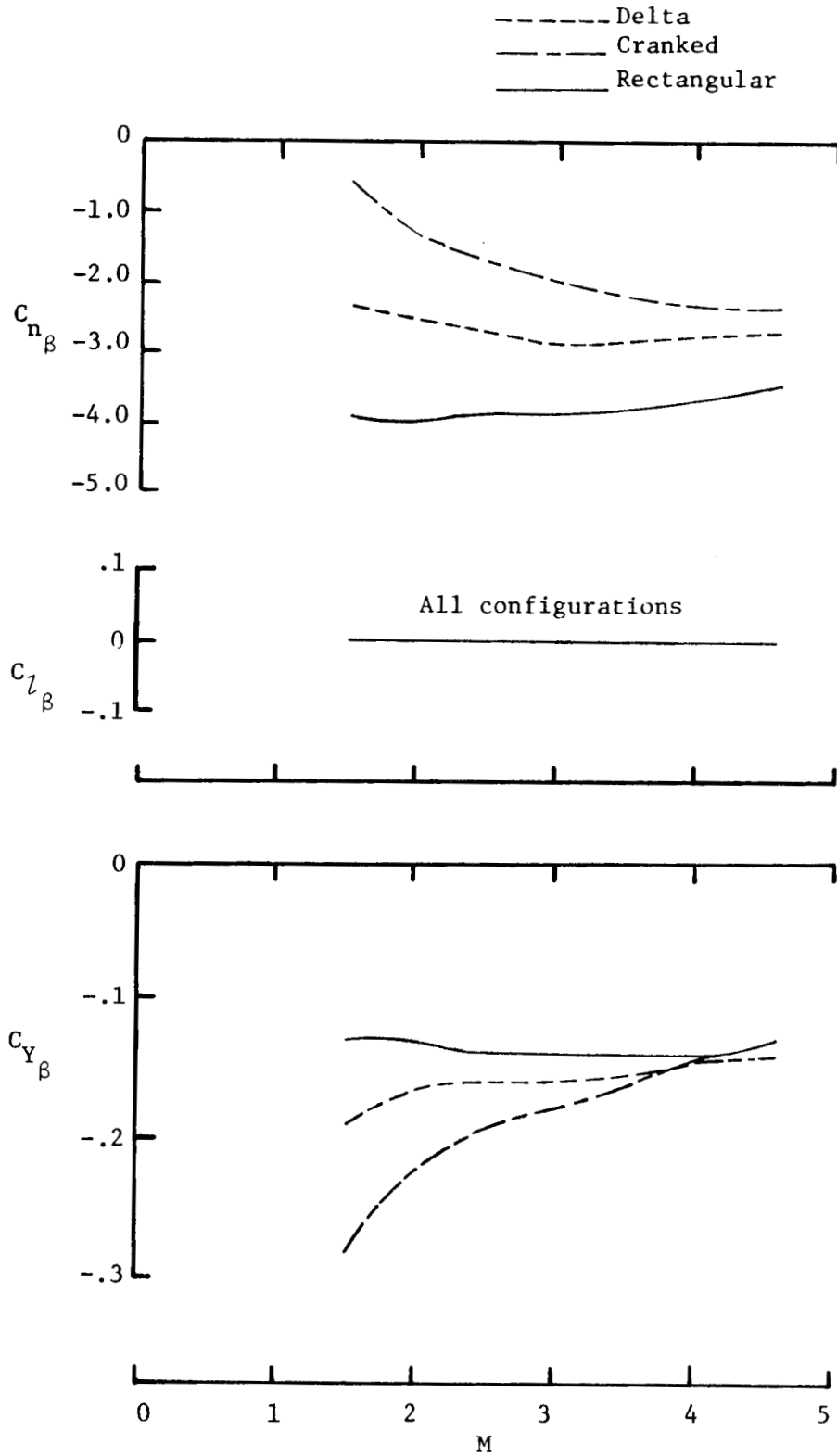


Figure 8. - Variation of sideslip derivatives with Mach number; $\alpha=0^\circ$, $\phi=0^\circ$, mid-sized wings.

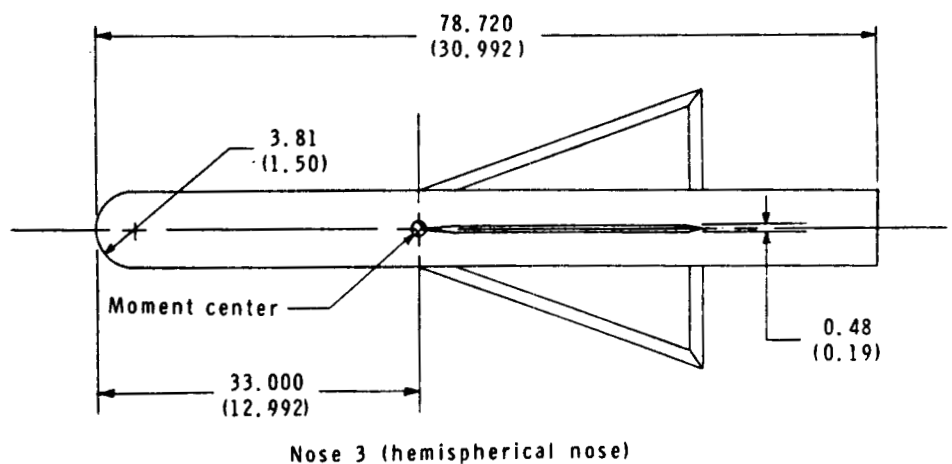
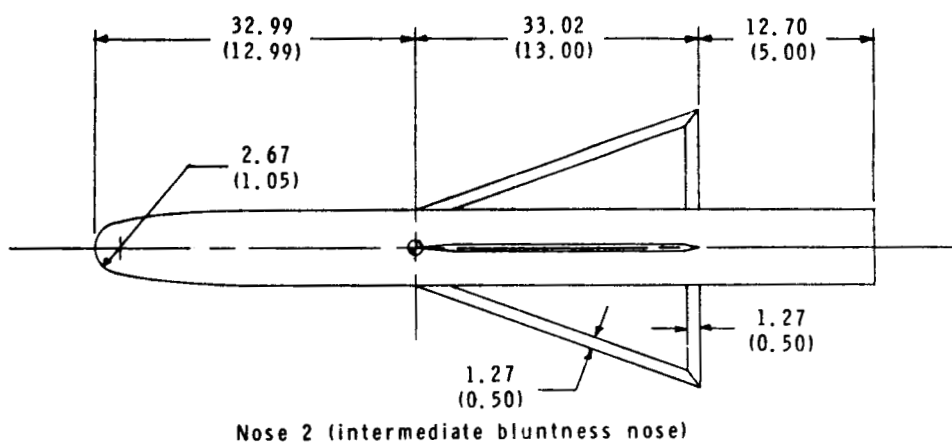
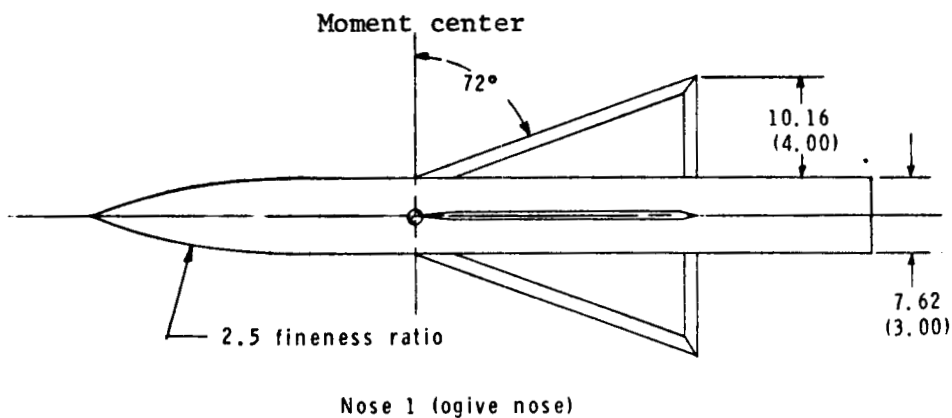


Figure 9. - Drawing of model showing nose shapes investigated. Linear dimensions are given in centimeters and parenthetically in inches.

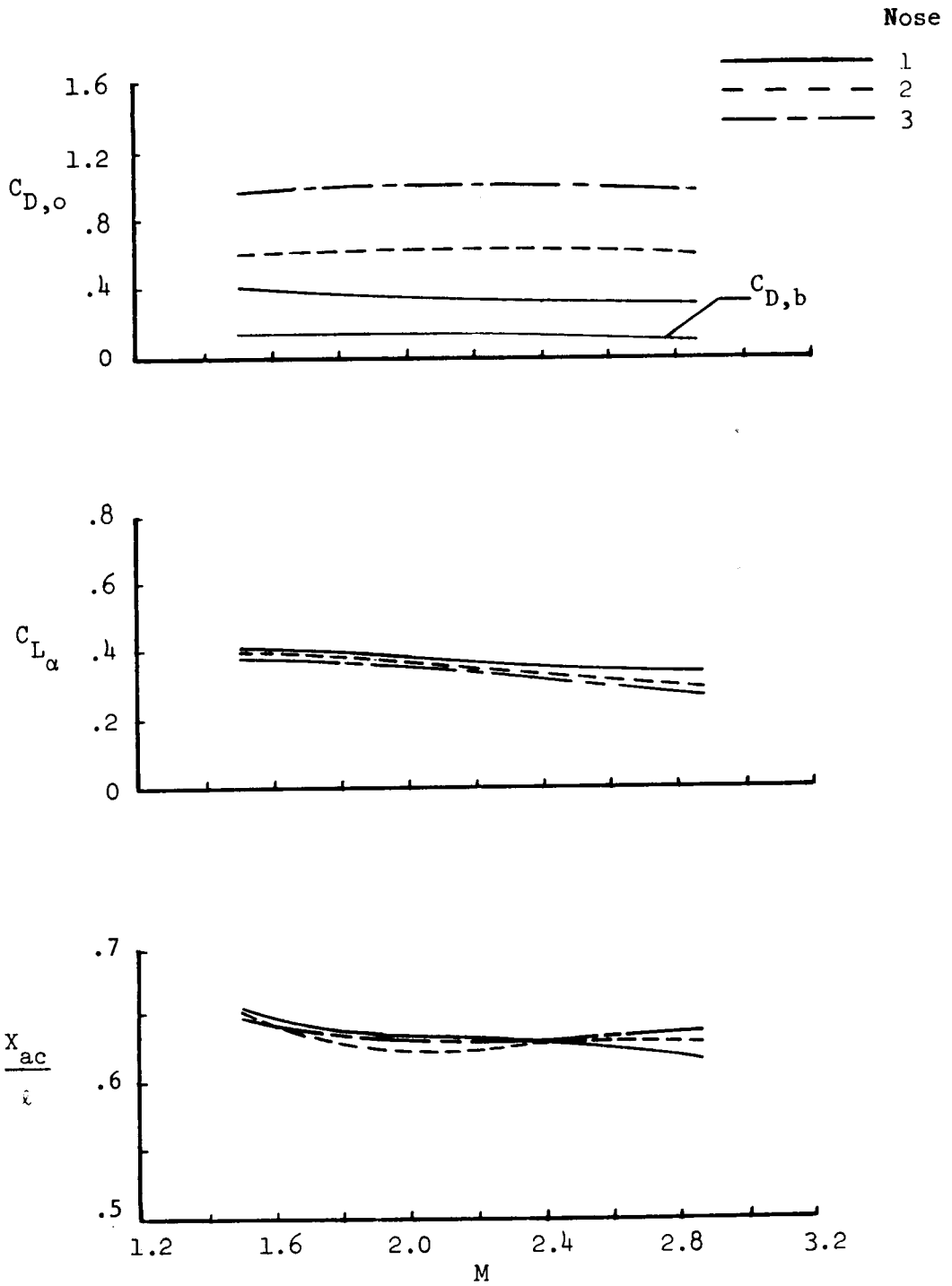


Figure 10. - Variation of longitudinal parameters with Mach number; $\alpha=0^\circ$
 $\phi=0^\circ$

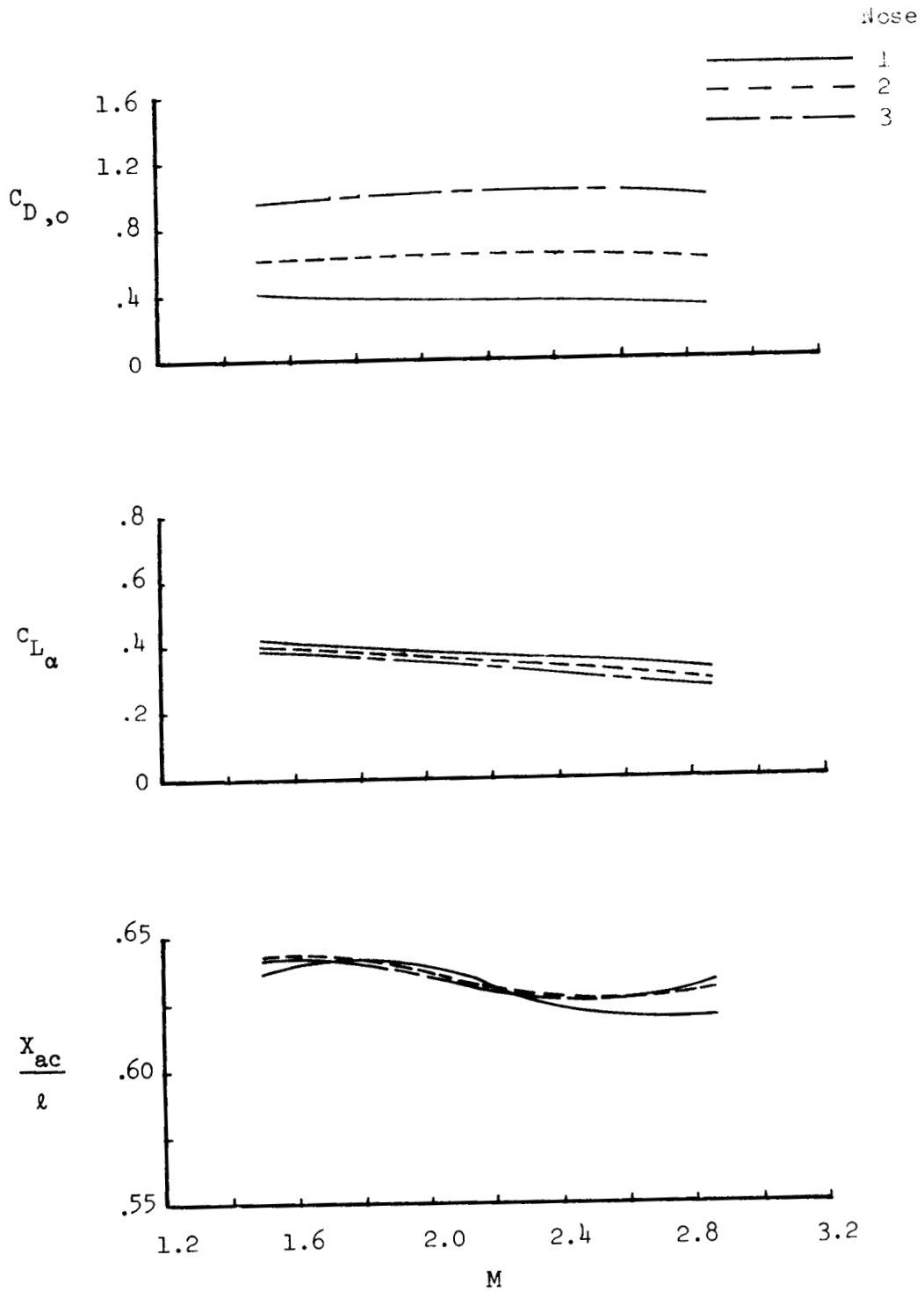


Figure 11. - Variation of longitudinal parameters with Mach number; $\alpha=0^\circ$
 $\phi=45^\circ$

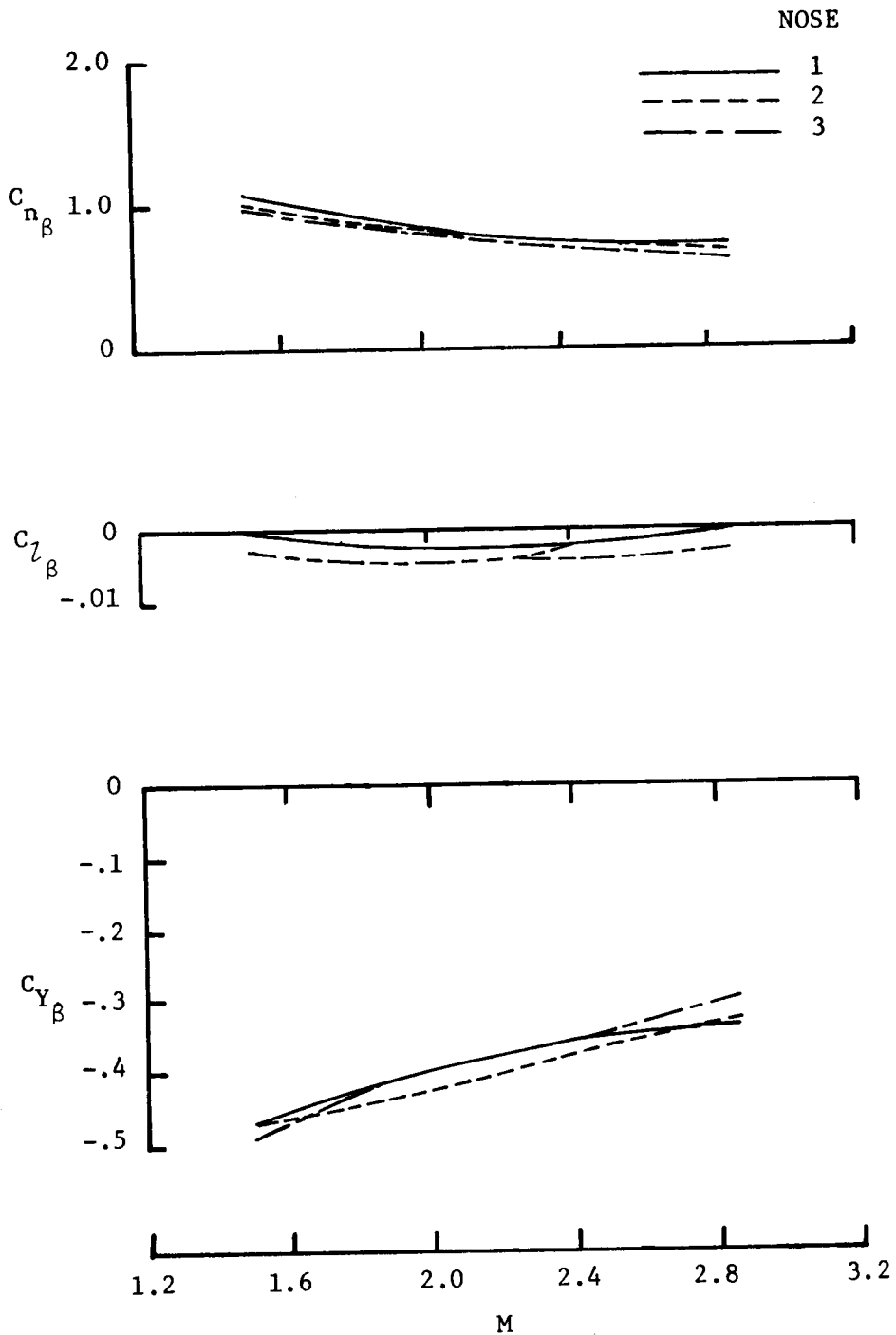


Figure 12. - Variation of sideslip derivatives with Mach number; $\alpha=0^\circ$, $\phi=0^\circ$.

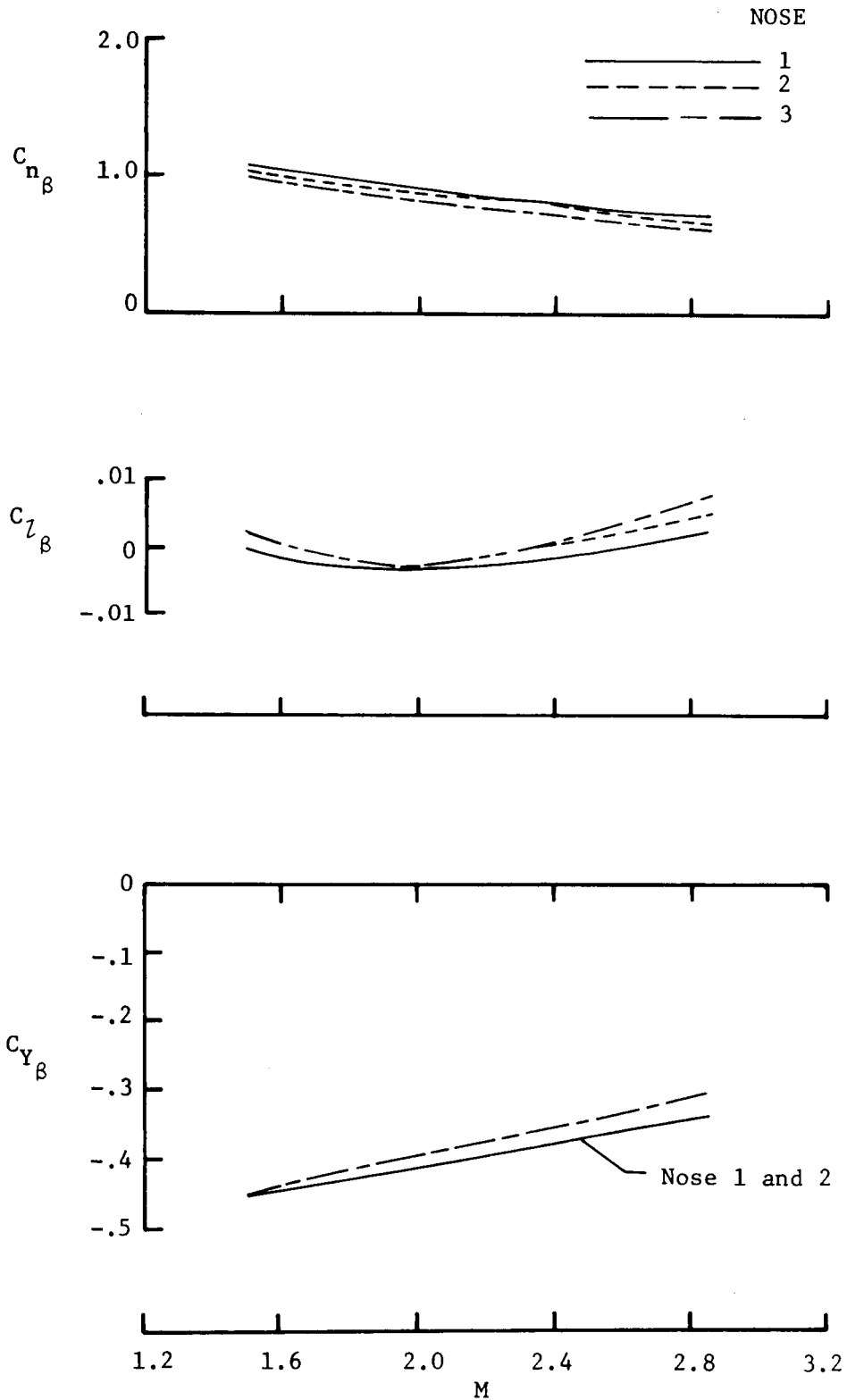


Figure 13. - Variation of sideslip derivatives with Mach number; $\alpha \approx 0^\circ$, $\phi = 45^\circ$.

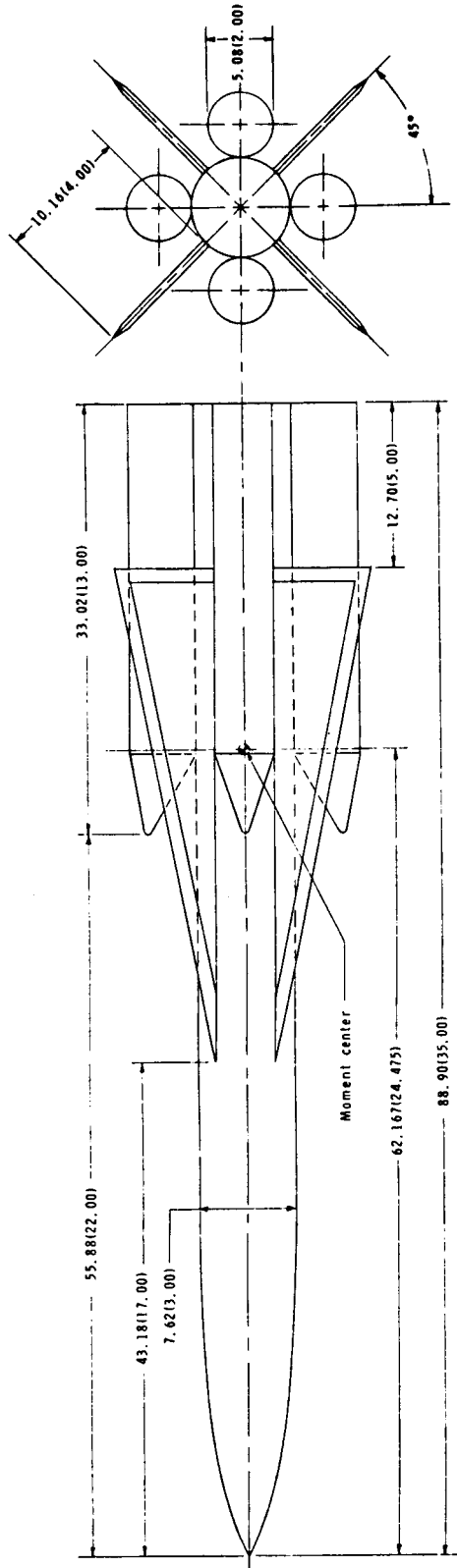


Figure 14. - Drawing of model. Dimensions are in centimeters (inches) unless otherwise noted.

Ref. TM X-2491

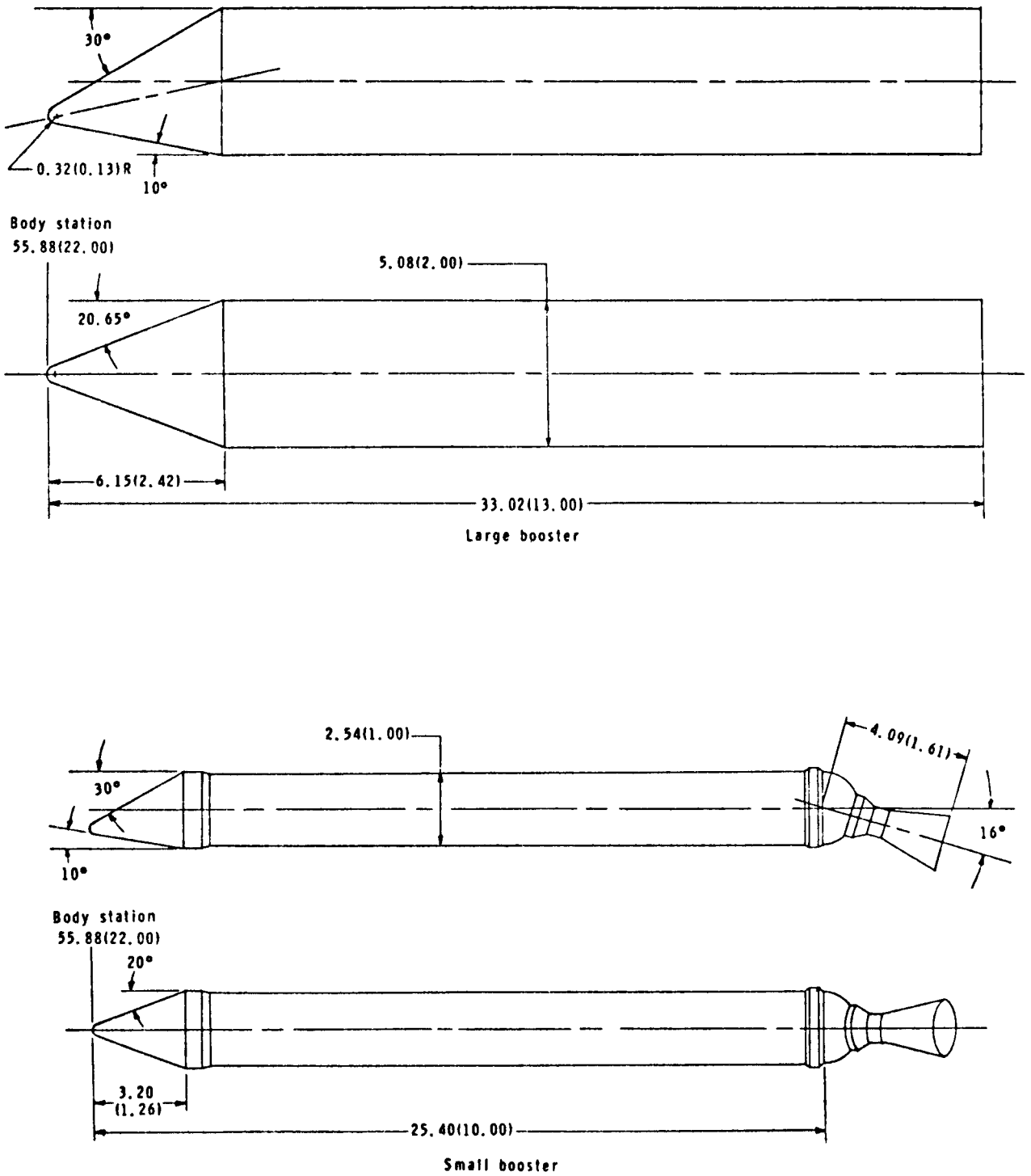


Figure 14 - Concluded.

Ref. TM X-2491

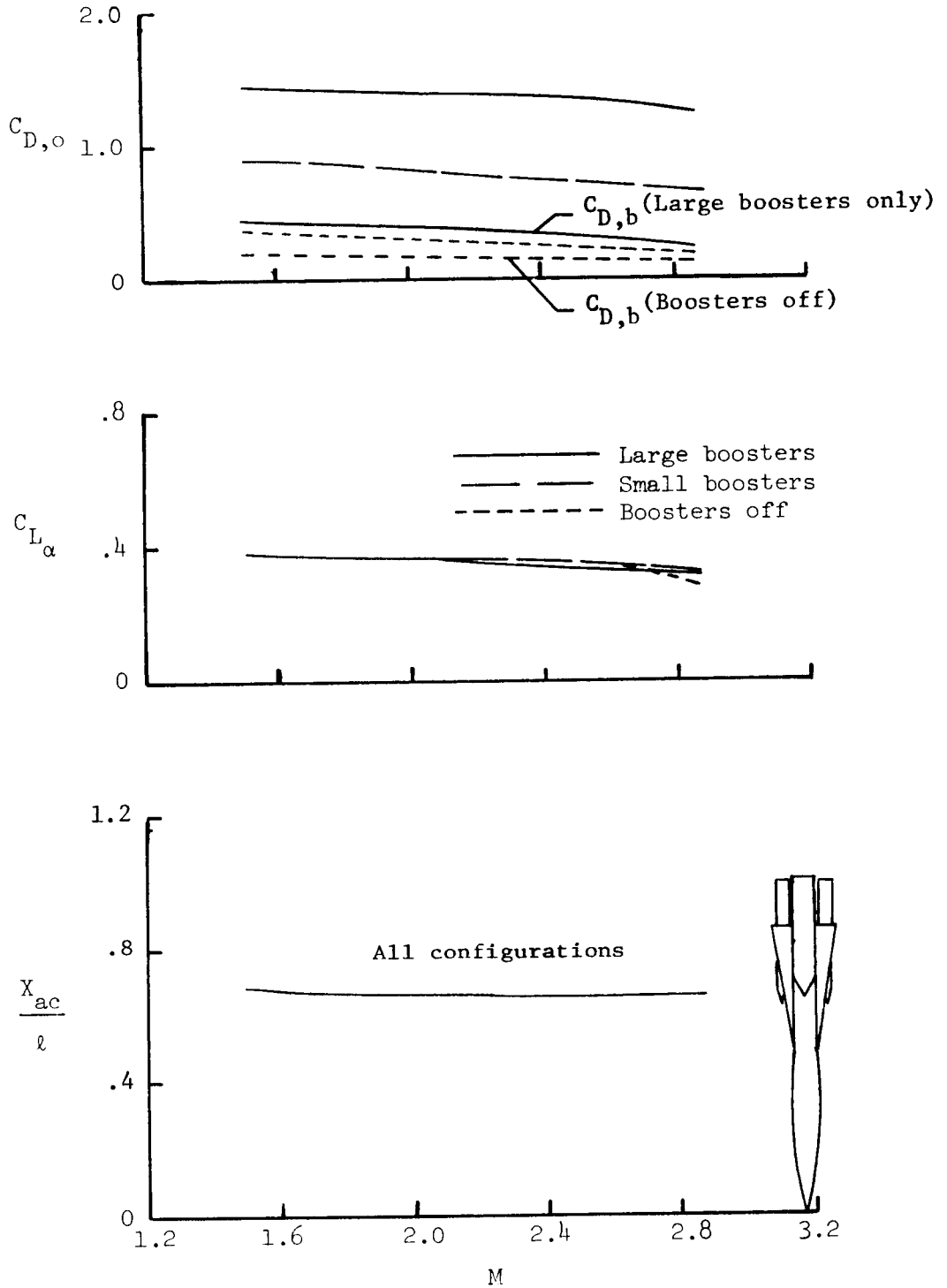


Figure 15 - Variation of longitudinal parameters with Mach number; $\alpha \approx 0^\circ$.

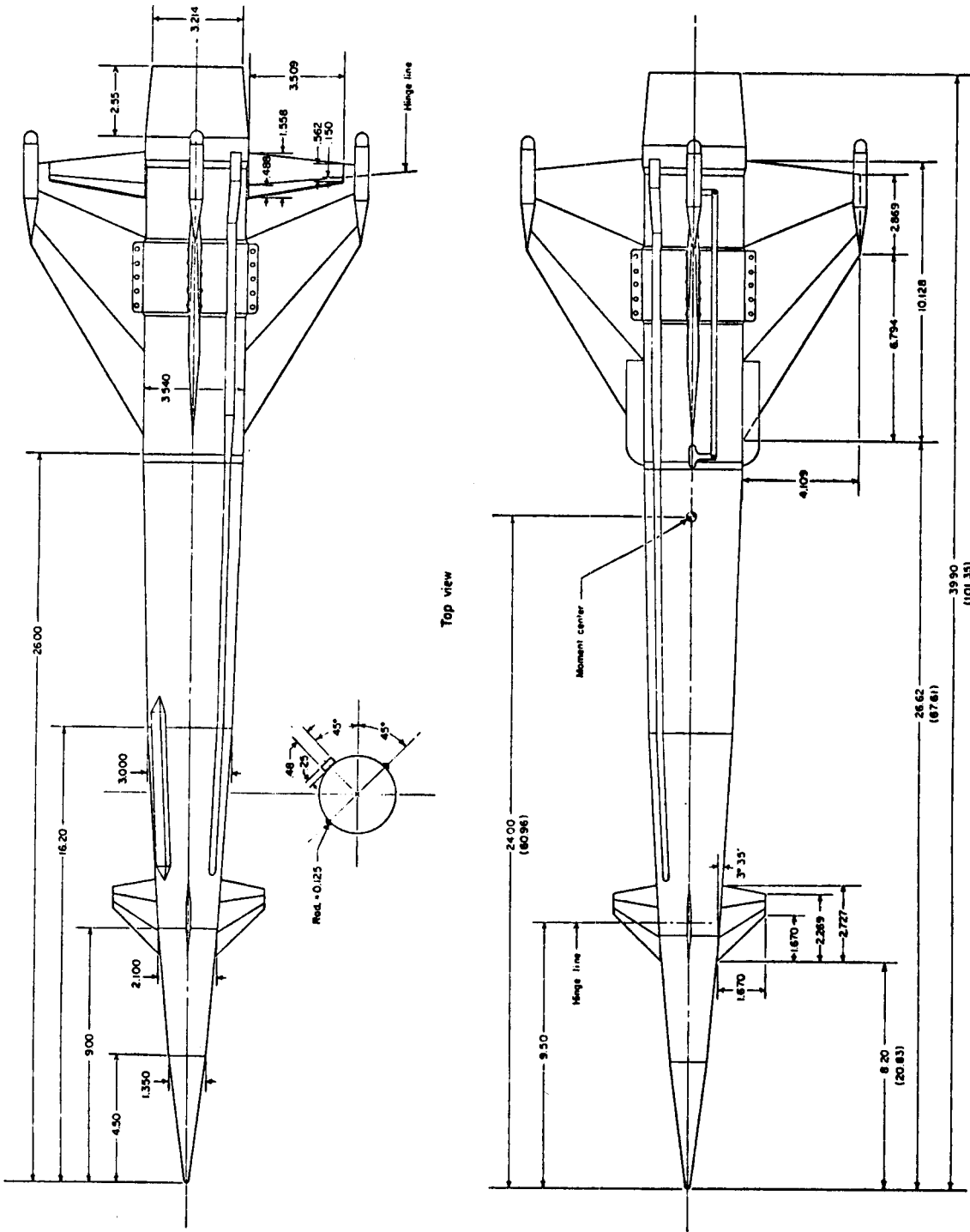


Figure 16. - Model shown with surfaces oriented in 0° roll plane.
Ref. TM X-1309, TM X-1352

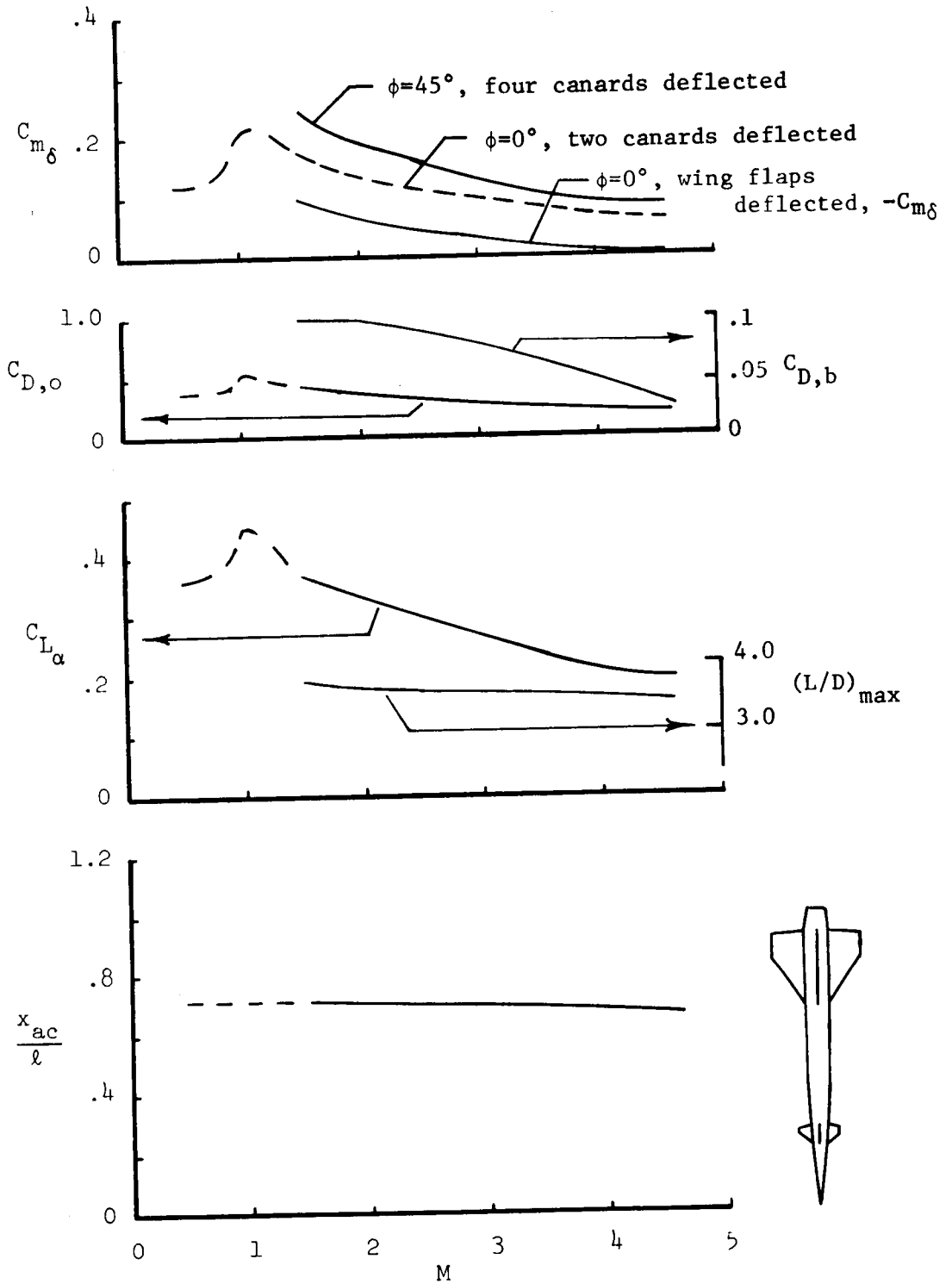


Figure 17. - Variation of longitudinal parameters with Mach number; $\alpha=0^\circ$

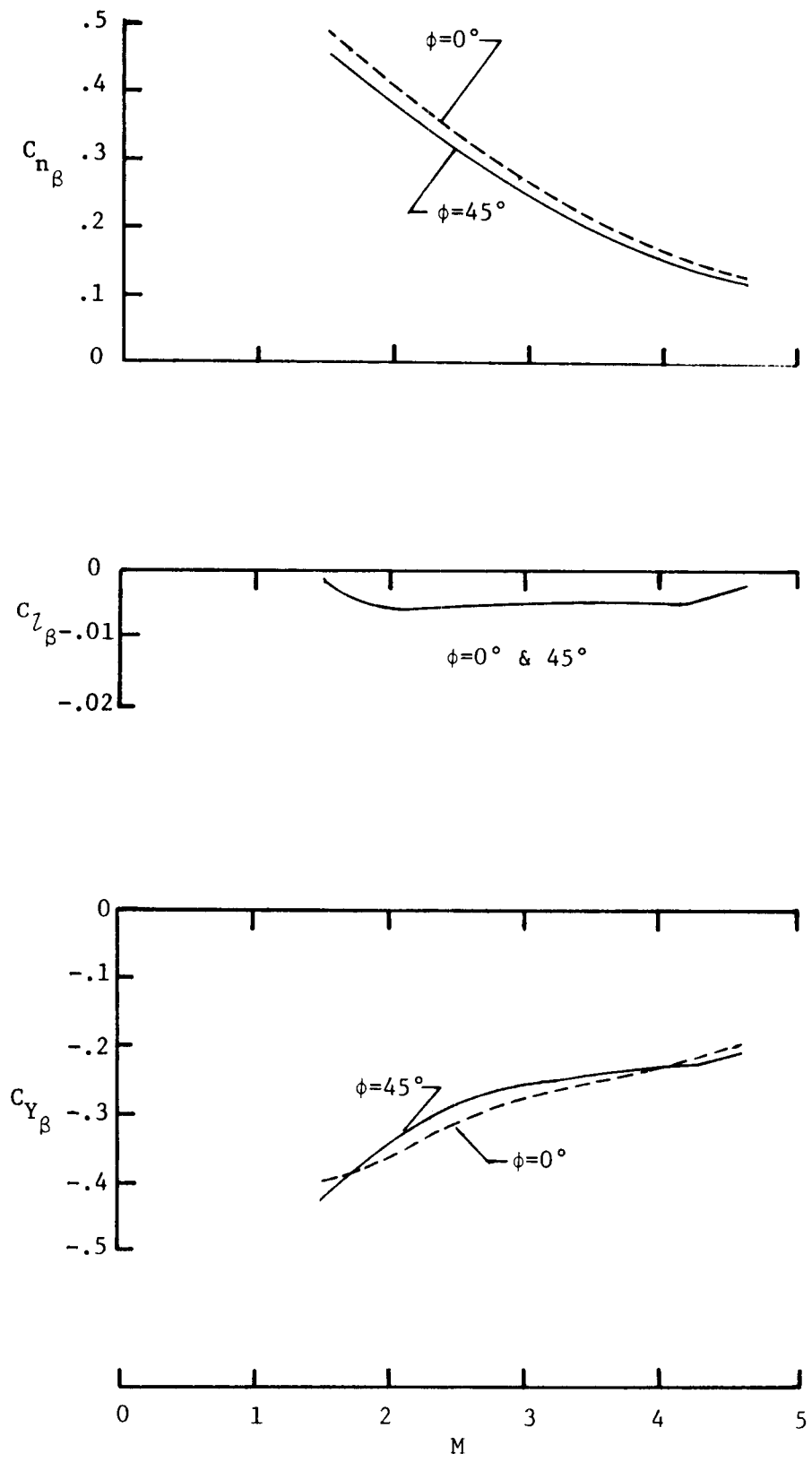


Figure 18. - Variation of sideslip derivatives with Mach number; $\alpha = 0^\circ$.

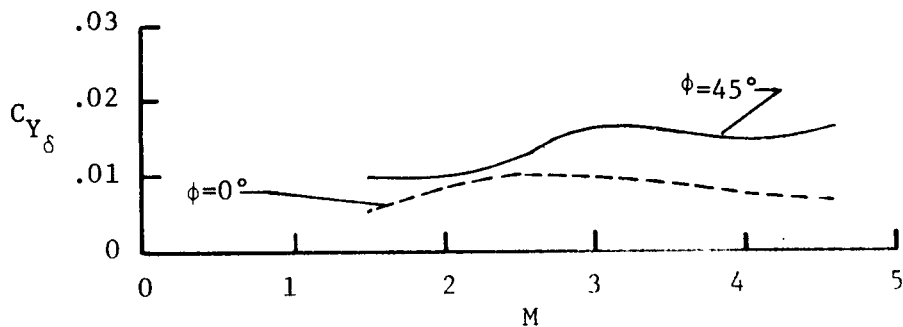
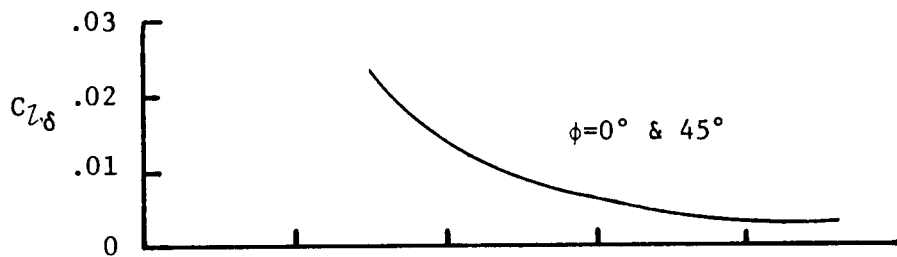
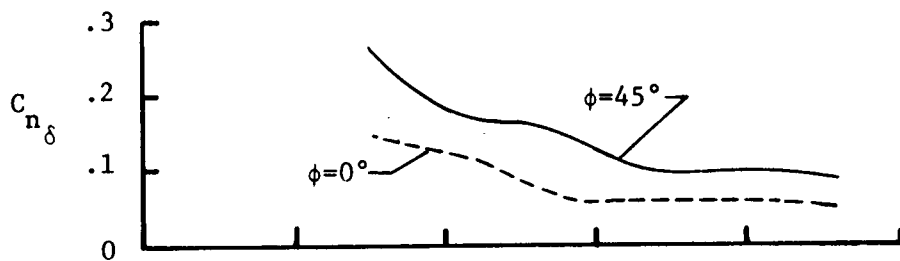


Figure 19. - Directional and lateral control effectiveness: $\alpha = 0^\circ$.

Ref. TM X-1309, TM X-1151

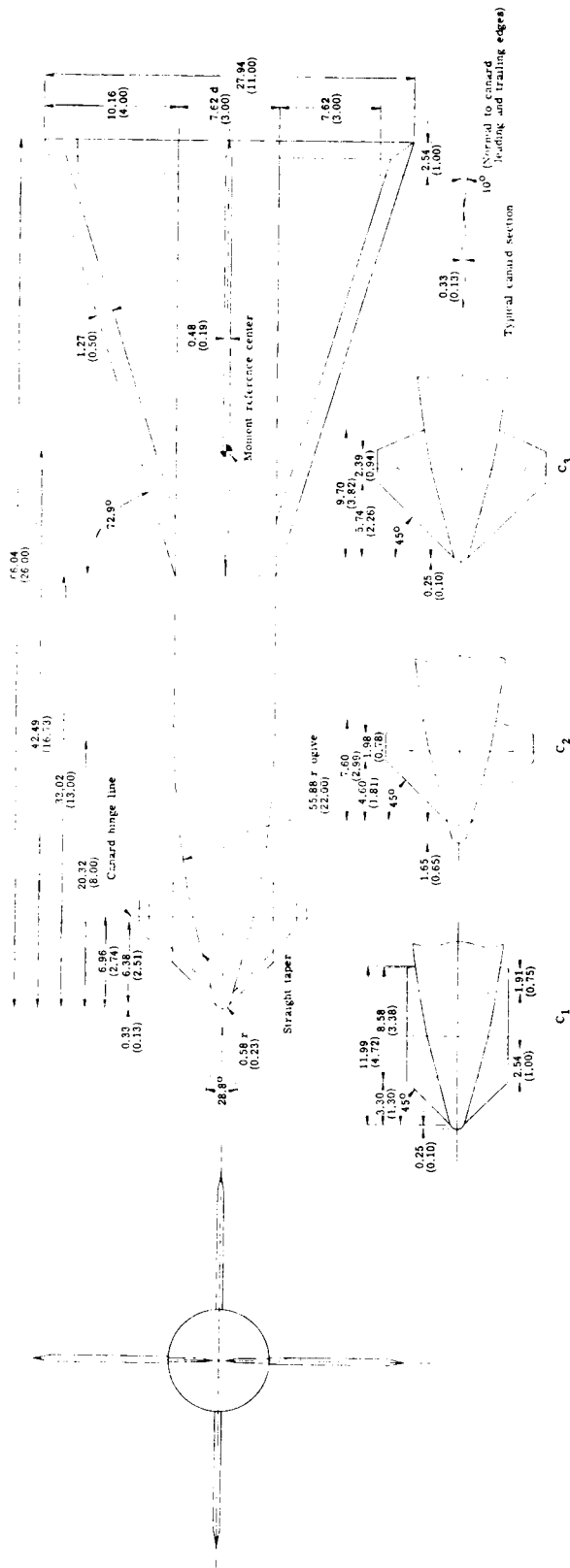


Figure 20. - Drawing of the model. All linear dimensions are in centimeters (inches).

Ref. TM X-2367

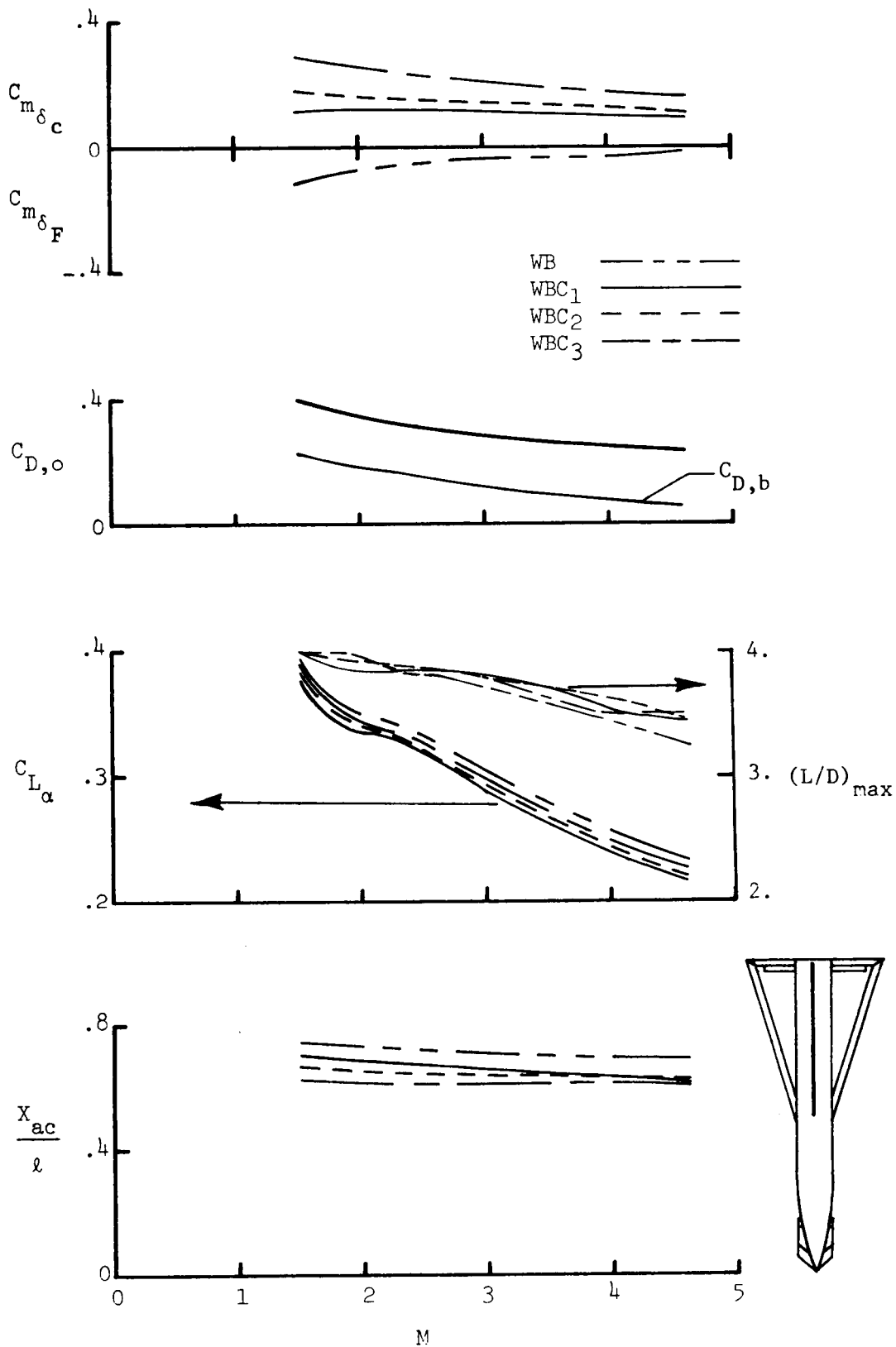


Figure 21. - Variation of longitudinal parameters with Mach number; $\alpha \approx 0^\circ$.

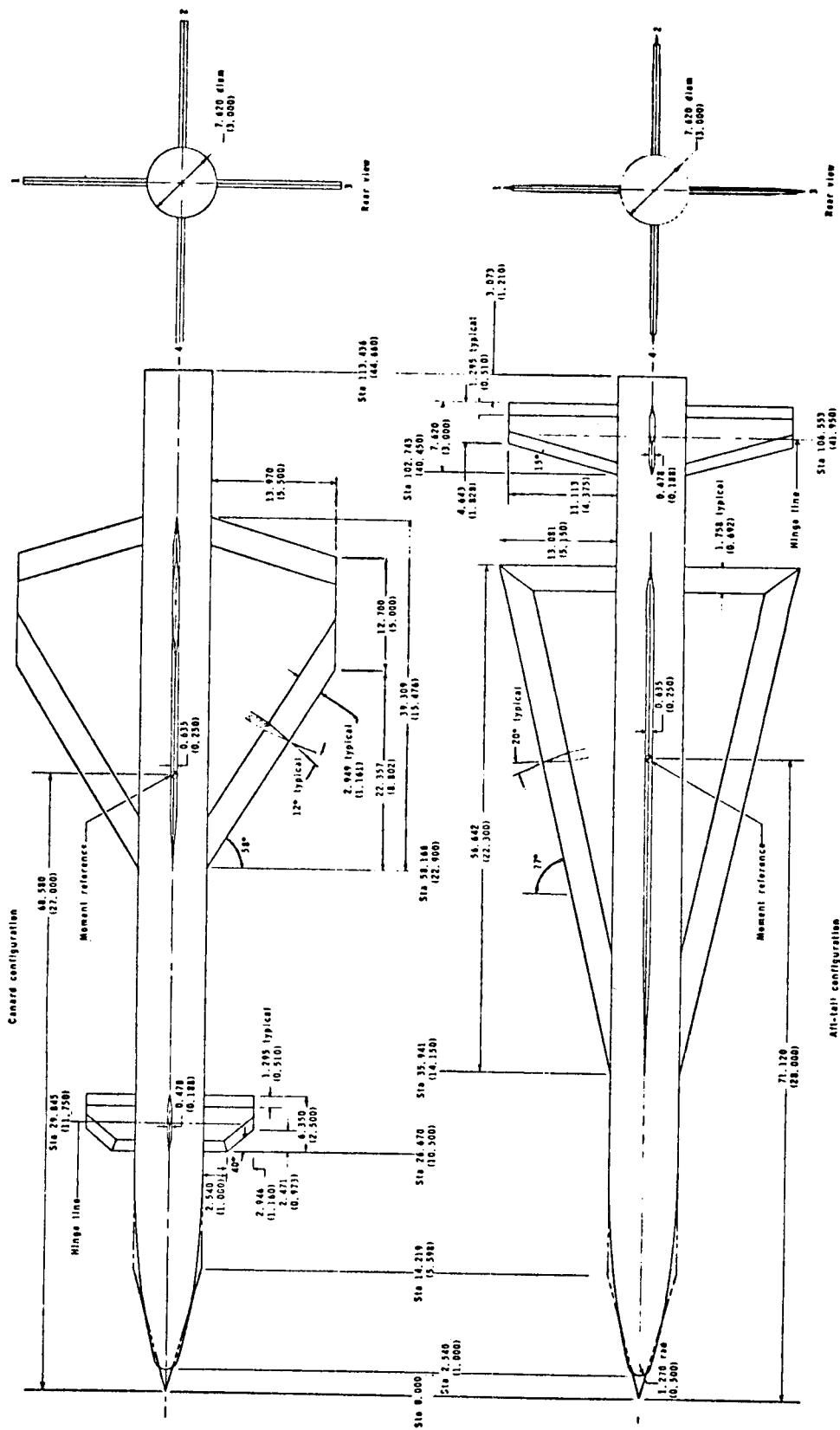


Figure 22. - Model details. All dimensions are in centimeters (inches) unless otherwise indicated.

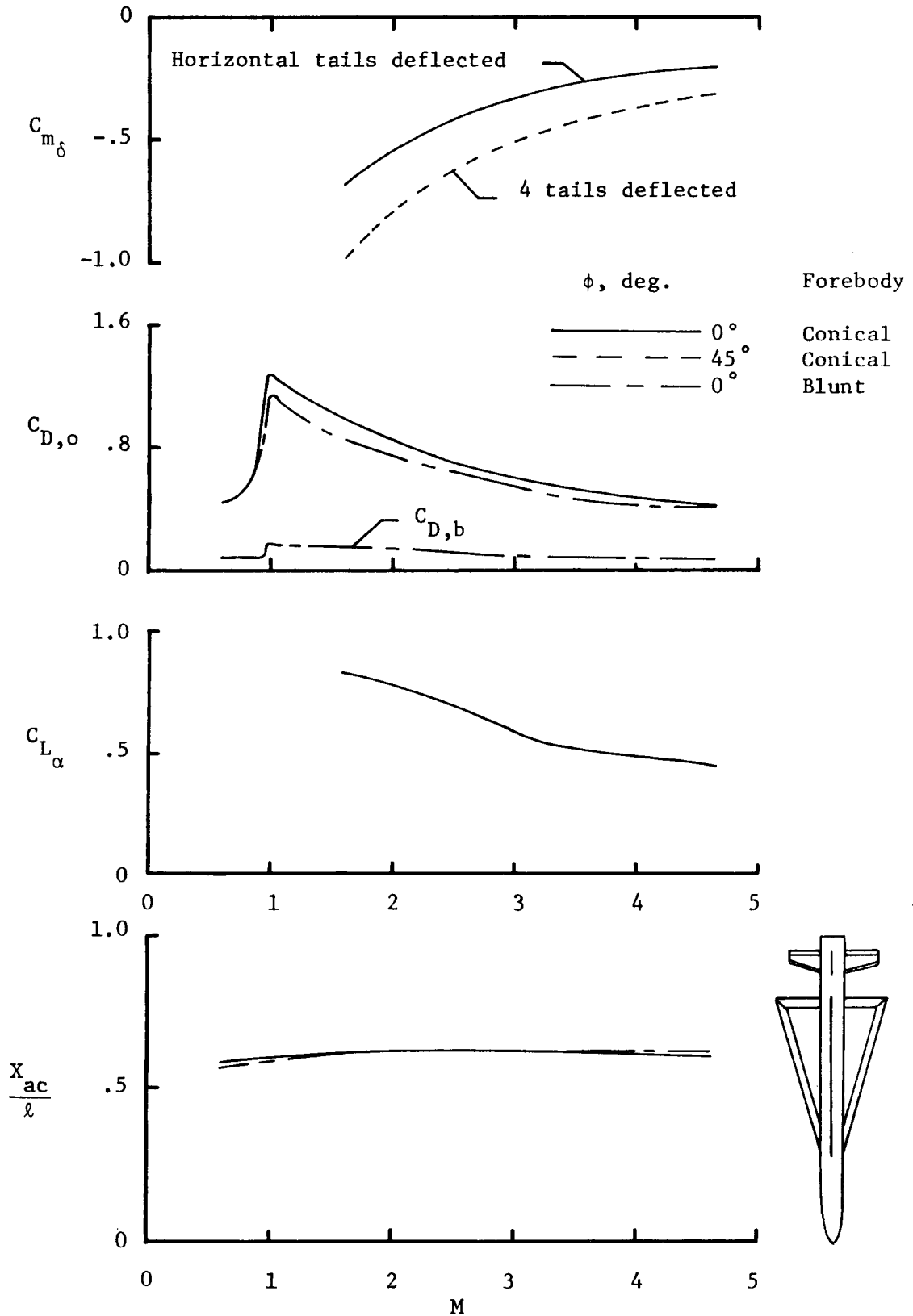


Figure 23. - Variation of longitudinal parameters with Mach number; $\alpha \approx 0^\circ$.

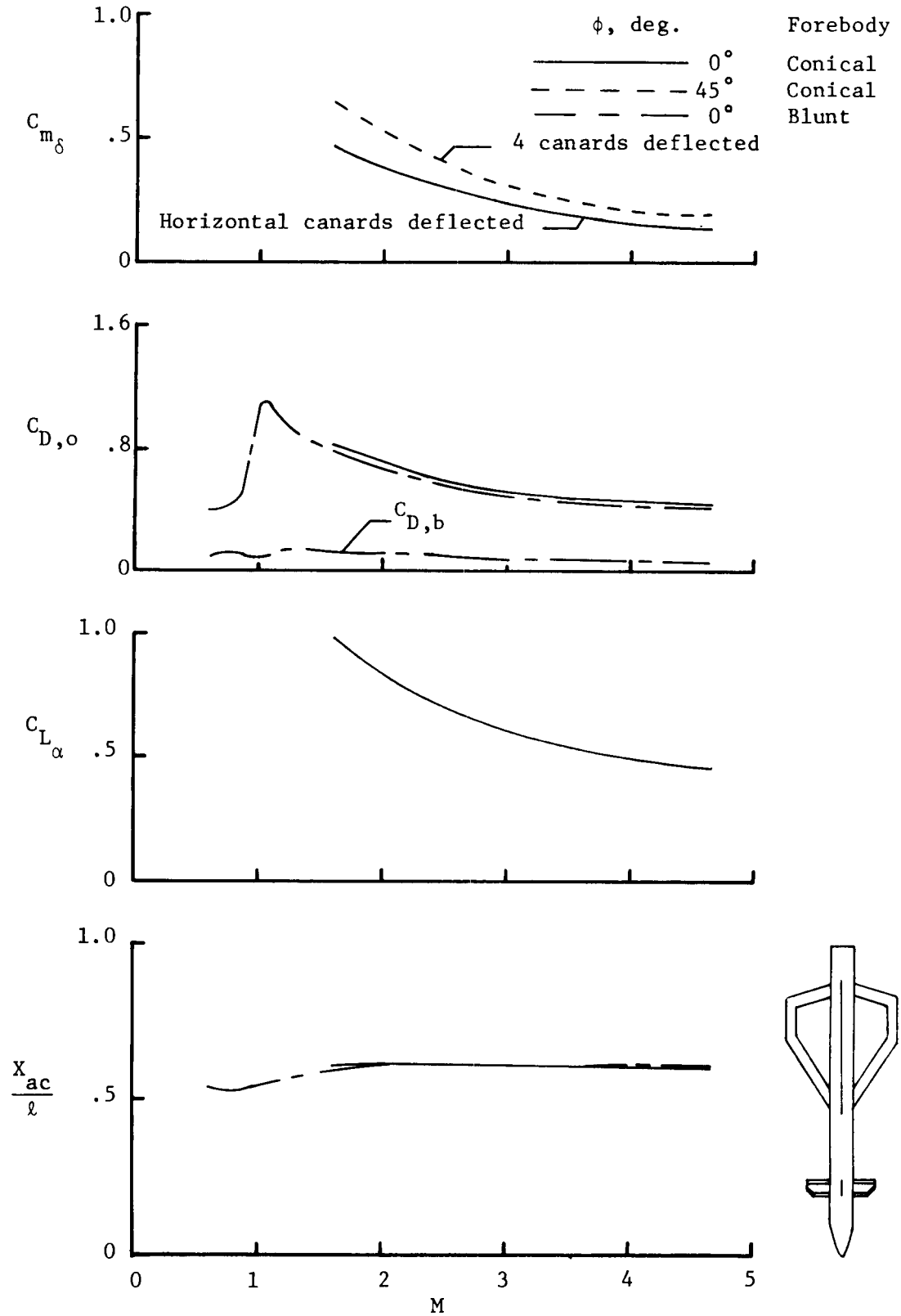


Figure 24. - Variation of longitudinal parameters with Mach number; $\alpha=0$.

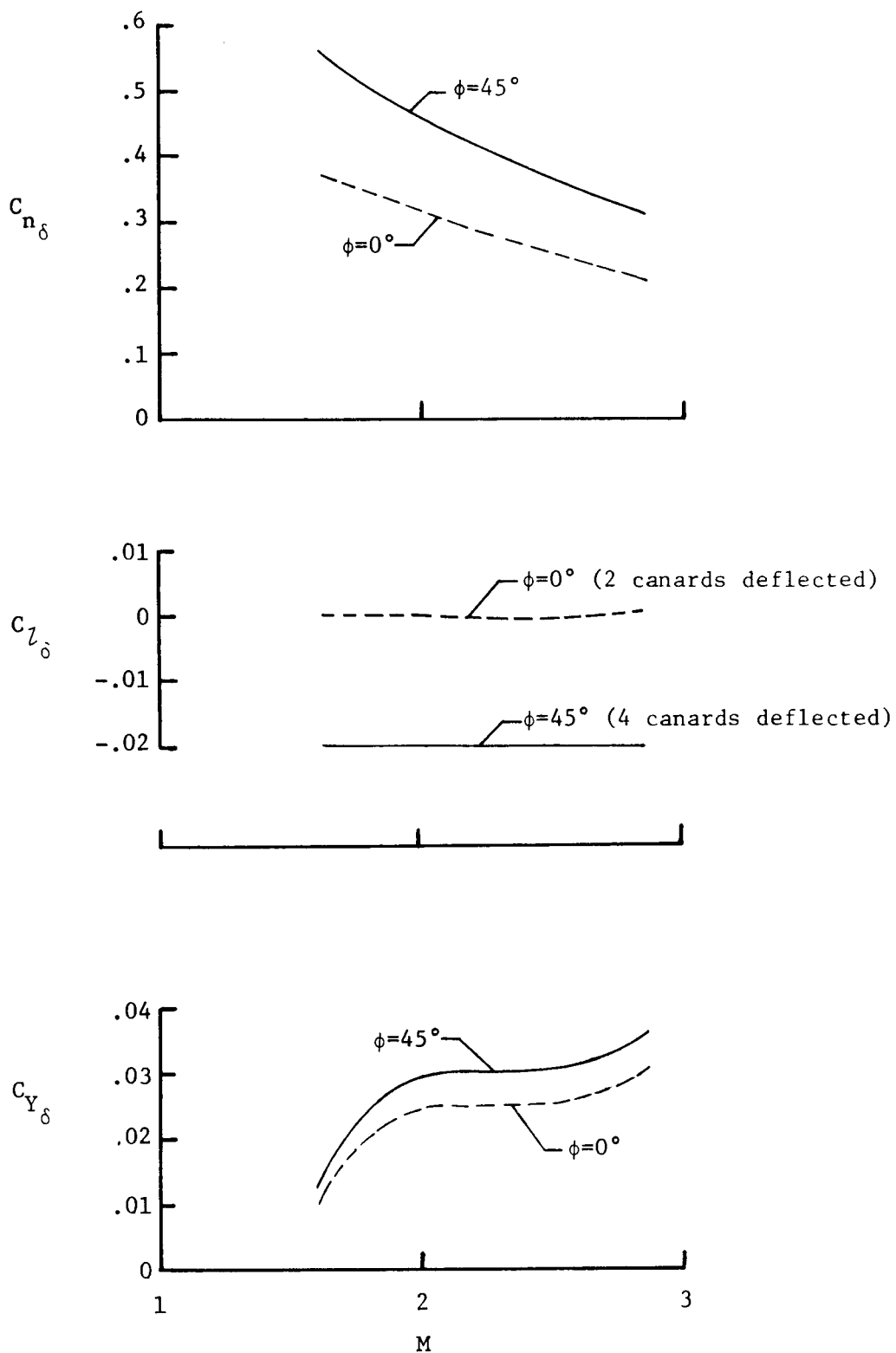
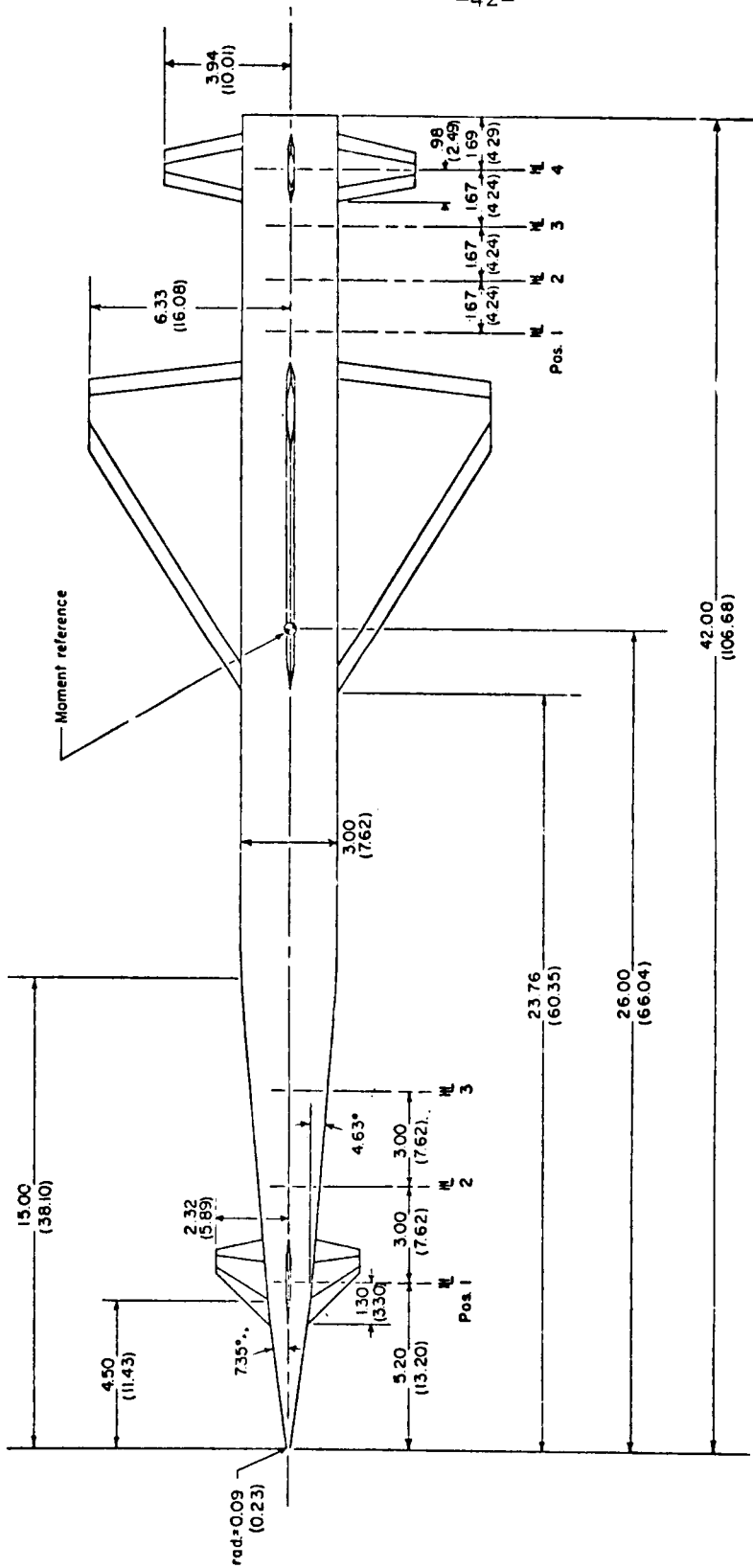
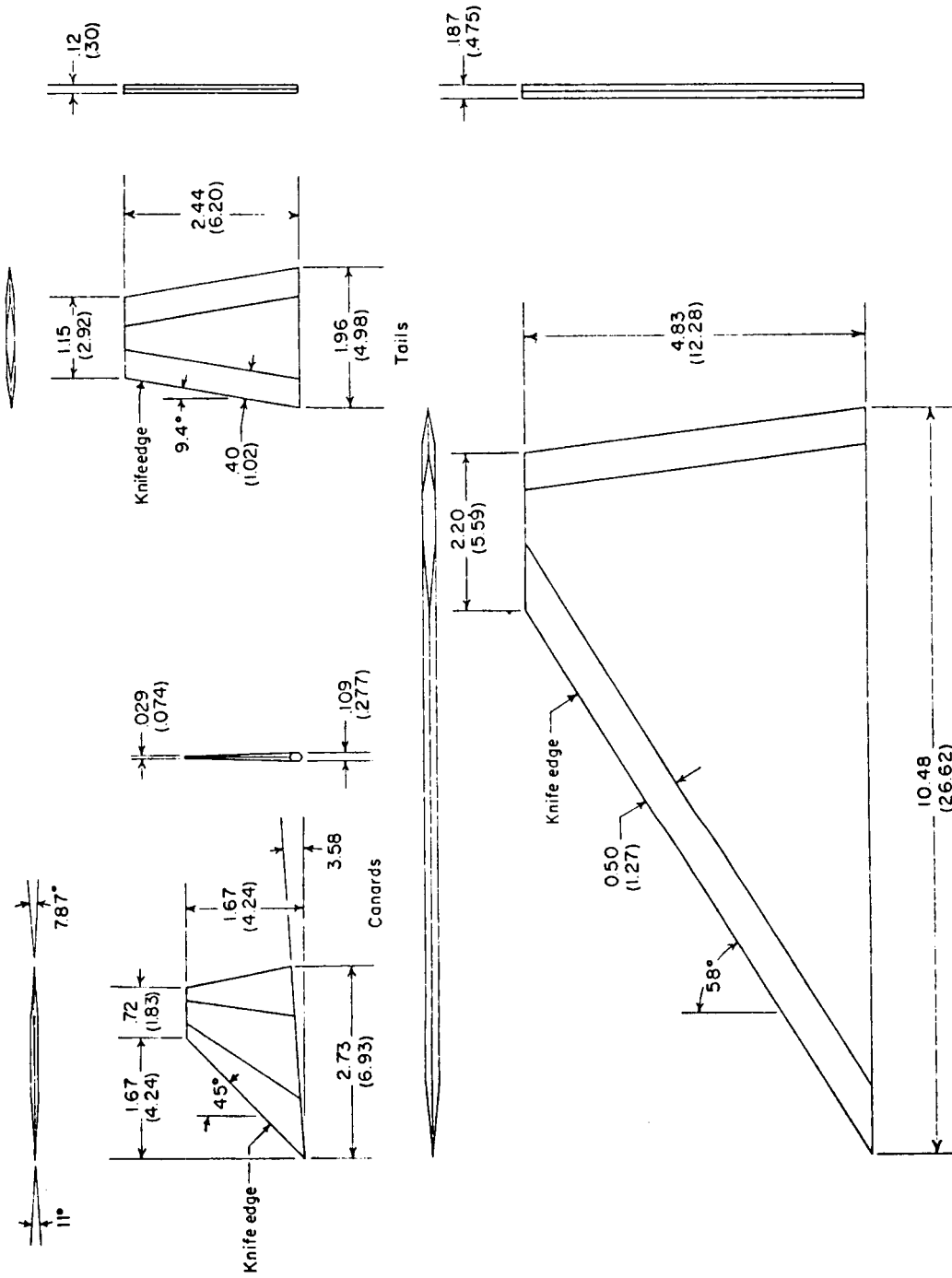


Figure 25. - Directional and lateral control effectiveness of canard configuration with blunted ogive nose; $\alpha=0^\circ$.



(a) Complete model.

Figure 26. - Model drawings. (All dimensions are given in inches and parenthetically in centimeters.)



(b) Details of canards, tails, and wing.

Figure 26. - Concluded

Ref. TM X-1834

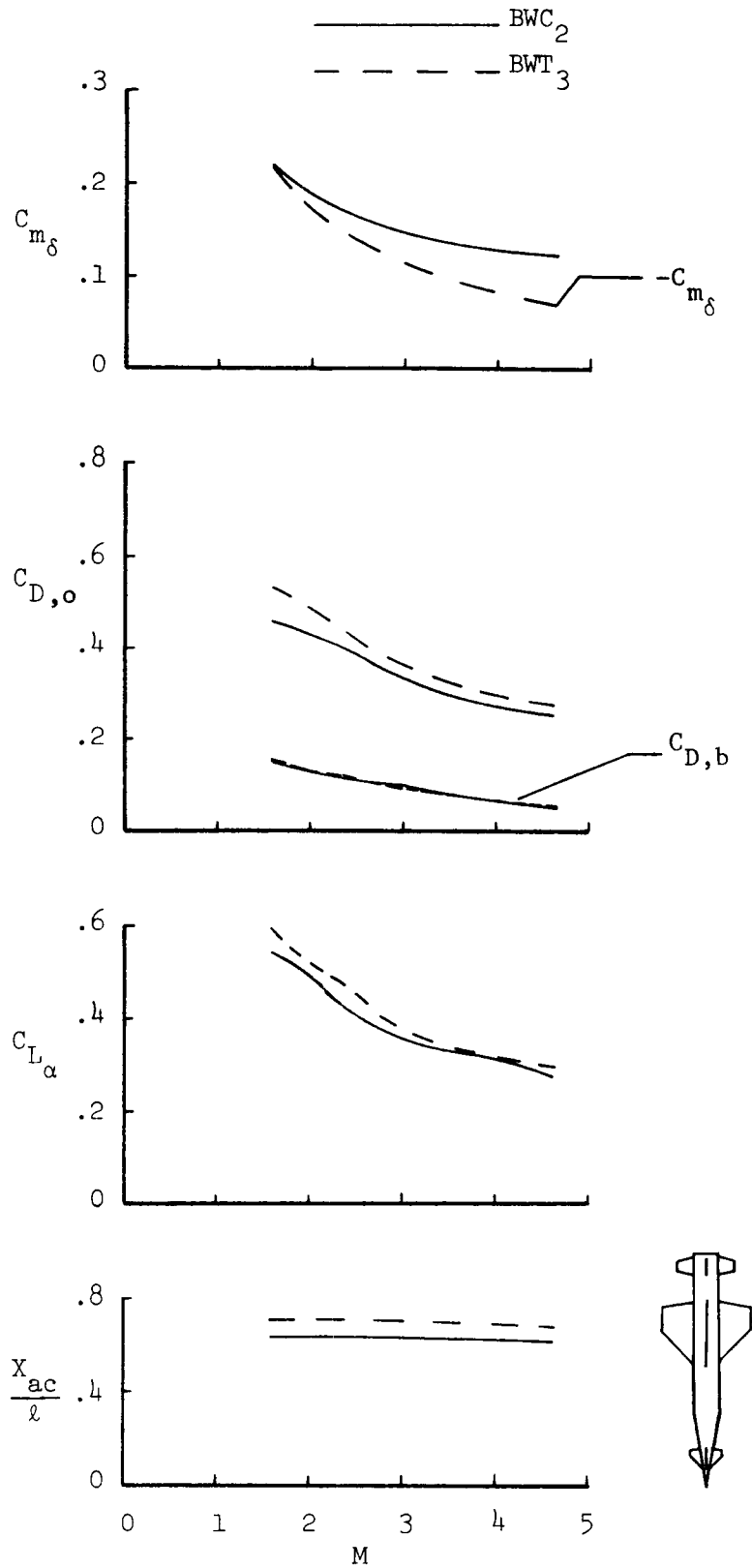


Figure 27. - Variation of longitudinal parameters with Mach number; $\alpha \approx 0^\circ$

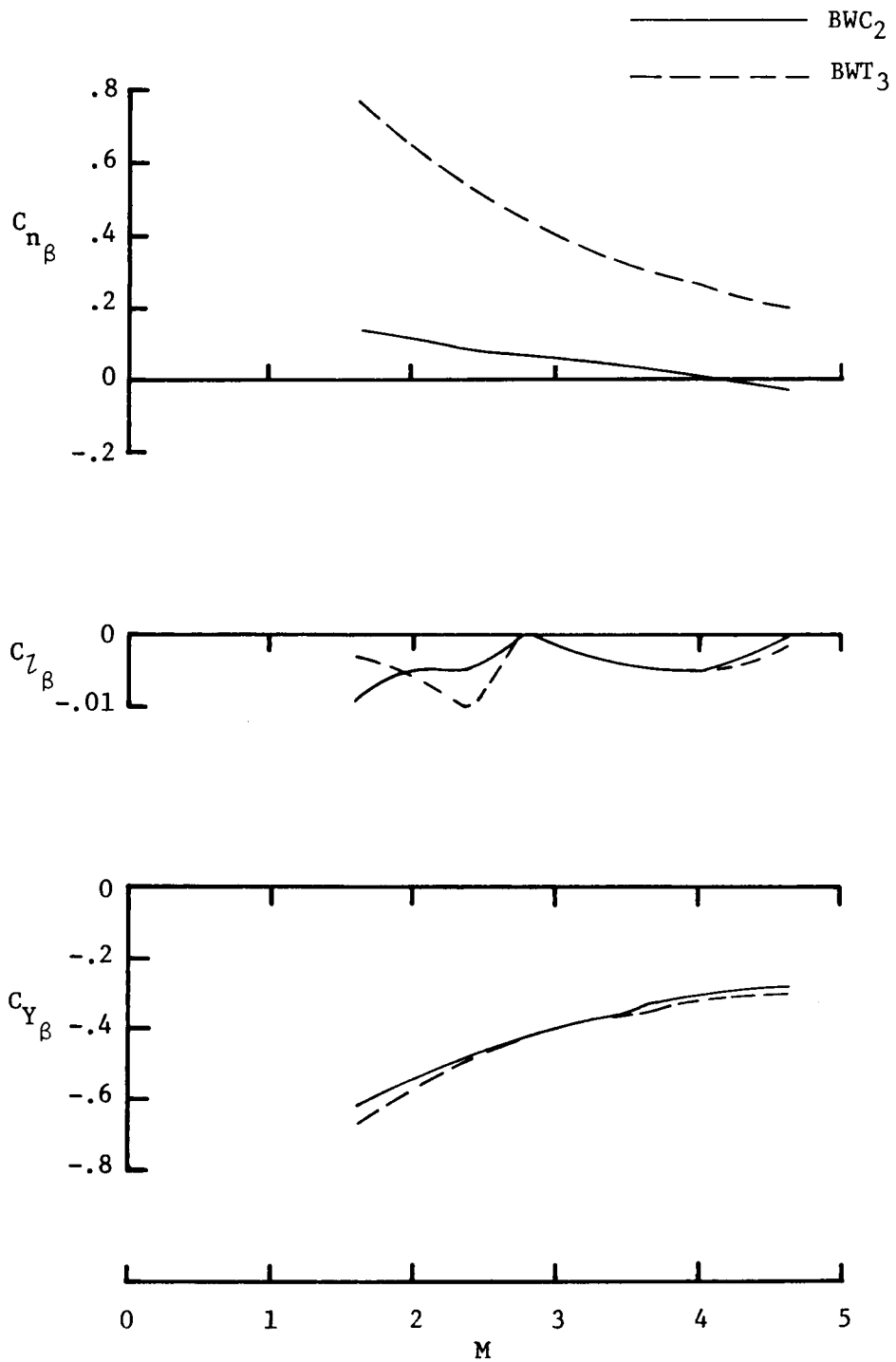
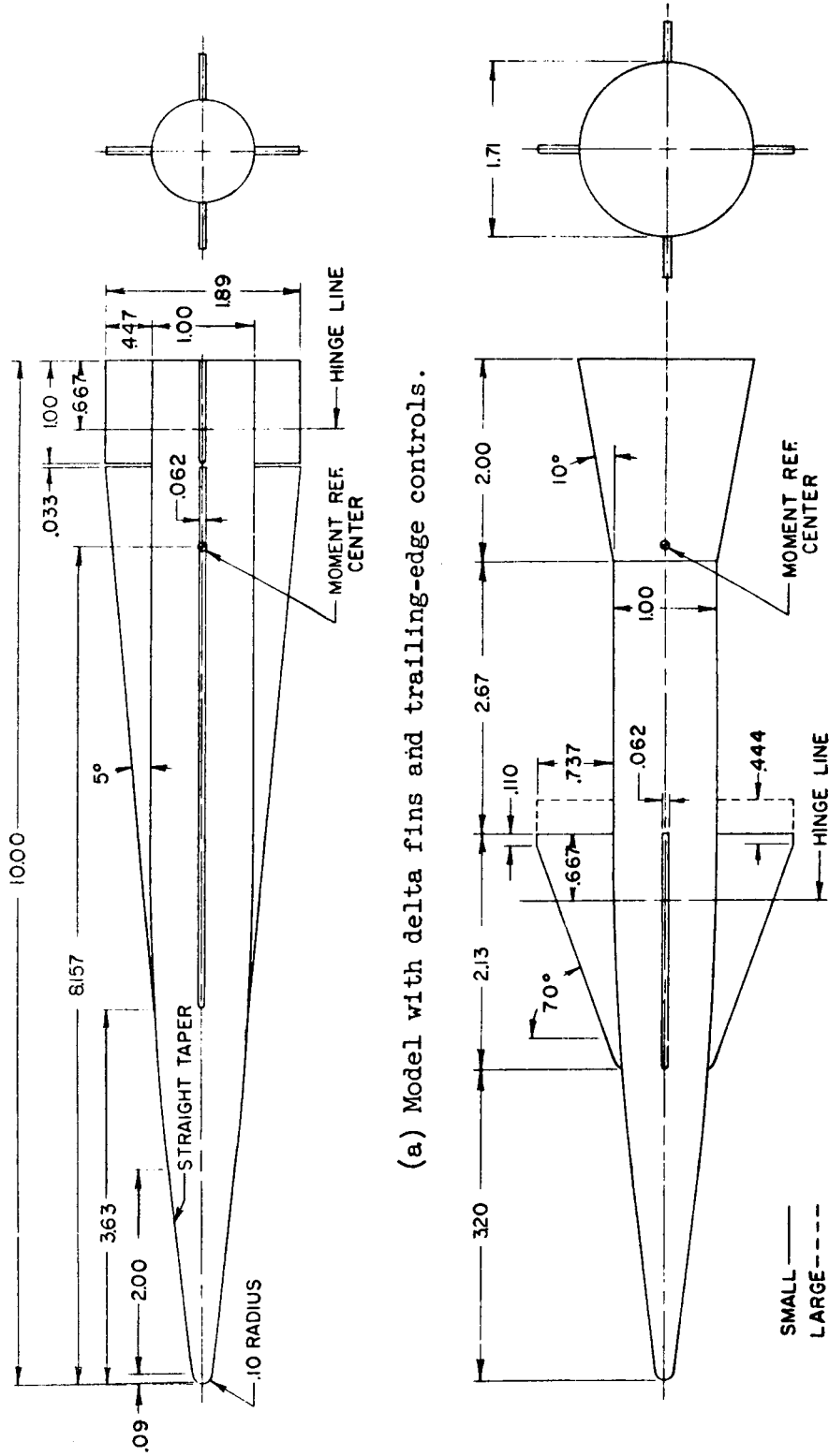


Figure 28. - Variation of sideslip derivatives with Mach number; $\alpha=0^\circ$.

Ref. TM X-1834



(a) Model with delta fins and trailing-edge controls.

(b) Model with flared skirt and large and small canard controls.

Figure 29. - Missile configurations tested. All linear dimensions are in diameters.

TABLE 3. - LONGITUDINAL PARAMETERS AT MACH NUMBER 4.65; $\alpha=0^\circ$

CCONFIGURATION	C_{m_δ}	$C_{D,o}$	C_{L_α}	$\frac{X_{ac}}{l}$
Delta Fins and Trailing-Edge Controls	-0.017	0.12	0.134	0.637
Large Canard Controls with Flared Skirt	0.166	0.36	0.175	0.593
Small Canard Controls with Flared Skirt	0.143	0.34	0.150	0.583
Small Canard Controls without Flared Skirt	—	0.18	0.105	0.445

TABLE 4. - SIDESLIP DERIVATIVES AT MACH NUMBER 4.65; $\alpha=0^\circ$

CONFIGURATION	C_{n_β}	C_{l_β}	C_{Y_β}
Delta Fins and Trailing-Edge Controls	-0.266	0	-0.153
Large Canard Controls with Flared Skirt	-0.418	0	-0.186
Small Canard Controls with Flared Skirt	-0.390	0	-0.177
Small Canard Controls without Flared Skirt	-0.433	0	-0.134

TABLE 5. - DIRECTIONAL AND LATERAL CONTROL EFFECTIVENESS
AT MACH NUMBER OF 4.65; $\alpha=0^\circ$

CONFIGURATION	C_{n_δ}	C_{l_δ}	C_{Y_δ} roll	C_{Y_δ} yaw
Delta Fins and Trailing Edge Controls	-0.0133	0.008*	-0.020*	0.0067
Small Canard Controls with Flared Skirt	—	0.026†	-0.015†	—

* All four control surfaces used for roll.

† Only two vertical canards used for roll.

Ref. TM X-187

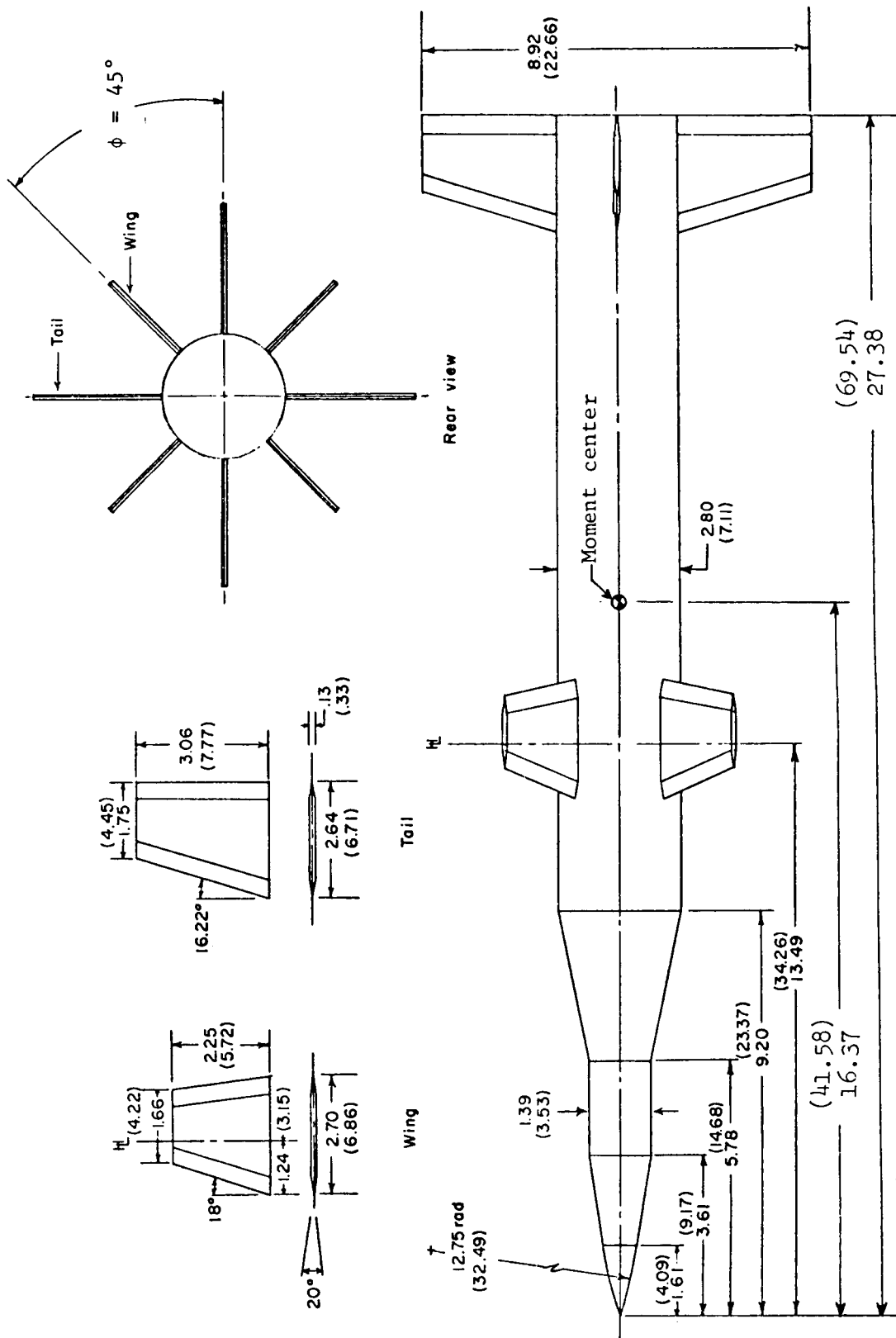


Figure 30. - Details of model. Linear dimensions are in inches (values within parentheses are centimeters).

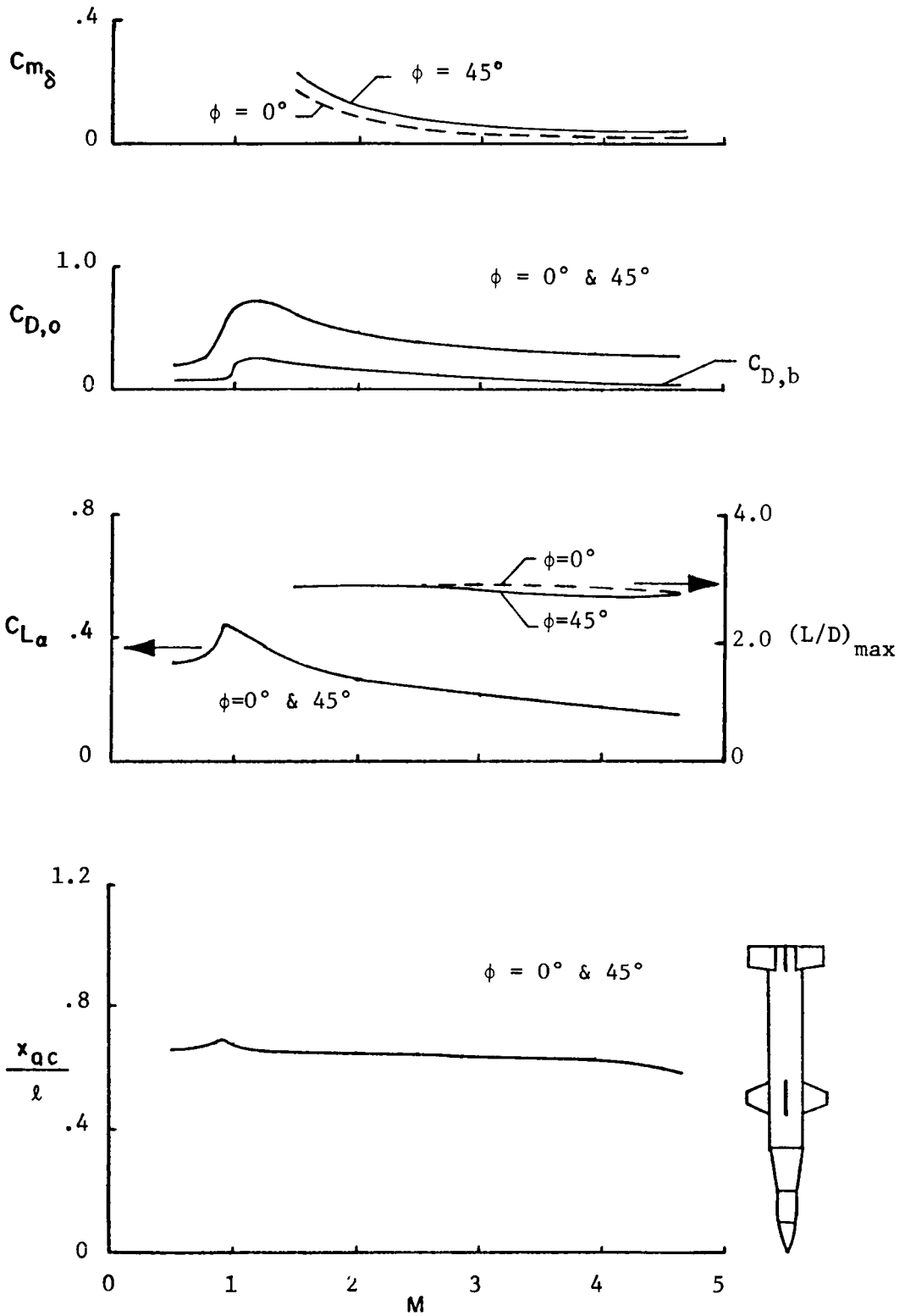


Figure 31. - Variation of longitudinal parameters with Mach numbers; $\alpha \approx 0$.

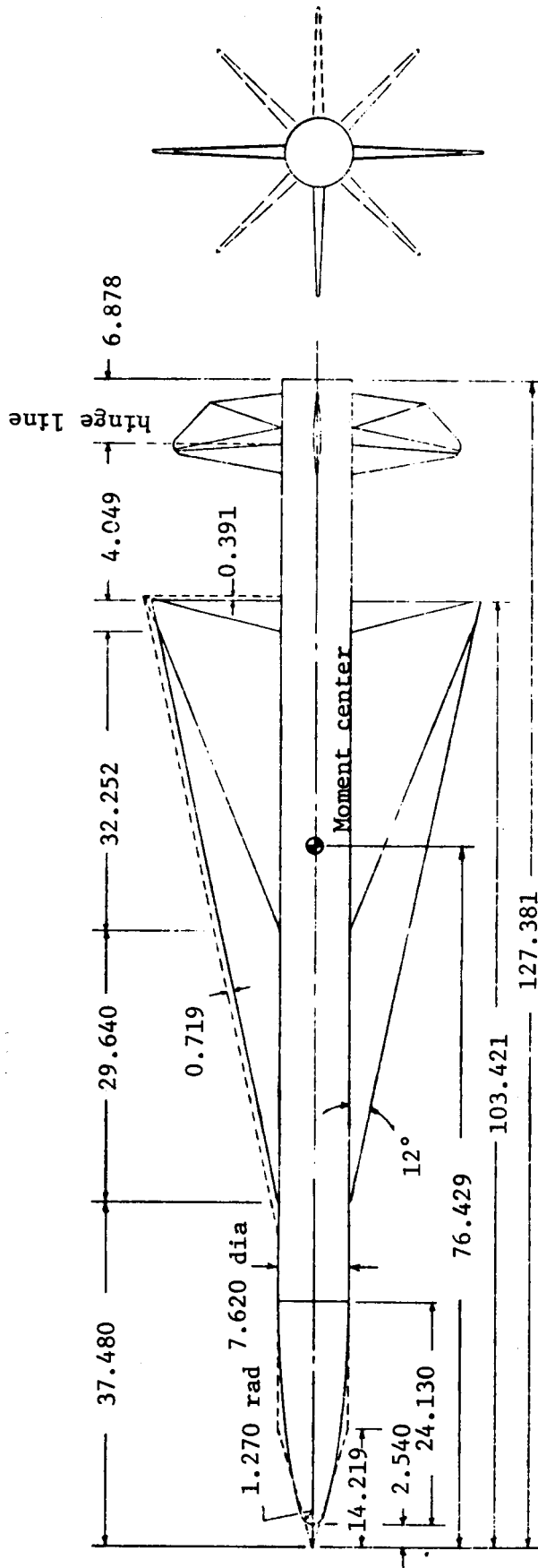


Figure 34. - Model drawings. Linear dimensions are in centimeters.

Ref. TM X-71984

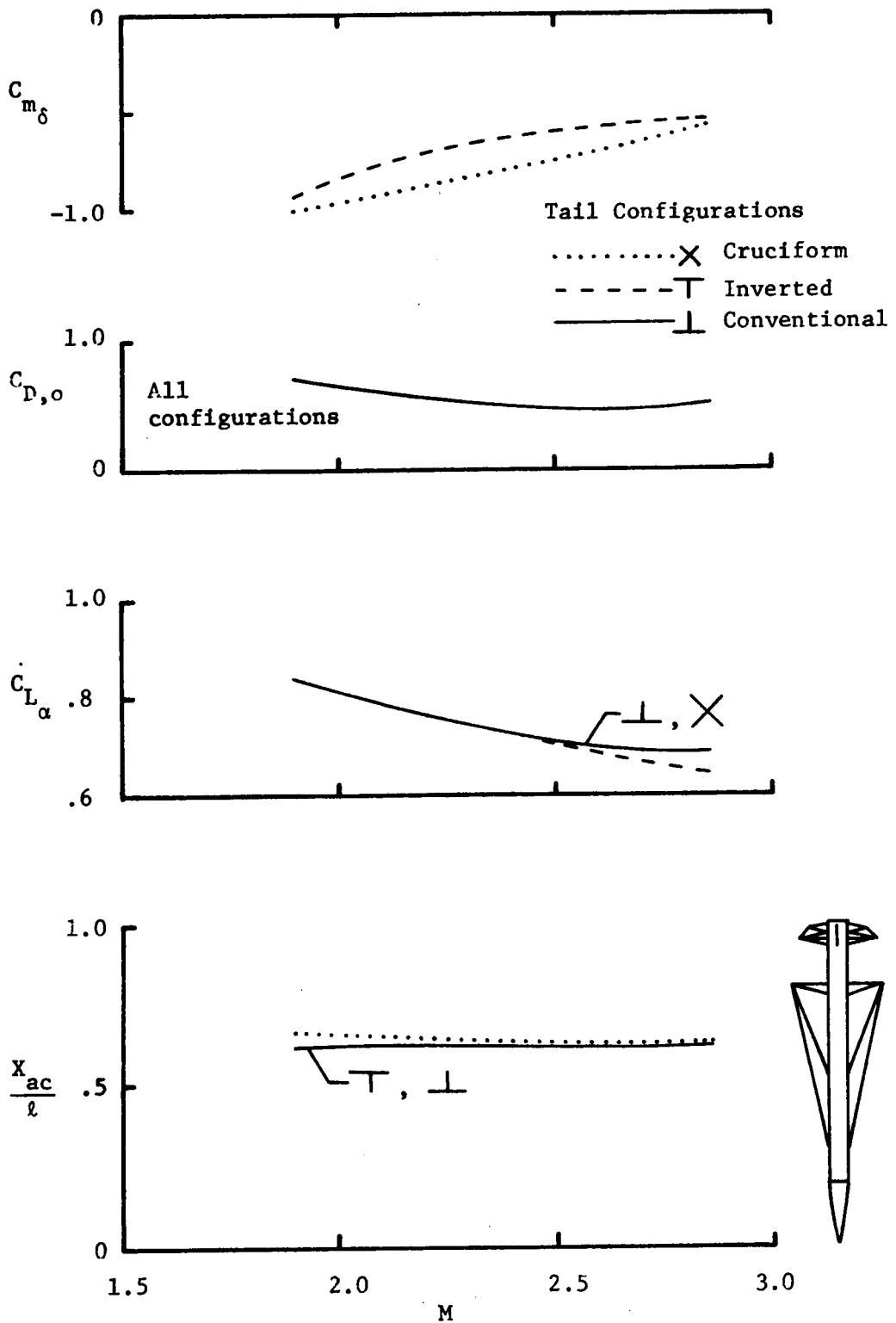


Figure 35. - Variation of longitudinal parameters with Mach number; $\alpha=0^\circ$.

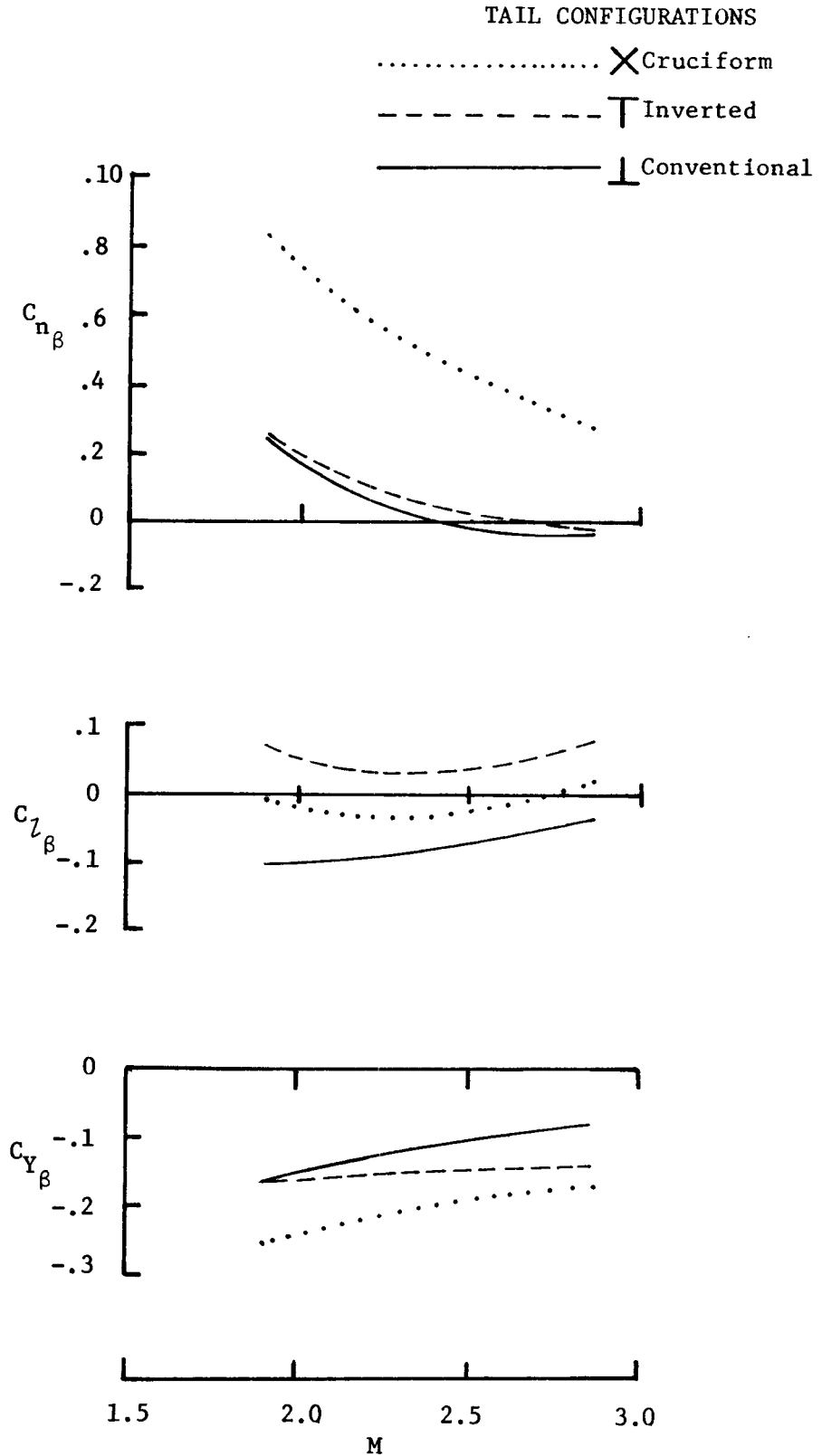


Figure 36. - Variation of sideslip derivatives with Mach number; $\alpha=0^\circ$.

TAIL CONFIGURATIONS

- X Cruciform
- T Inverted
- _____ ⊥ Conventional

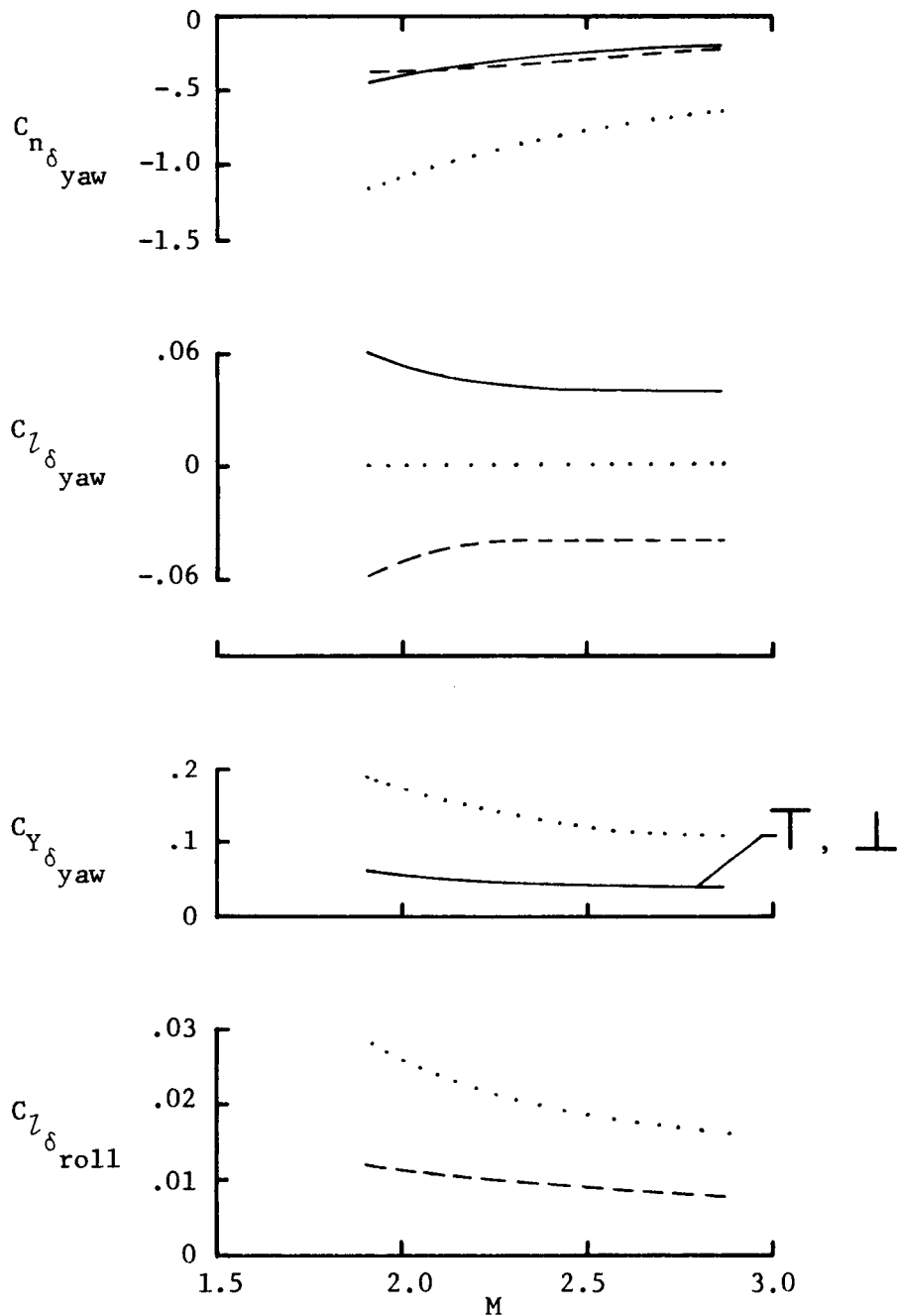


Figure 37. - Directional and lateral control effectiveness; $\alpha=0^\circ$.

SURFACE-TO-AIR MISSILES (SAM)

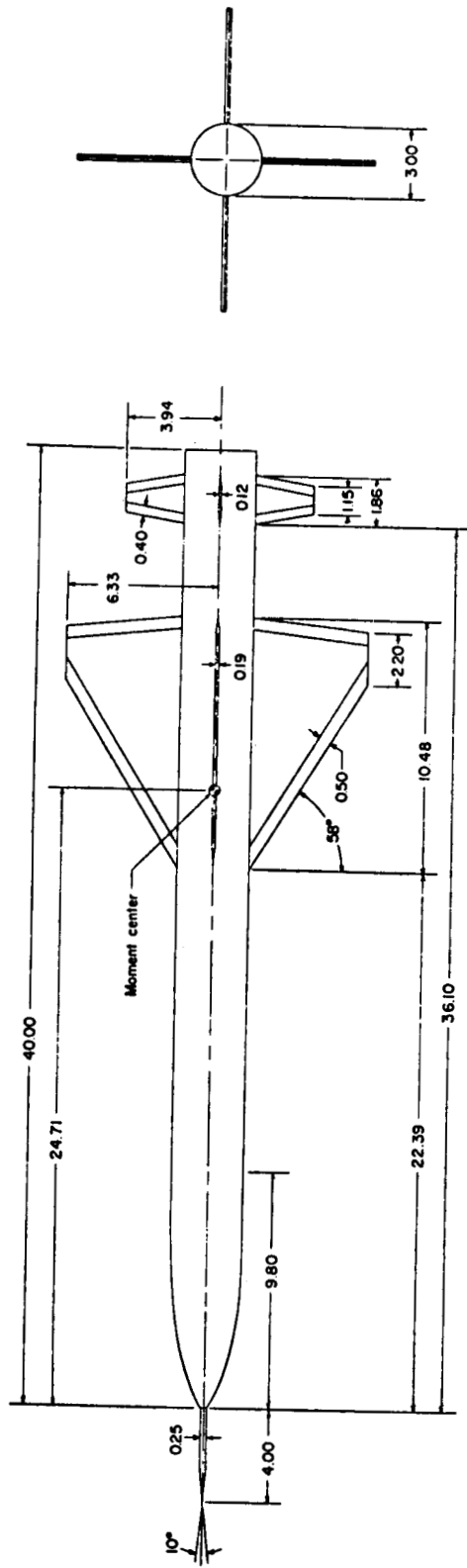


Figure 38. - Details of model. (All linear dimensions are in inches.)

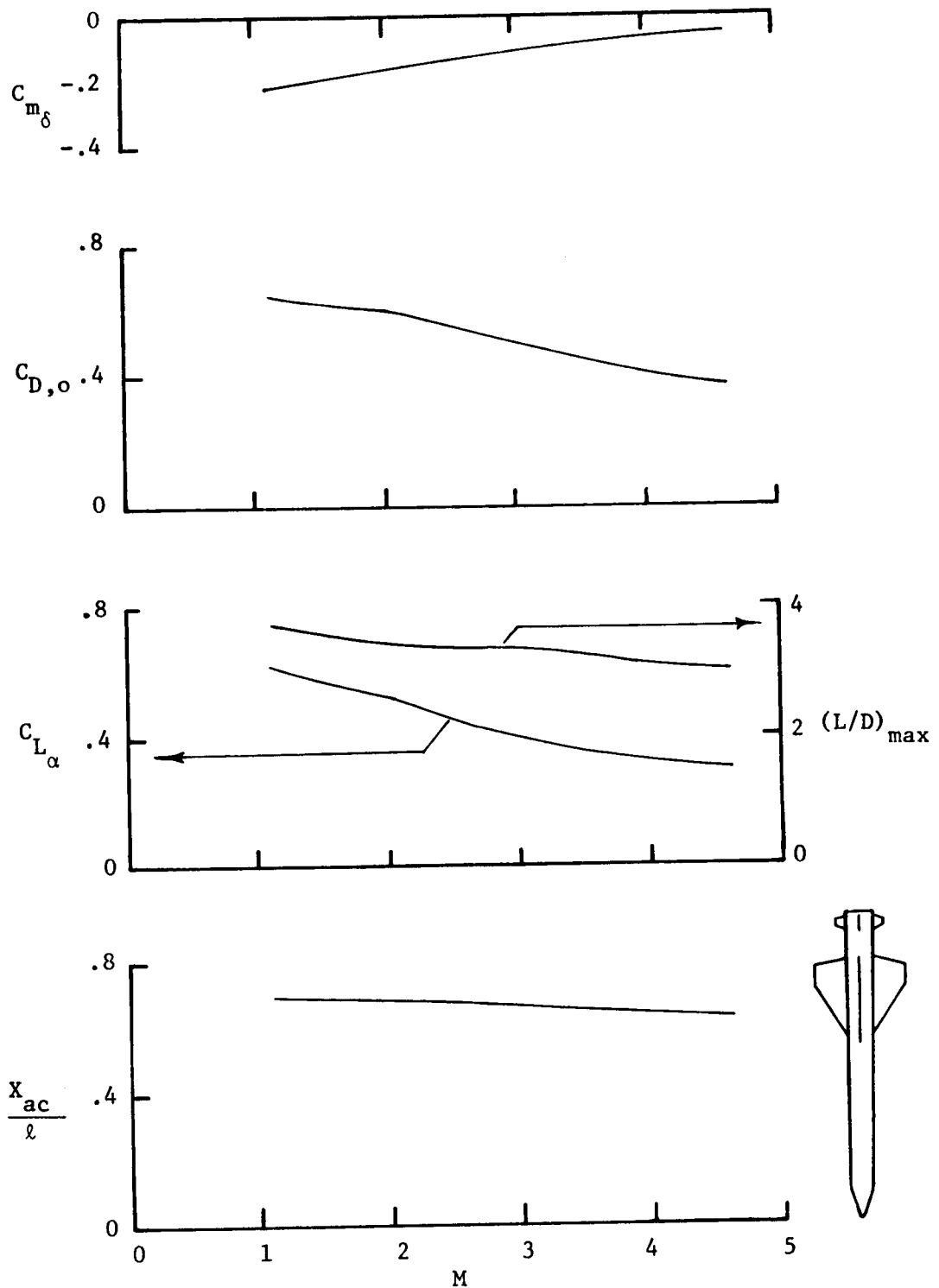


Figure 39. - Variation of longitudinal parameters with Mach number; $\alpha=0^\circ$.

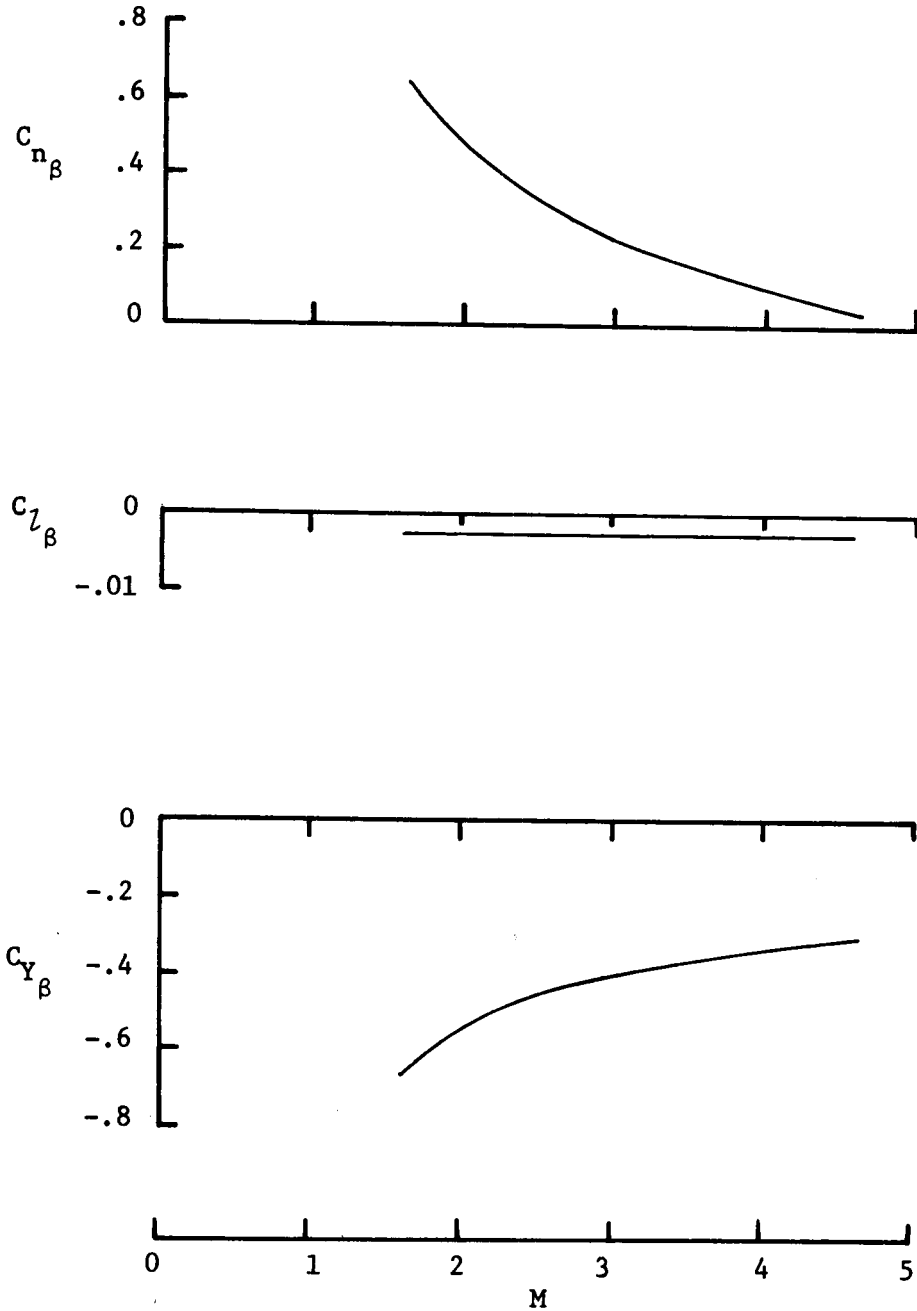


Figure 40. - Variation of sideslip derivatives with Mach number; $\alpha=0^\circ$.

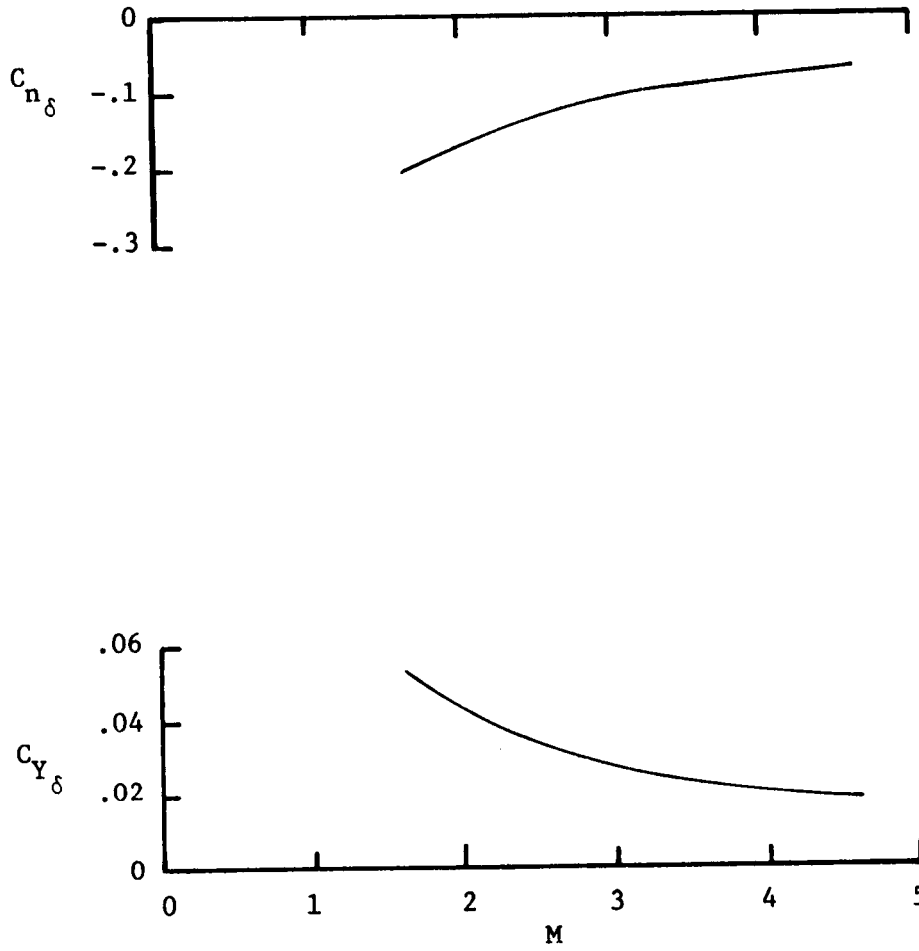


Figure 41. - Directional control effectiveness; $\alpha \approx 0^\circ$.

Ref. TM X-1025

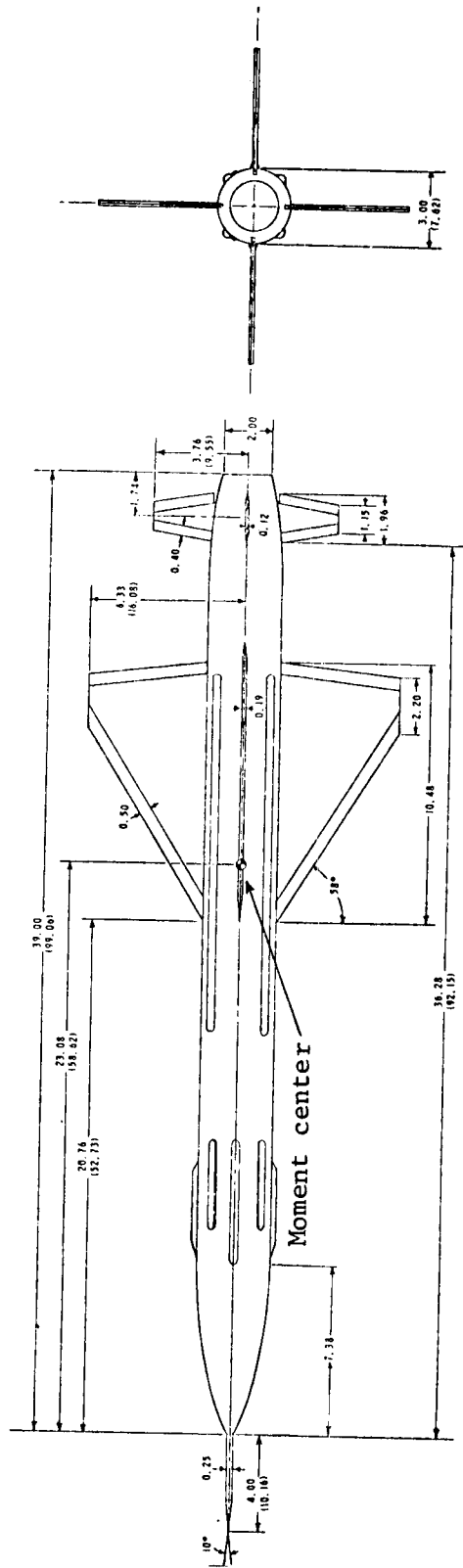


Figure 42. - Details of model. (All linear dimensions are given in inches and parenthetically in centimeters. Because of space limitations, conversions to the International System of units are presented for only a few representative dimensions.)

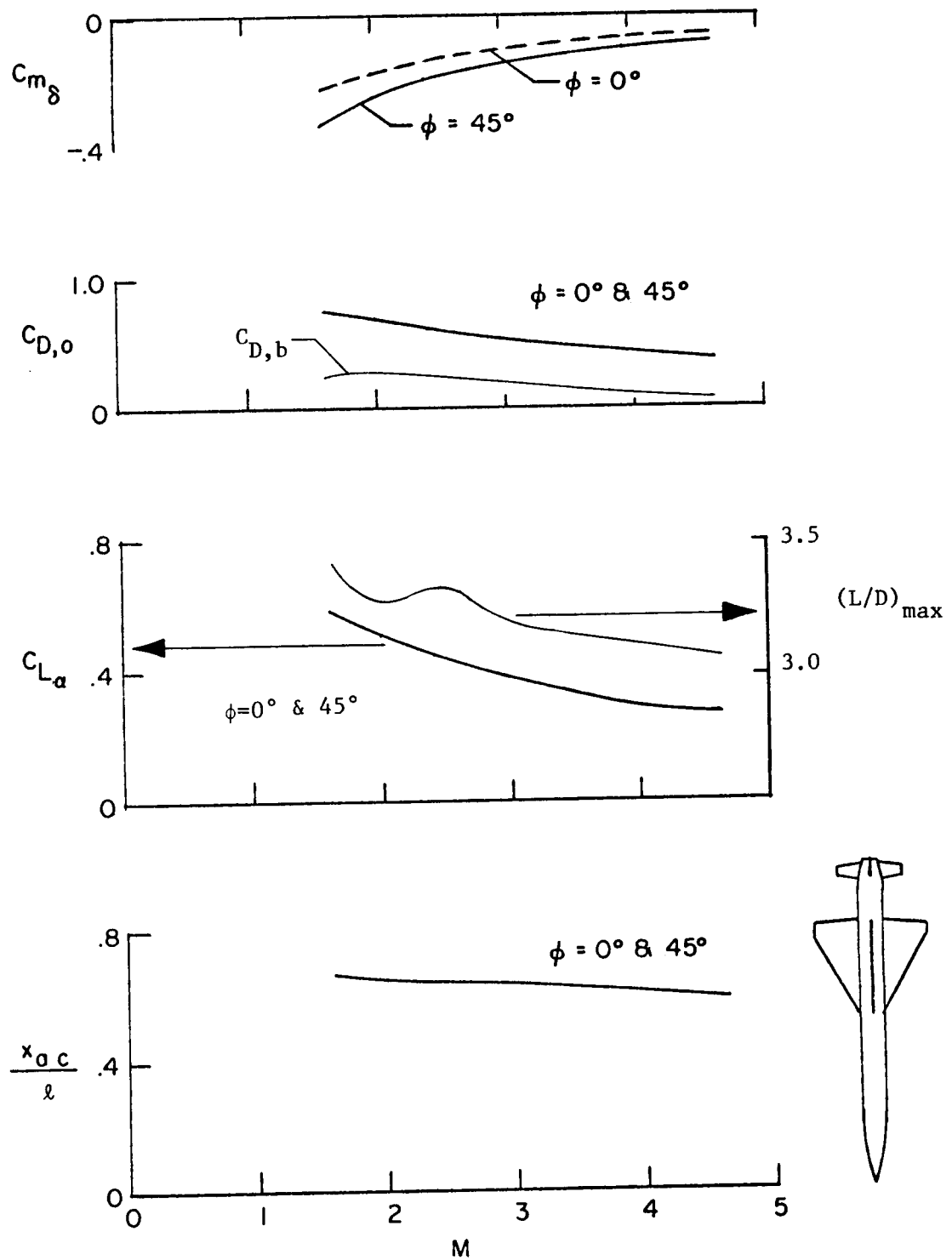


Figure 43. - Variation of longitudinal parameters with Mach number; $\alpha=0$.

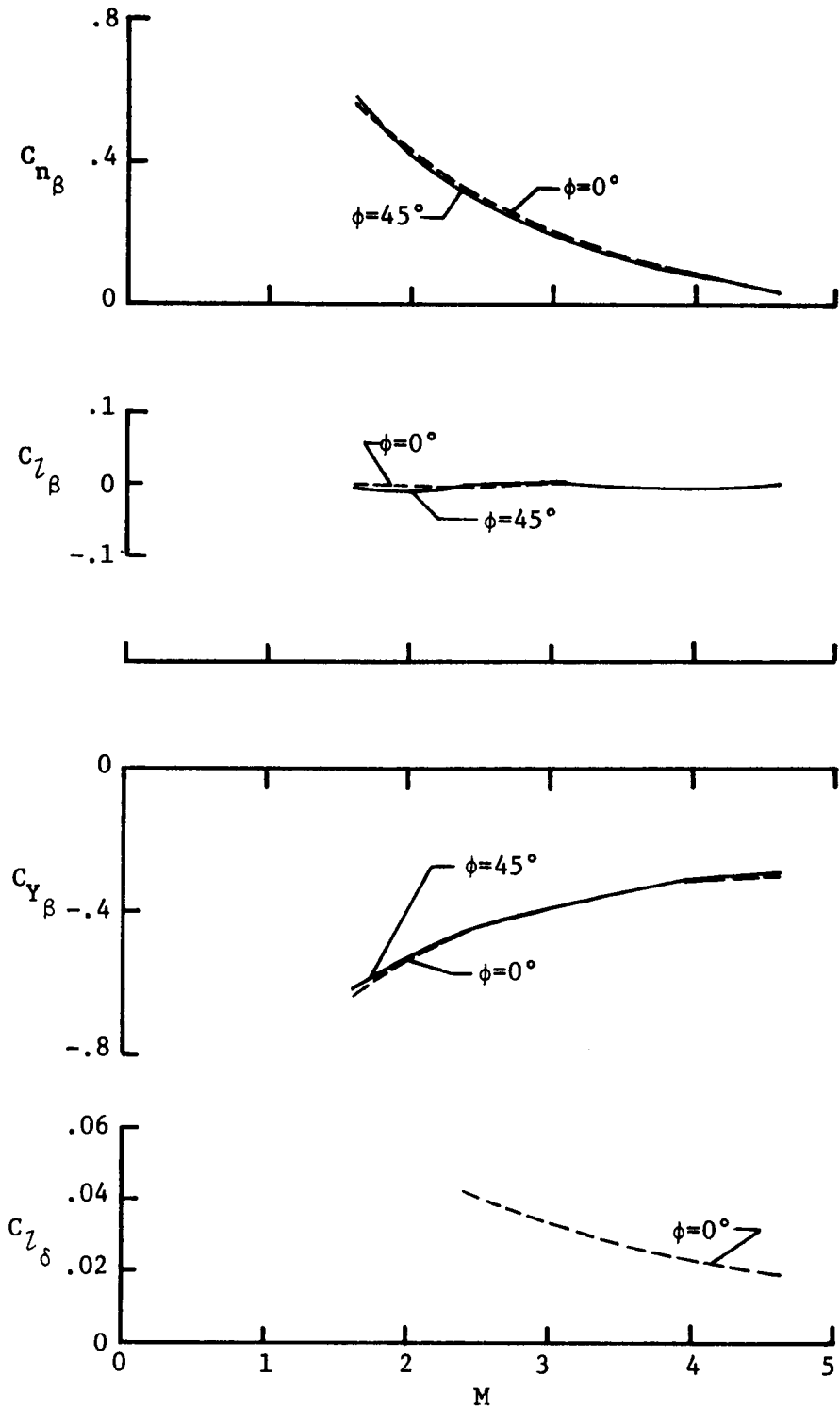


Figure 44. - Variation of sideslip derivatives and roll control effectiveness with Mach number; $\alpha=0^\circ$.

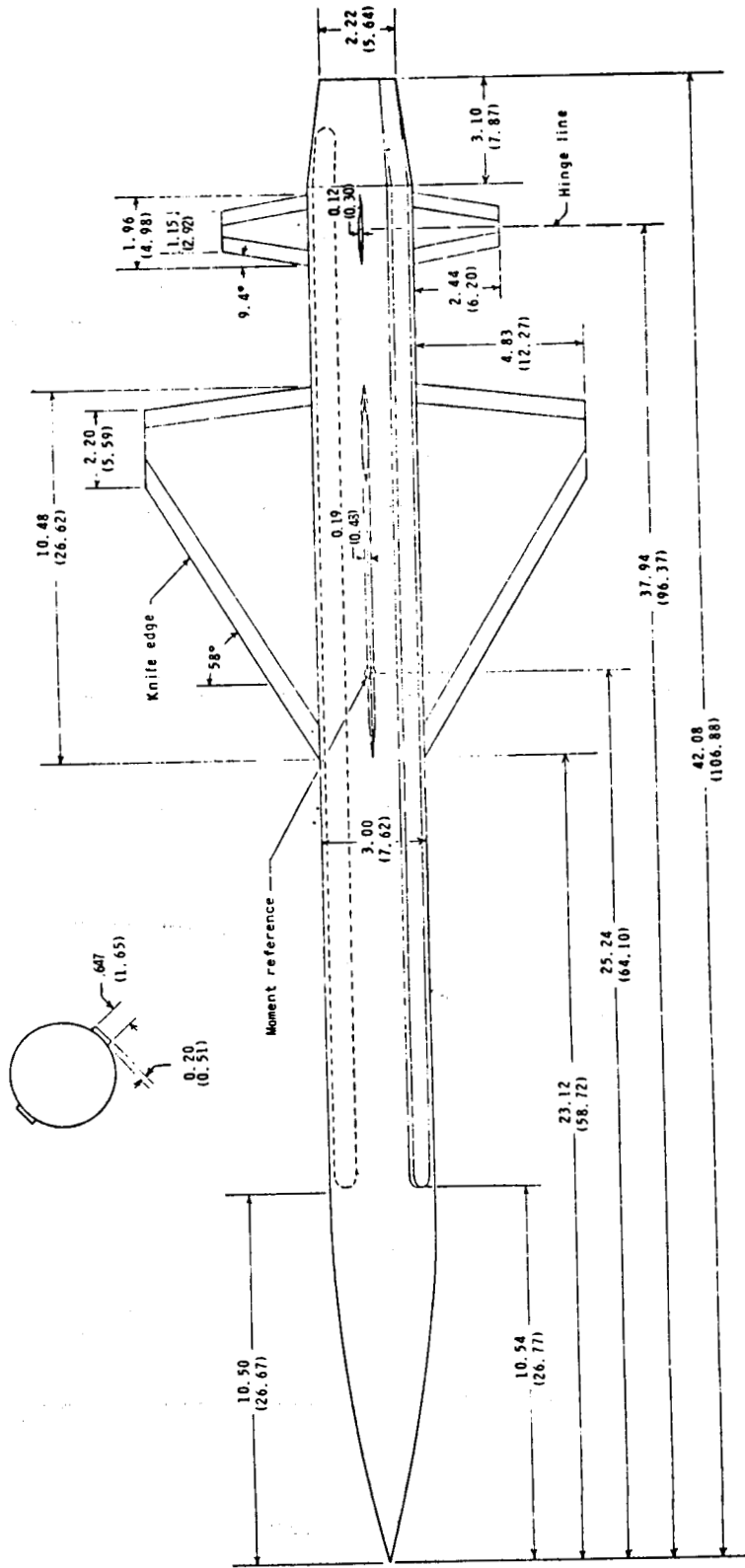


Figure 45. - Model details. Dimensions are in inches and parenthetically in centimeters.

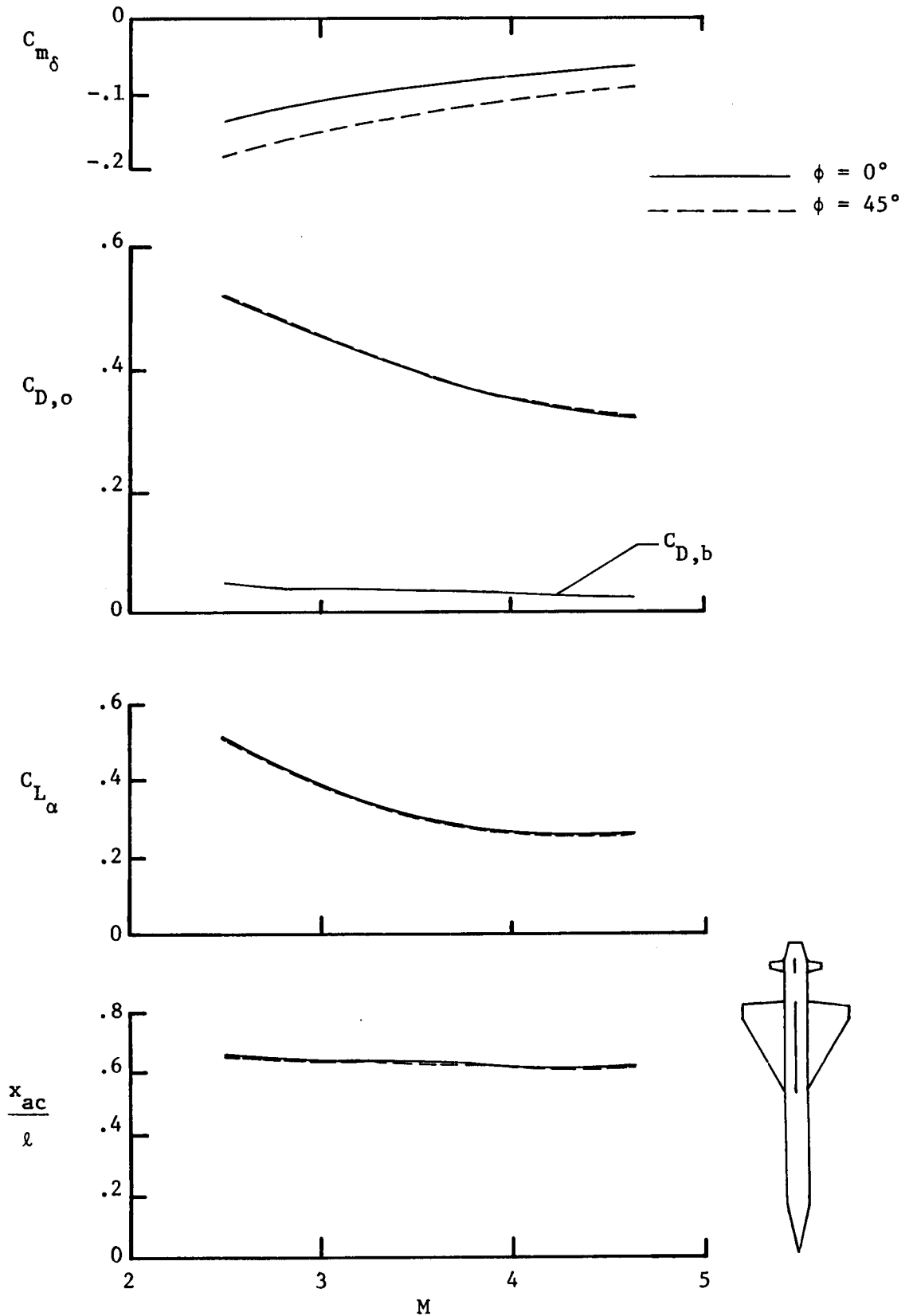
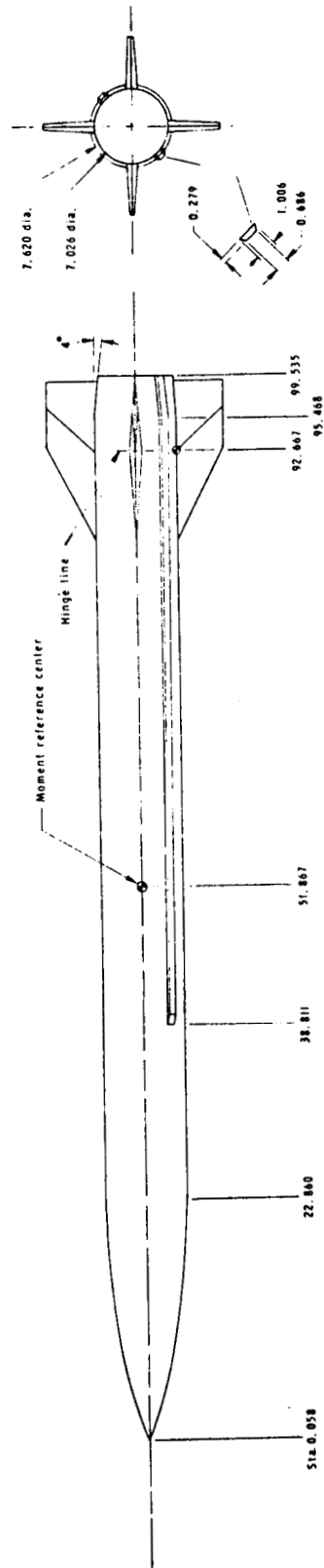


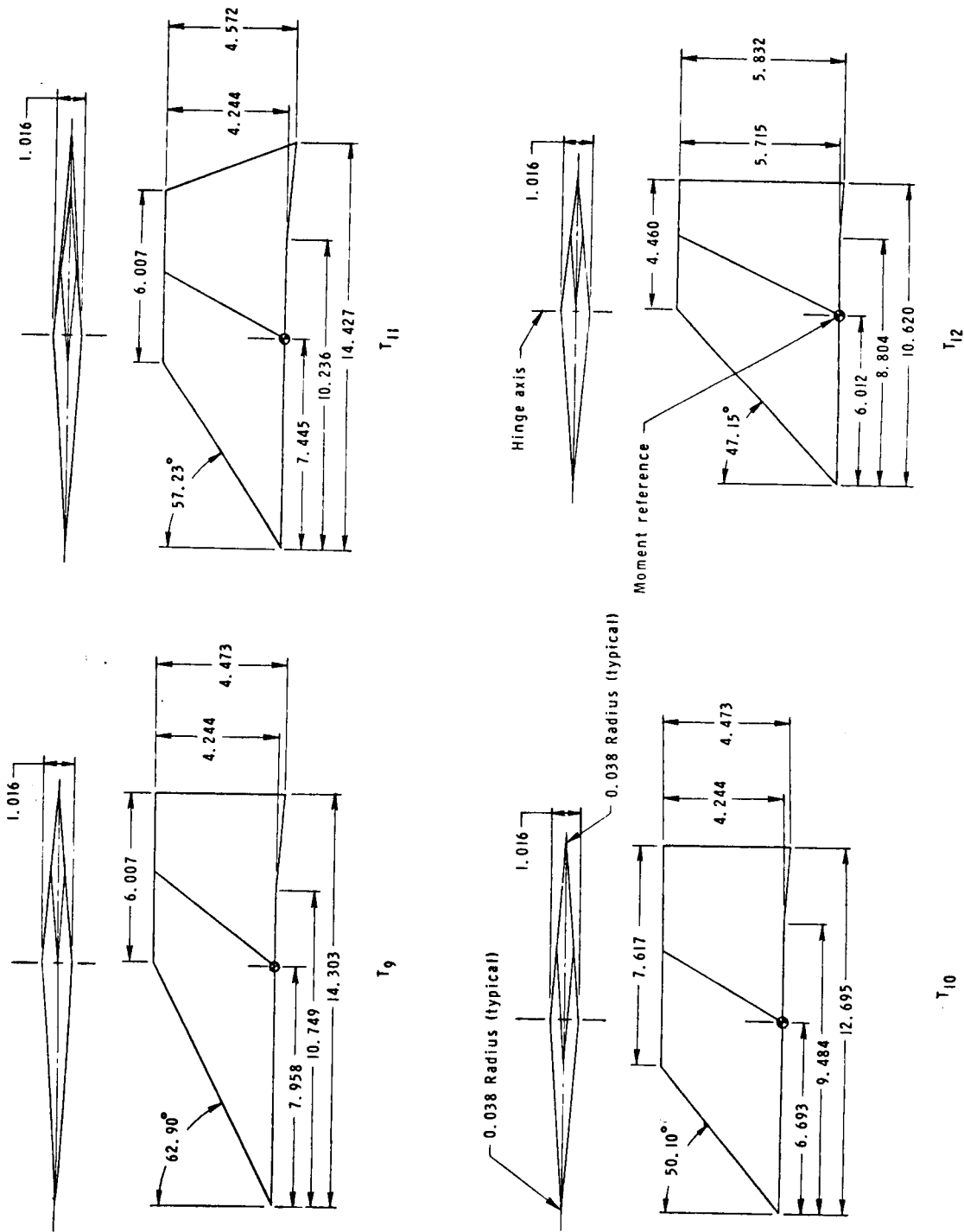
Figure 46. - Variation of longitudinal parameters with Mach number; $\alpha \approx 0^\circ$.



(a) Model details.

Figure 47. - Drawing of model. All dimensions are in centimeters unless otherwise noted.

Ref. TM X-2774



(b) Fin details.

Figure 47. - Concluded.

$\phi = 0^\circ$

$\phi = 45^\circ$

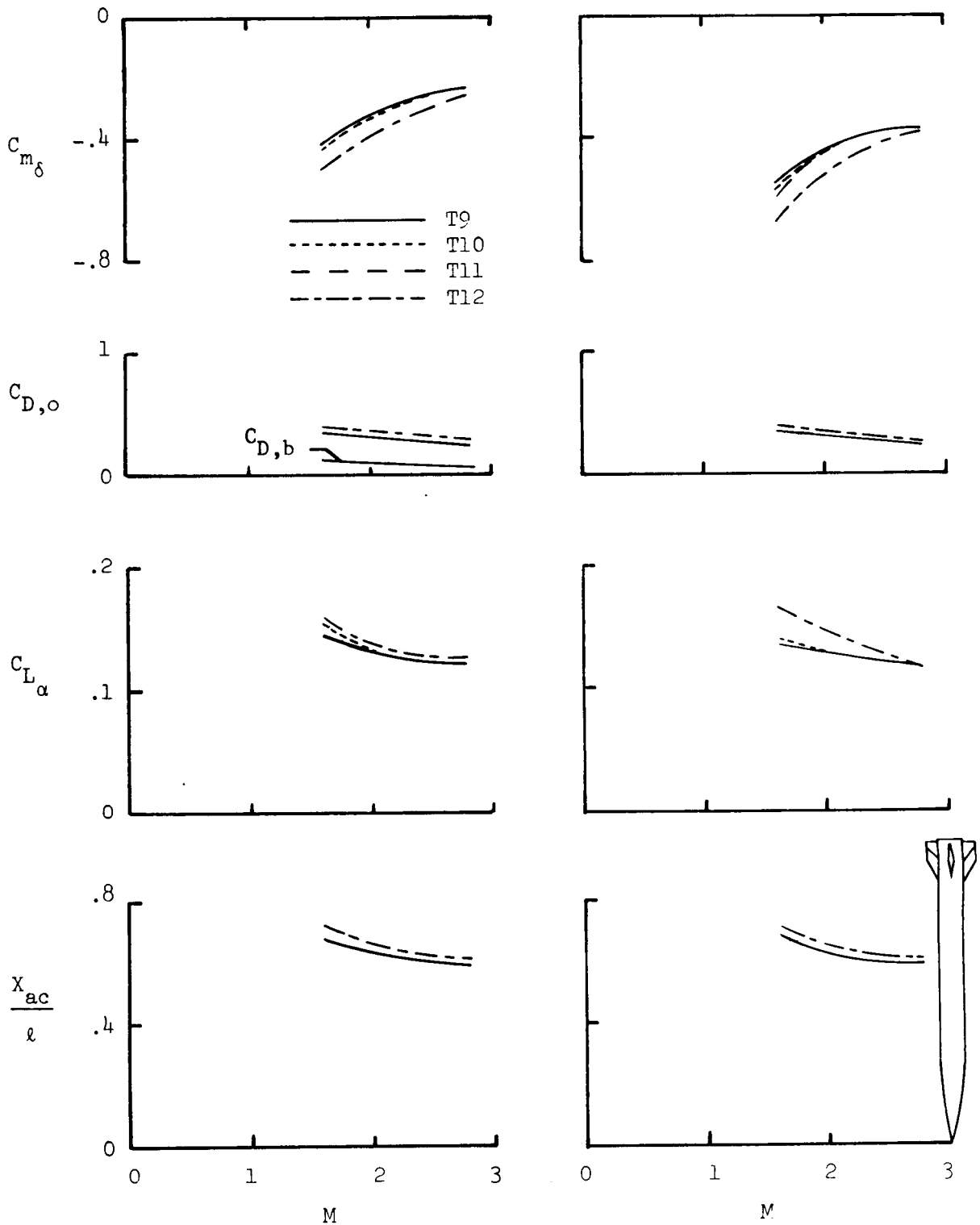


Figure 48. - Variation of longitudinal parameters with Mach number; $\alpha = 0^\circ$.

AIR-TO-SURFACE MISSILES (ASM)

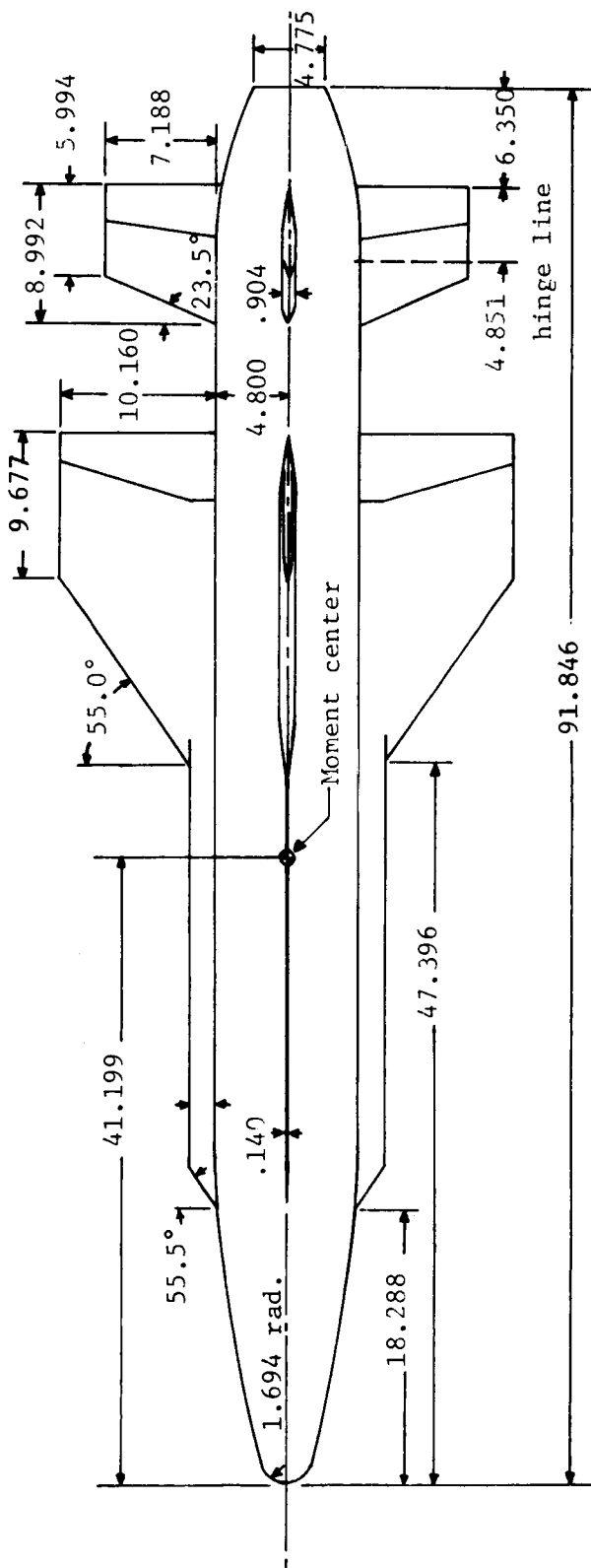


Figure 49. - Model details. (All dimensions are in centimeters.)

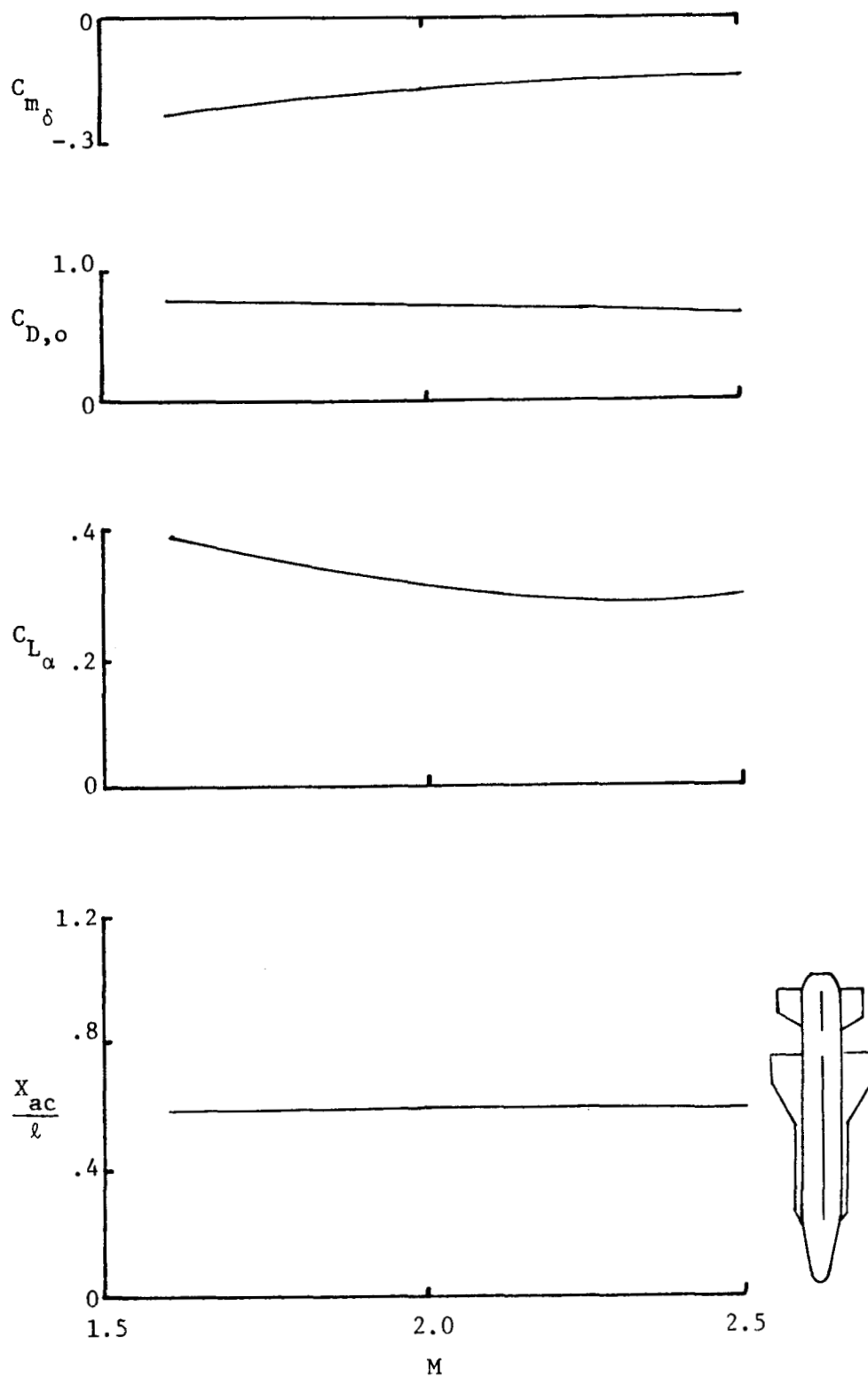


Figure 50. - Variation of longitudinal parameters with Mach number; $\alpha \approx 0^\circ$.

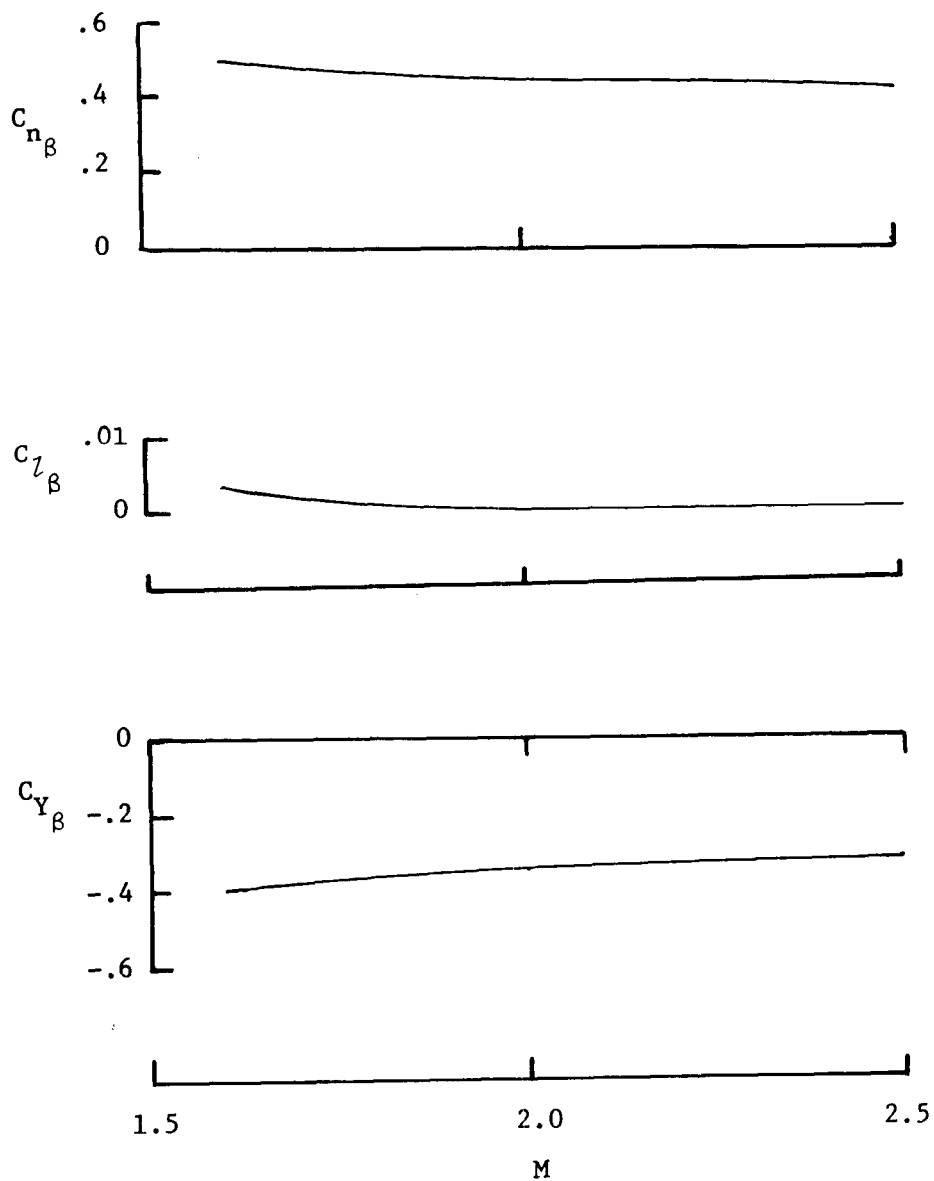


Figure 51. - Variation of sideslip derivatives with Mach number; $\alpha=0^\circ$

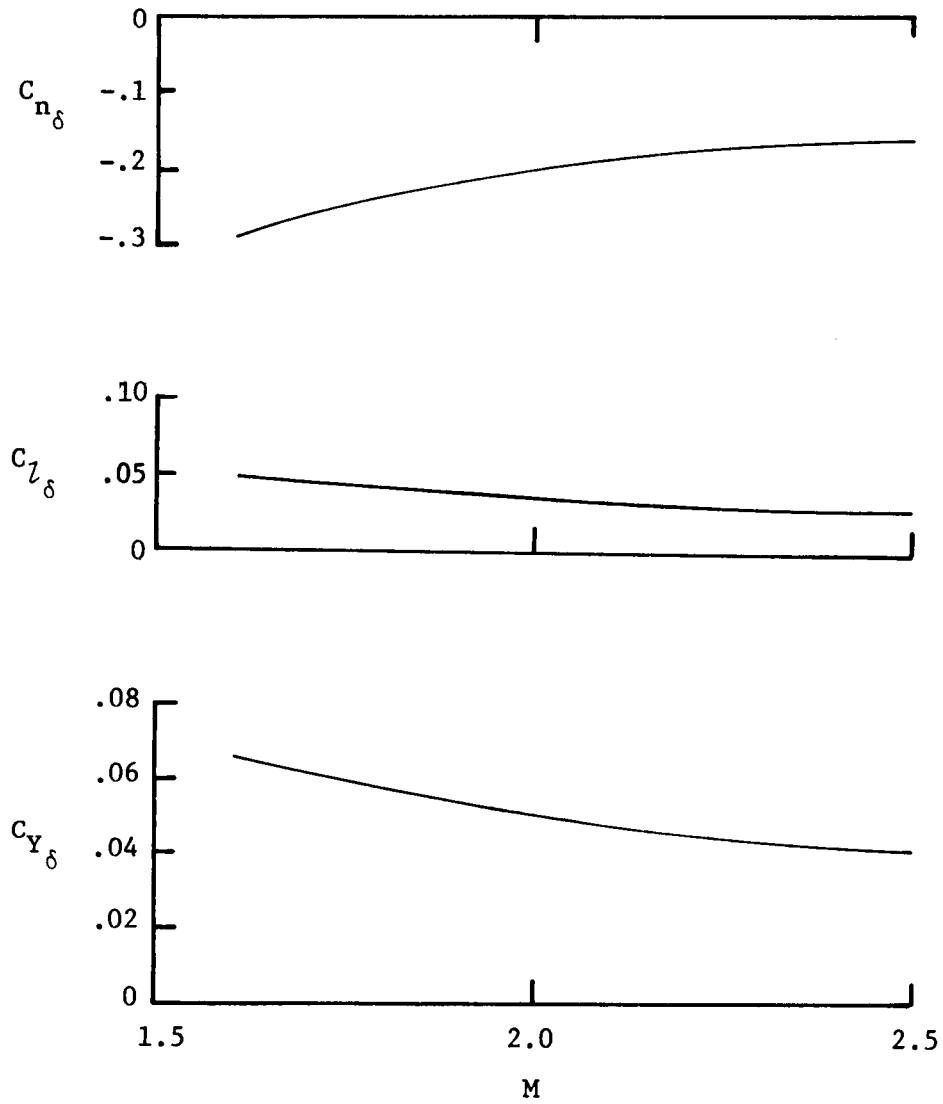


Figure 52. - Directional and lateral control effectiveness; $\alpha=0^\circ$.

Ref. TM X-1112

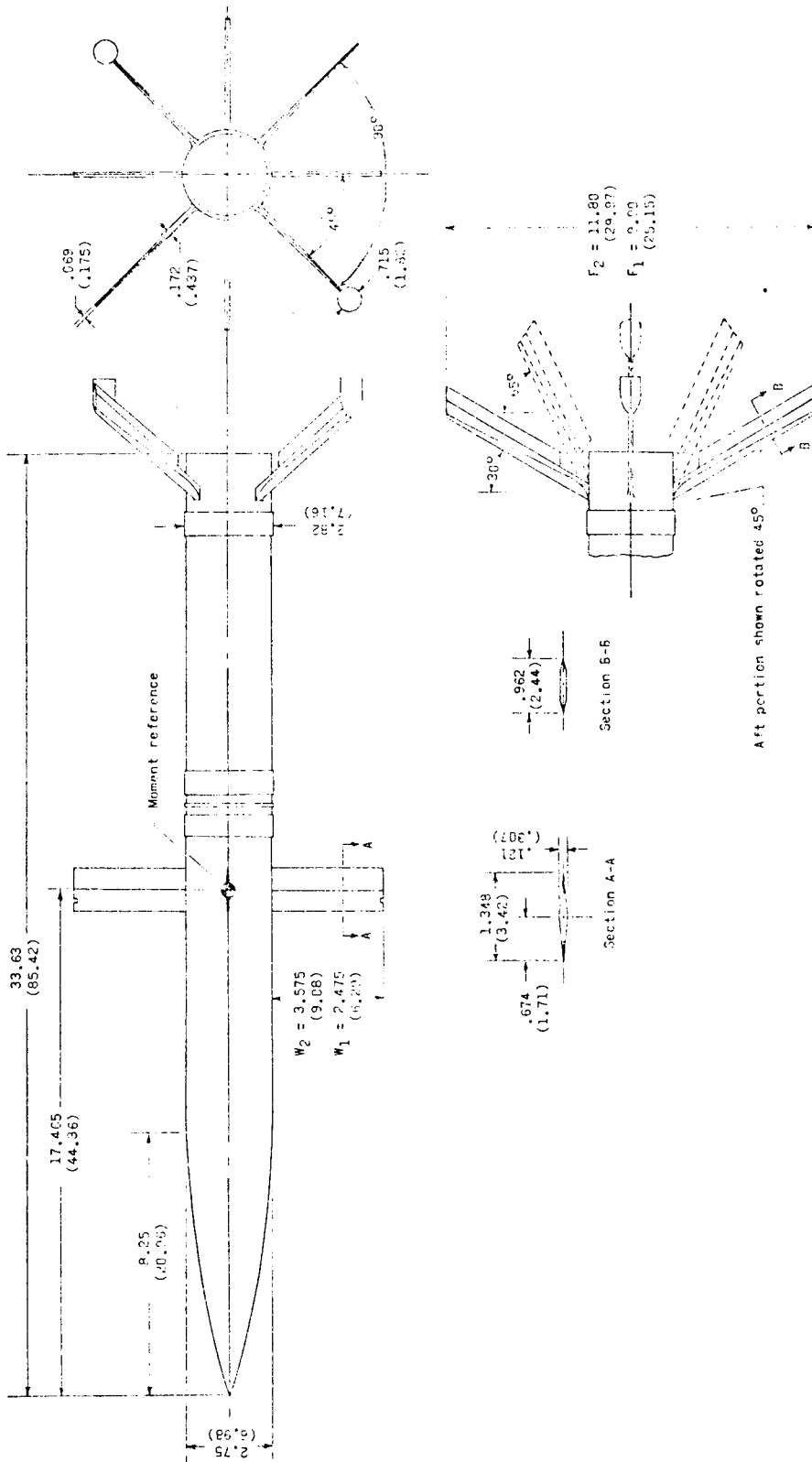


Figure 53. - Details of the model. Dimensions are in inches (centimeters) unless otherwise noted.

Ref. TM X-1491

TABLE 6. - LONGITUDINAL PARAMETERS; $\alpha \approx 0^\circ$.

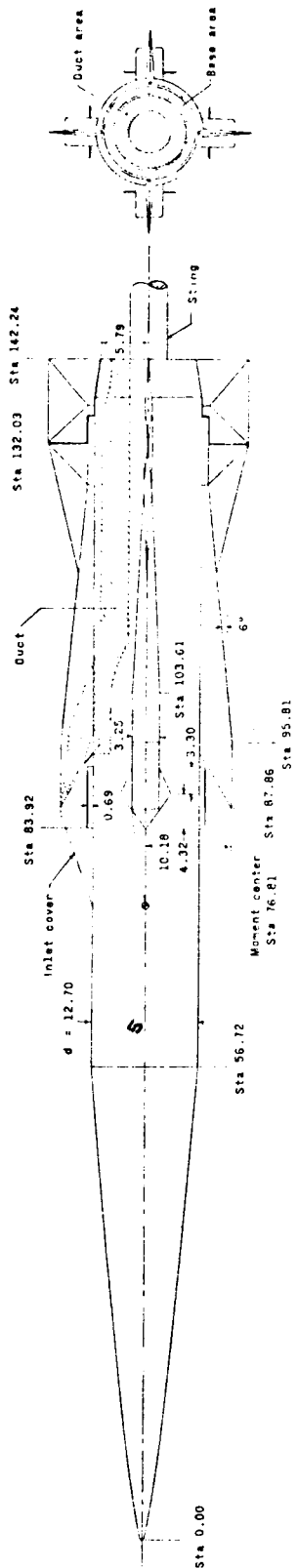
Mach Number 1.6

Config- uration	Fin Sweep	$C_{m\delta}$		$C_{D,o}$		$C_{L\alpha}$		X_{ac}/ℓ	
		$\phi=0^\circ$	$\phi=45^\circ$	$\phi=0^\circ$	$\phi=45^\circ$	$\phi=0^\circ$	$\phi=45^\circ$	$\phi=0^\circ$	$\phi=45^\circ$
BF ₁	65°	—	—	.380	—	.083	—	.617	.697
BF ₂	65°	—	—	.400	.398	.104	.108	.684	.697
BF ₂	30°	—	—	.565	.560	.114	.114	.702	.720
BF ₂ W ₂	30°	-.012	-.016	.688	.690	.218	.227	.619	.619
BF ₁ W ₁	30°	-.012	-.016	.610	.590	.174	.185	.606	.603

Mach Number 2.0

Config- uration	Fin Sweep	$C_{m\delta}$		$C_{D,o}$		$C_{L\alpha}$		X_{ac}/ℓ	
		$\phi=0^\circ$	$\phi=45^\circ$	$\phi=0^\circ$	$\phi=45^\circ$	$\phi=0^\circ$	$\phi=45^\circ$	$\phi=0^\circ$	$\phi=45^\circ$
BF ₁	65°	—	—	.36	.368	.075	.083	.581	.549
BF ₂	65°	—	—	.38	.38	.100	.107	.630	.622
BF ₂	30°	—	—	.508	.509	.110	.106	.683	.694
BF ₂ W ₂	30°	0	.01	.628	.628	.194	.239	.609	.612
BF ₁ W ₁	30°	-.012	0	.542	.54	.161	.156	.590	.598

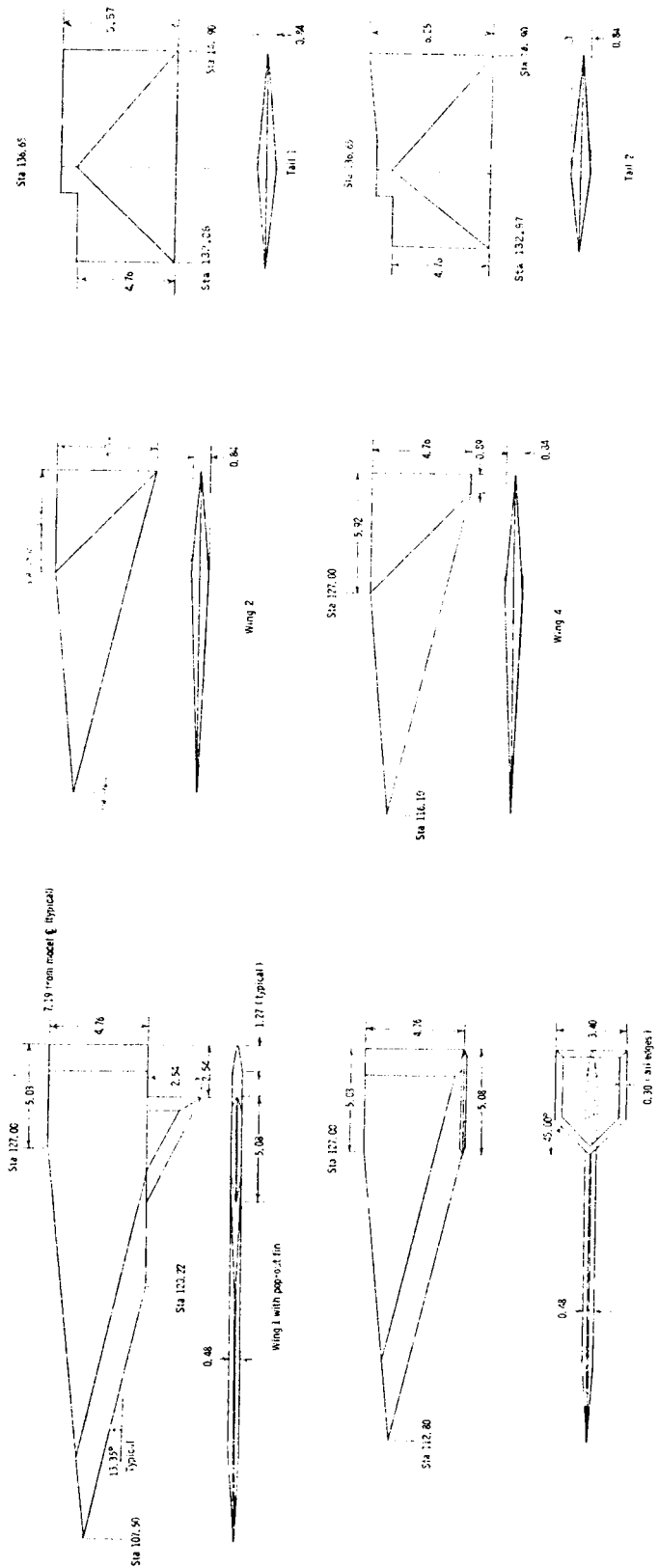
Ref. TM X-1491



(a) Basic model W_2I_1 .

Figure 54. - Model details. (All linear dimensions are in centimeters.)

Ref. TM X-1492



(b) Wings and tails.

Figure 54. - Concluded

Ref. TM X-1492

TABLE 7. - LONGITUDINAL PARAMETERS AT MACH NUMBER 2.5
WITH INLETS COVERED; $\alpha=0^\circ$.

$\phi = 0^\circ$

CONFIGURATION	C_{m_δ}	$C_{D,o}$	C_{L_α}	$\frac{x_{ac}}{l}$
Wing 1, Tail 1	-0.0829	0.247	0.155	0.611
Wing 1, Tail 1, Pop-out Fin	-0.0859	0.255	0.159	0.628
Wing 2, Tail 1	-0.0933	0.245	0.124	0.581
Wing 3, Tail 1	-0.0773	0.242	0.125	0.602
Wing 3, Tail 1, End Plate	-0.0762	0.255	0.148	0.622
Wing 4, Tail 2	-0.0821	0.240	0.129	0.574

$\phi = 45^\circ$

CONFIGURATION	C_{m_δ}	$C_{D,o}$	C_{L_α}	$\frac{x_{ac}}{l}$
Wing 1, Tail 1	-0.1176	0.250	0.146	0.603
Wing 1, Tail 1, Pop-out Fin	-0.1165	0.257	0.154	0.624
Wing 2, Tail 1	-0.1262	0.247	0.122	0.574
Wing 3, Tail 1	-0.1198	0.247	0.135	0.584
Wing 3, Tail 1, End Plate	-0.1142	0.256	0.150	0.614
Wing 4, Tail 2	-0.1128	0.243	0.128	0.563

TABLE 8. - SIDESLIP DERIVATIVES AND ROLL CONTROL EFFECTIVENESS
 AT MACH NUMBER 2.5 WITH INLETS COVERED: $\alpha = 0^\circ$.

$\phi = 0^\circ$

Configuration	C_{n_β}	C_{l_β}	C_{Y_β}	$C_{l_\delta}^*$ roll
Wing 1, Tail 1	.1008	0	-.147	—
Wing 1, Tail 1, Popout Fin	.1568	0	-.163	.0118
Wing 2, Tail 1	.0560	0	-.137	.0127
Wing 3, Tail 1, End Plate	.1344	0	-.155	—

$\phi = 45^\circ$

Configuration	C_{n_β}	C_{l_β}	C_{Y_β}	$C_{l_\delta}^\dagger$ roll
Wing 1, Tail 1	.0974	0	-.142	—
Wing 1, Tail 1, Popout Fin	.1456	0	-.152	.0235
Wing 2, Tail 1	.0482	0	-.125	.0252
Wing 3, Tail 1, End Plate	.1378	0	-.156	—
Wing 4, Tail 2	—	—	—	.0224

* Horizontal tails were deflected.

† All four tails were deflected.

Ref. TM X-1492

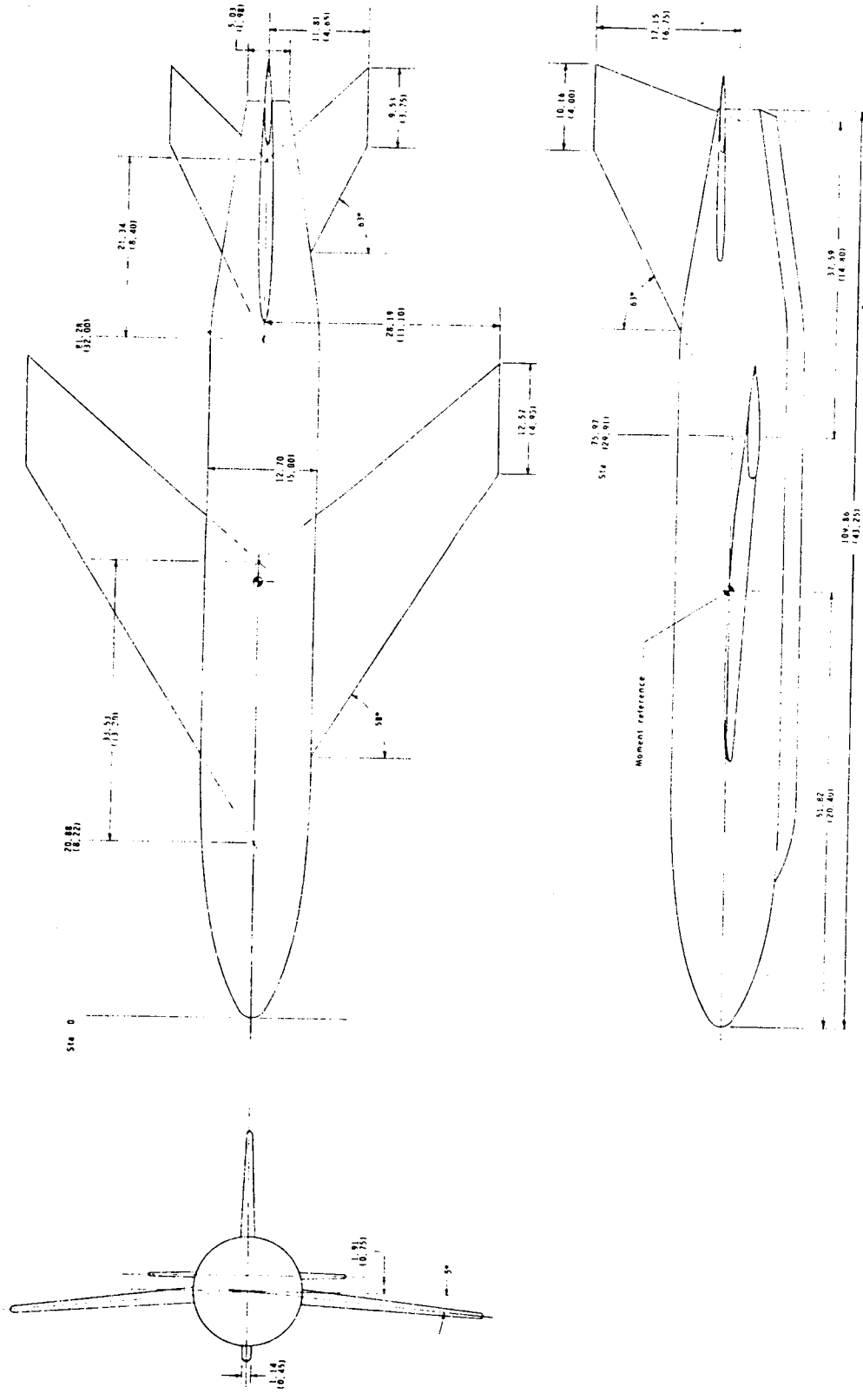


Figure 57. - Details of model. Linear dimensions are in centimeters (inches).

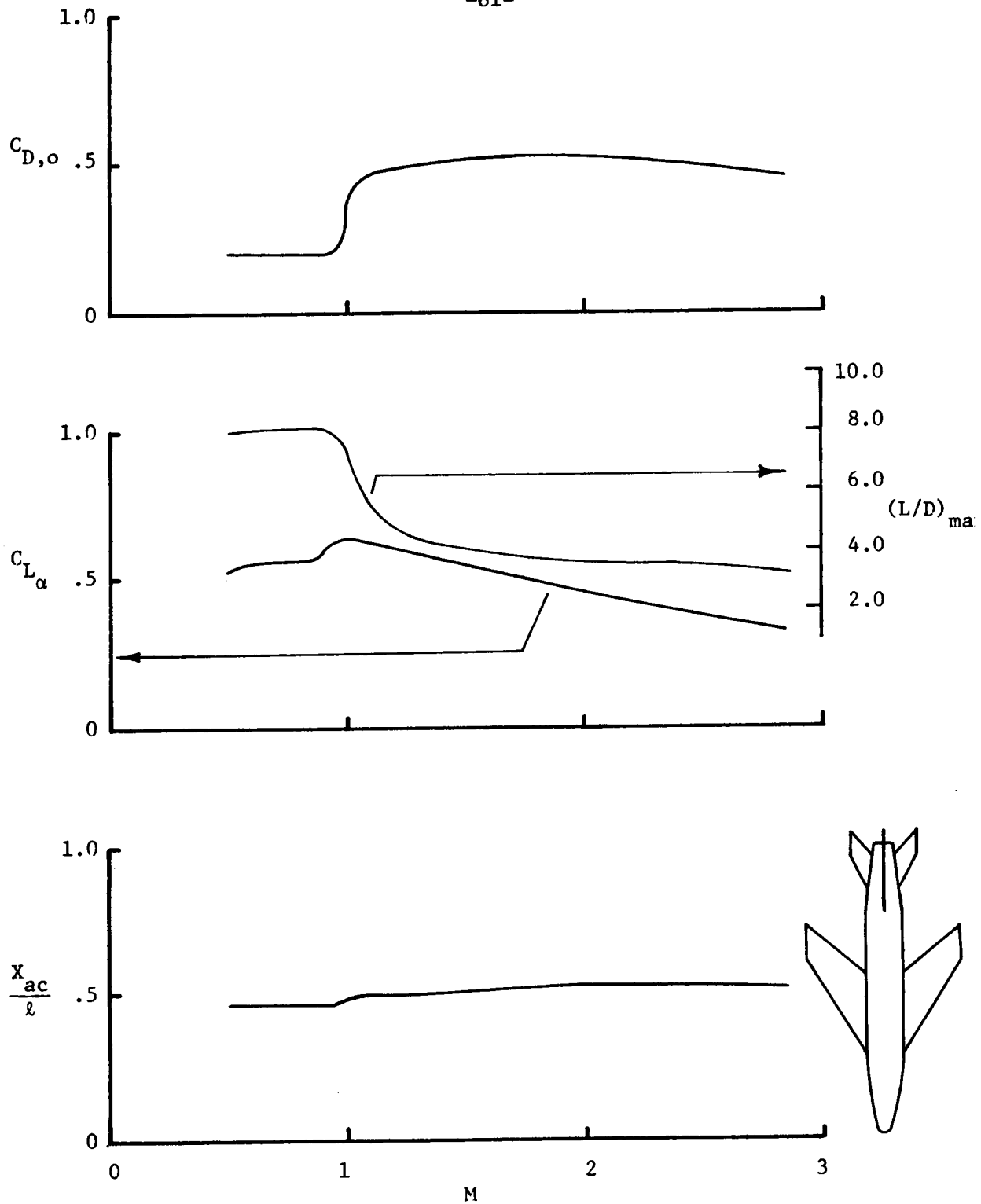


Figure 58. - Variation of longitudinal parameters with Mach number; $\alpha=0^\circ$.

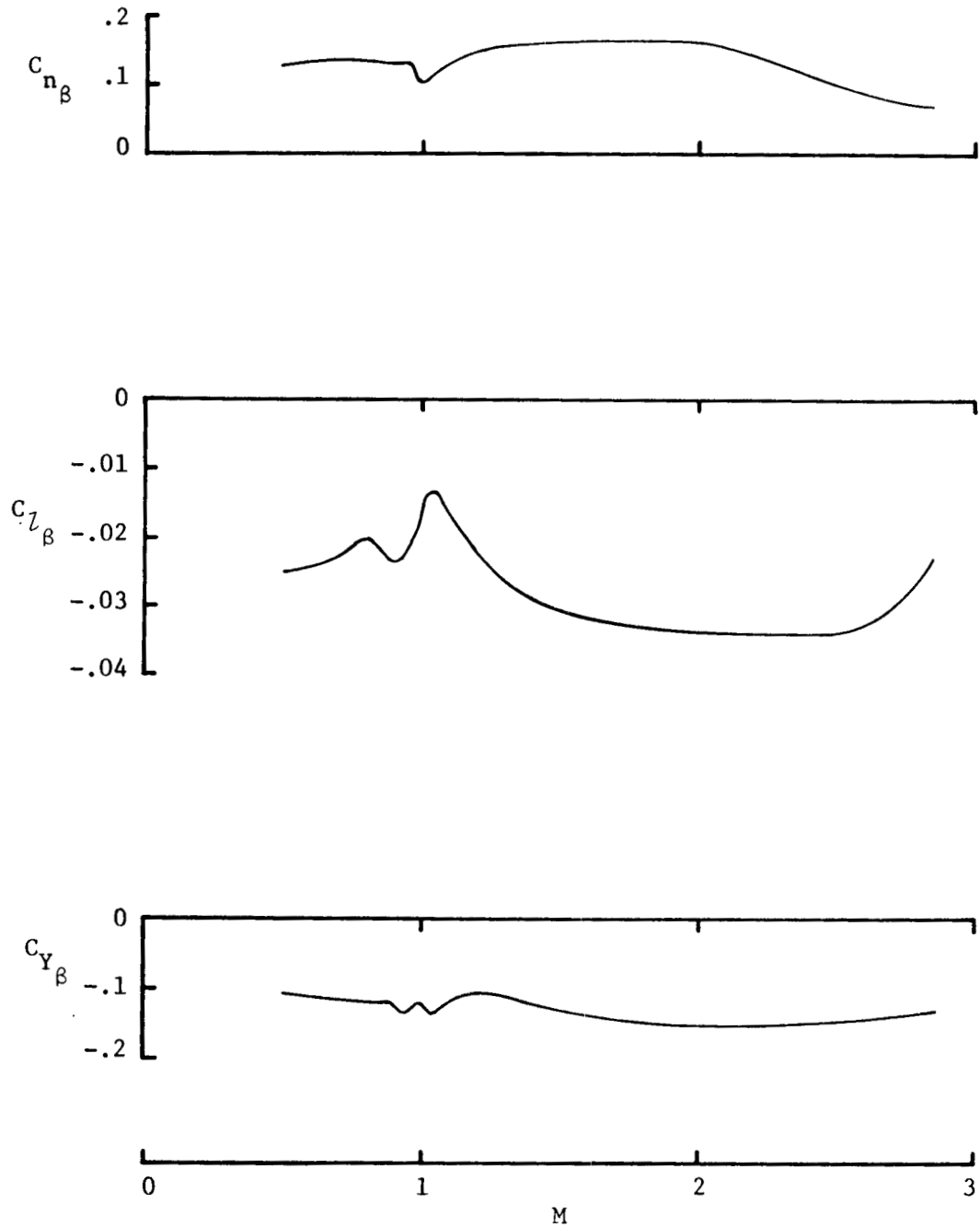


Figure 59. - Variation of sideslip derivatives with Mach number; $\alpha=0^\circ$.

Ref. TN D-7069

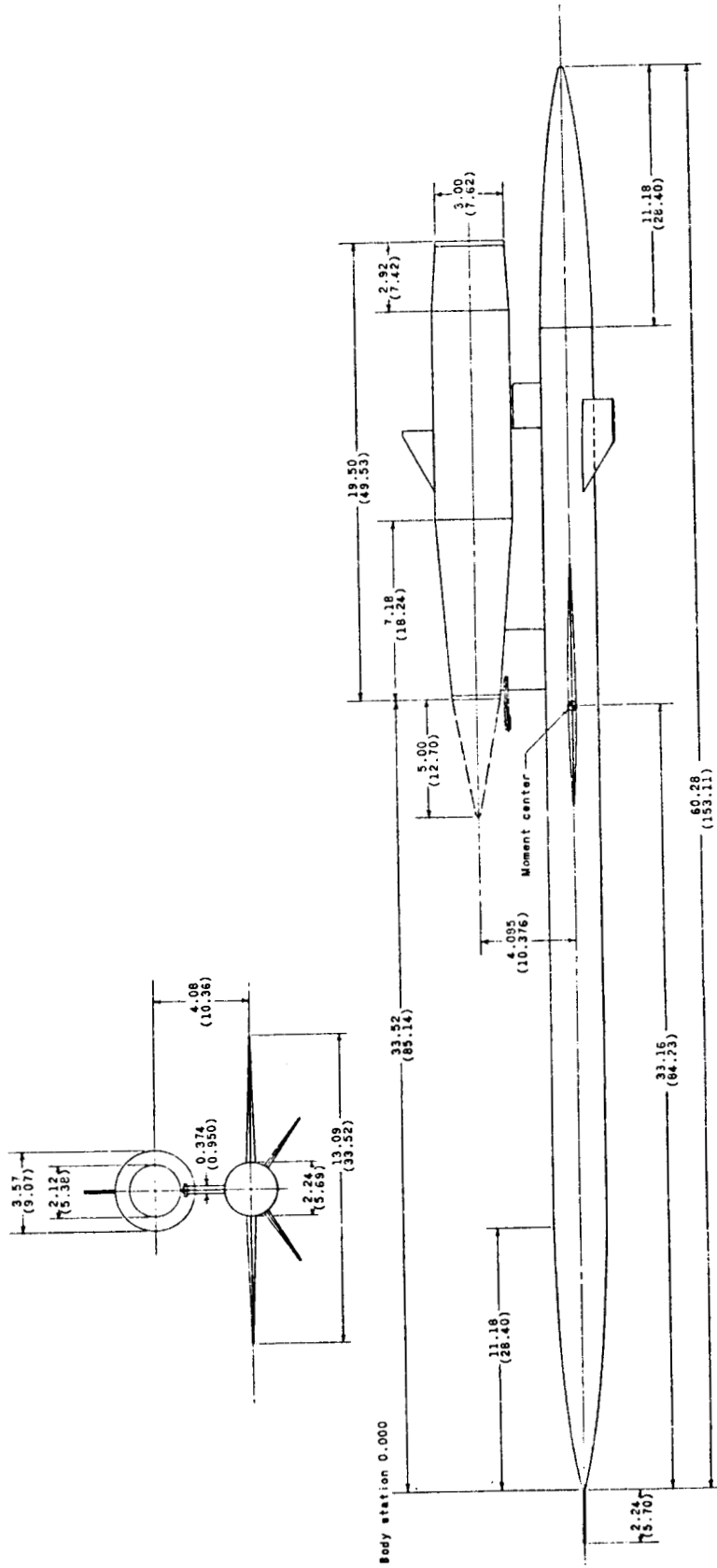


Figure 60. - Model details. (All dimensions are given in inches and parenthetically in centimeters.)

Ref. TM X-1304

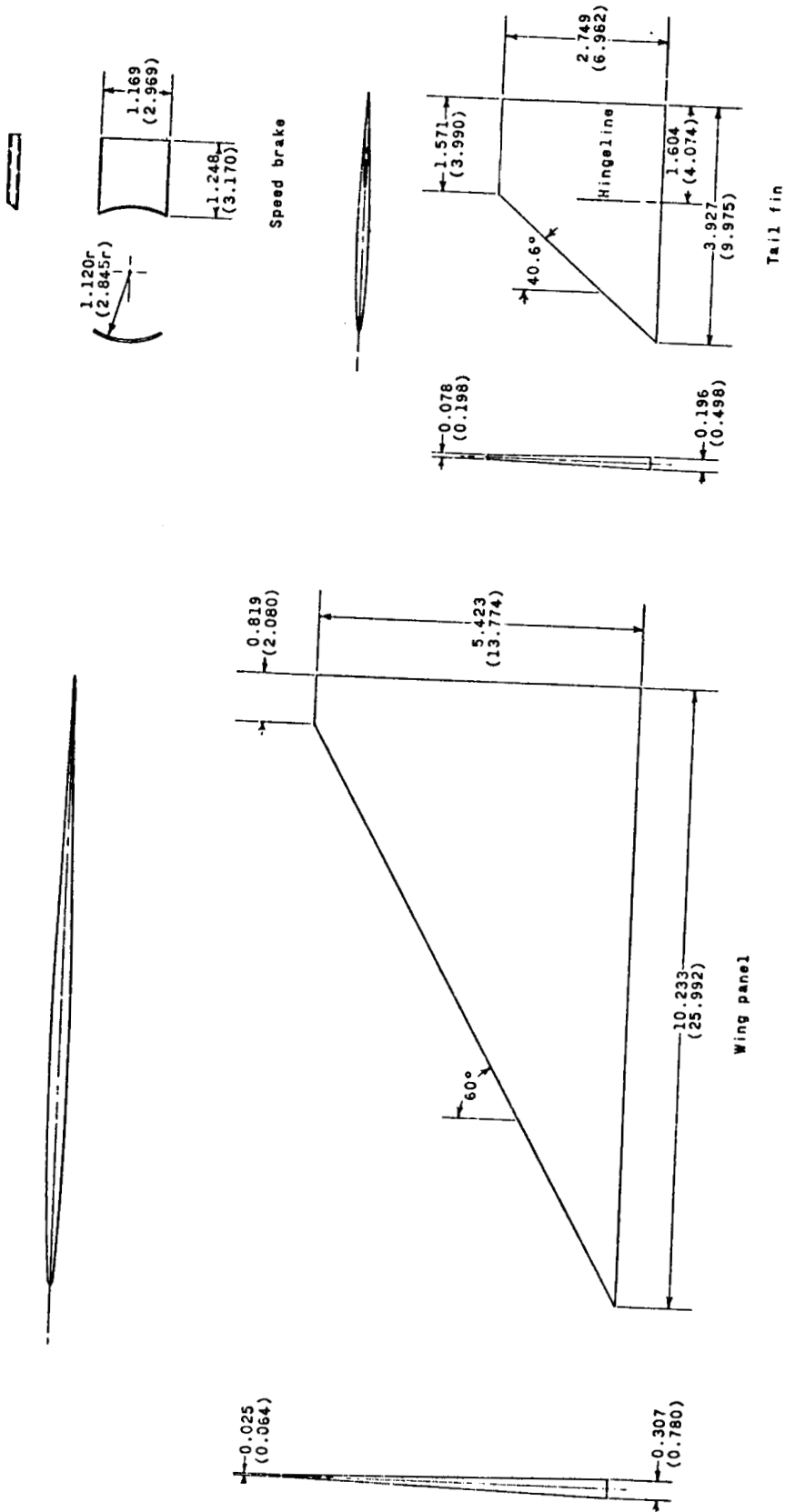


Figure 60. - Concluded

Ref. TM X-1304

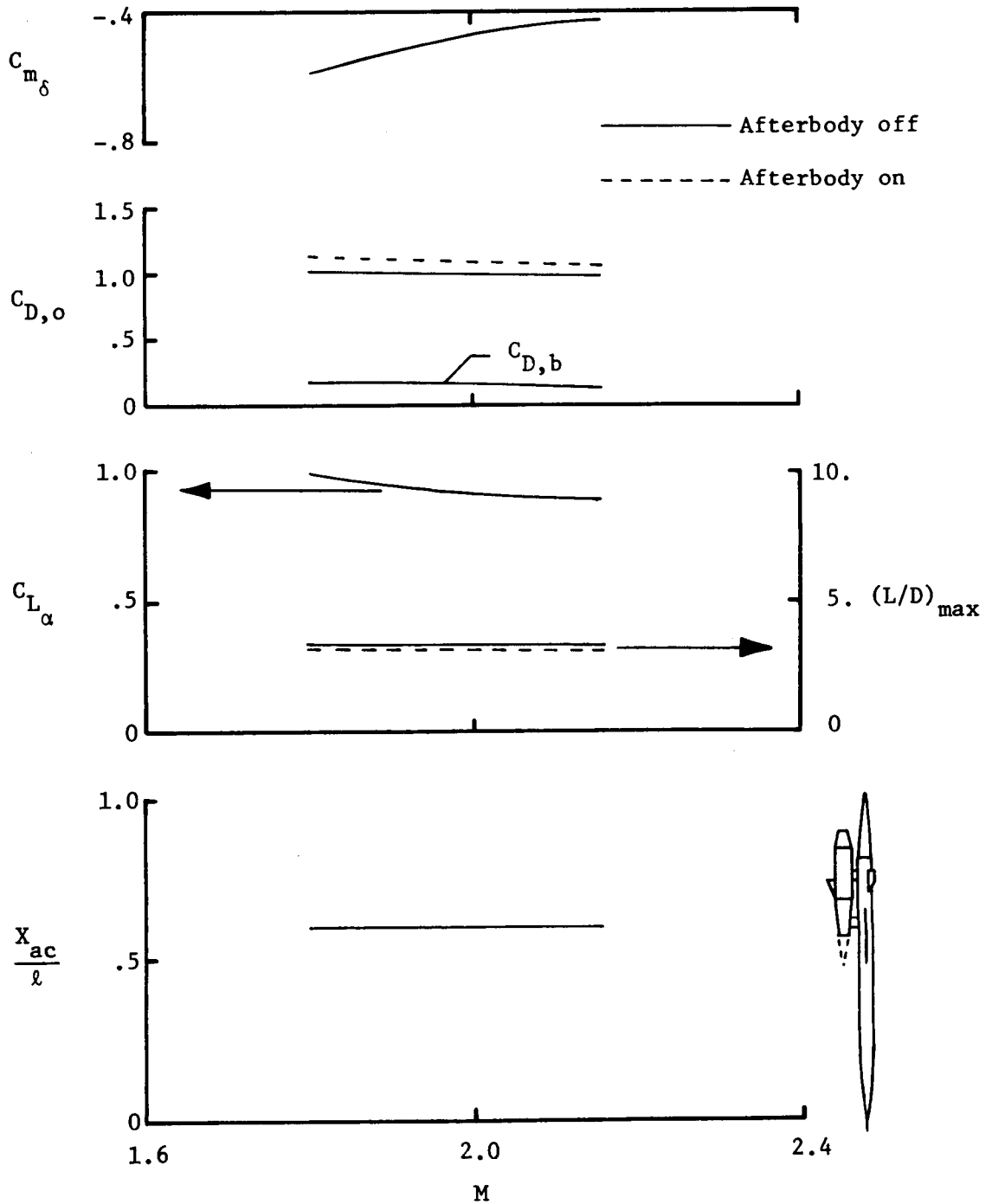


Figure 61. - Variation of longitudinal parameters with Mach number; $\alpha=0^\circ$. Cone-shaped fairing attached to nacelle inlet.

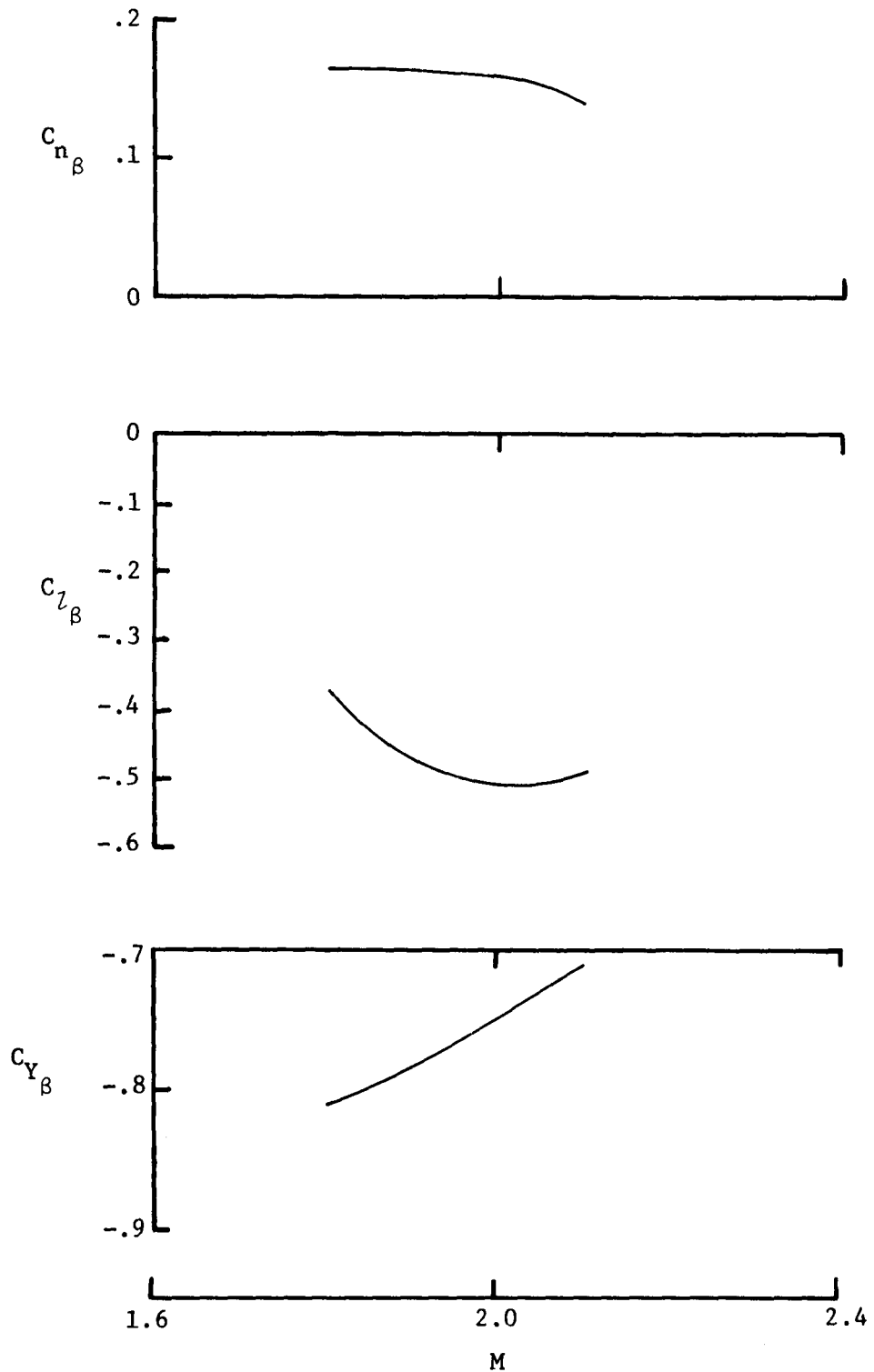


Figure 62. - Variation of sideslip derivatives with Mach number; $\alpha \approx 0^\circ$.
Cone-shaped fairing attached to nacelle inlet.

TABLE 9. - DIRECTION AND LATERAL CONTROL EFFECTIVENESS;* $\alpha=0^\circ$.

Mach No.	Yaw Control [†]			Roll Control ^{††}		
	C_{n_δ}	C_{l_δ}	C_{Y_δ}	C_{n_δ}	C_{l_δ}	C_{Y_δ}
1.80	-.161	.032	.040	.437	.102	-.075
2.00	-.215	.027	.040	.437	.075	-.118

* With cone-shaped fairing attached to nacelle inlet.

† Yaw control provided by pylon rudder.

††Roll control provided by differential deflection of tail fins.

Ref. TM X-1304

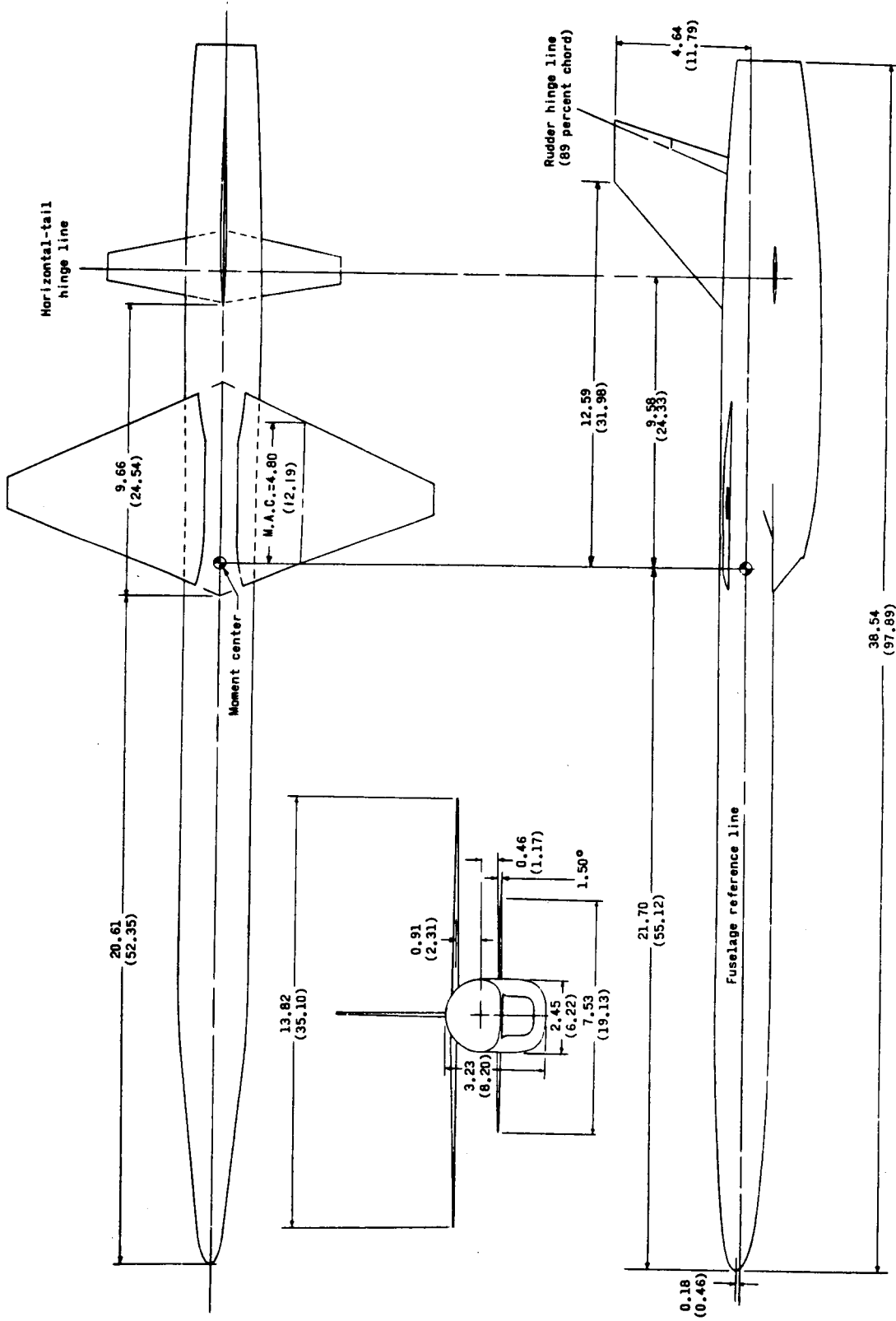


Figure 63. - Three-view drawing of the model. Dimensions are given in inches and parenthetically in centimeters.

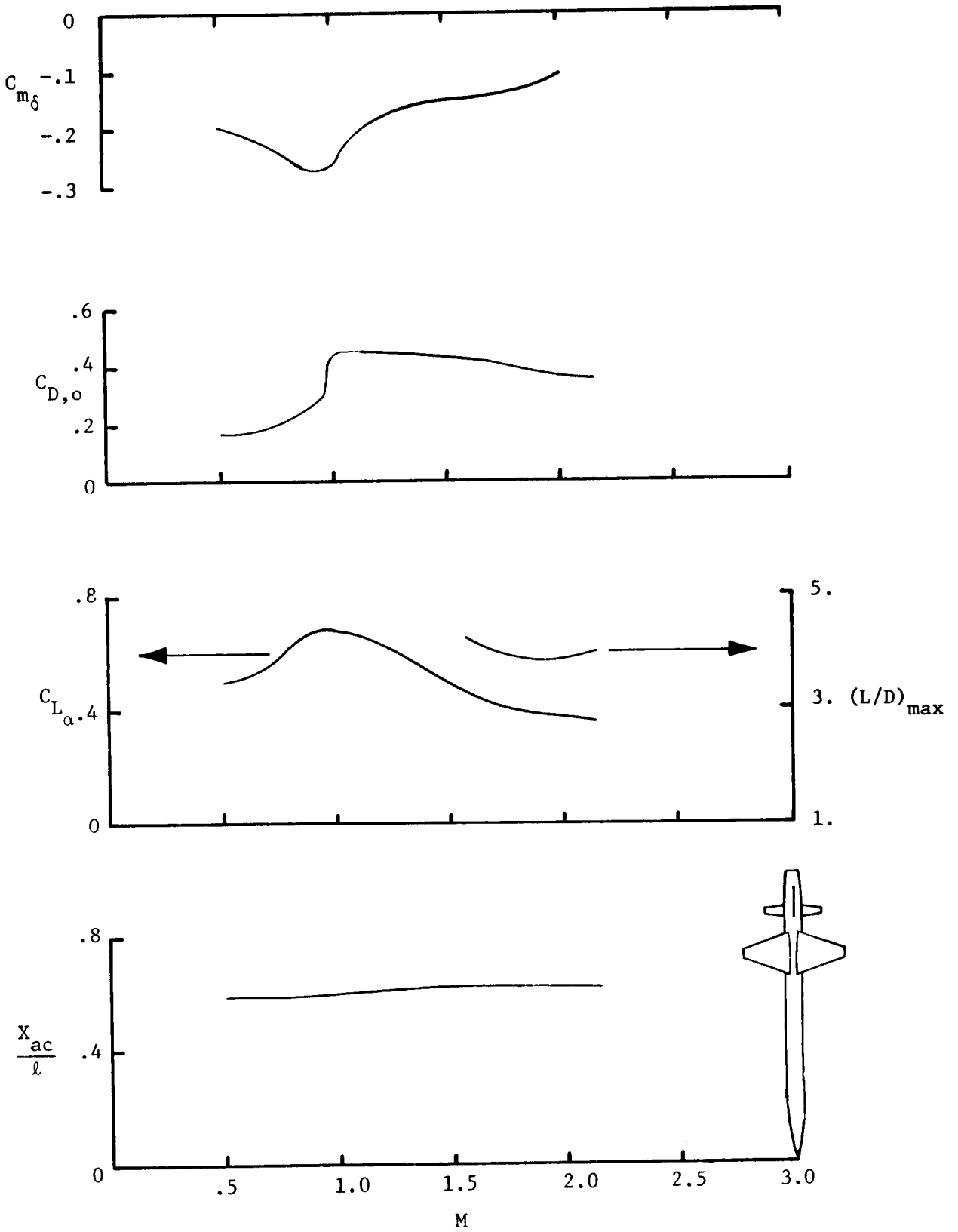


Figure 64. - Variation of longitudinal parameters with Mach number, configuration BW₁HV; $\alpha=0^\circ$.

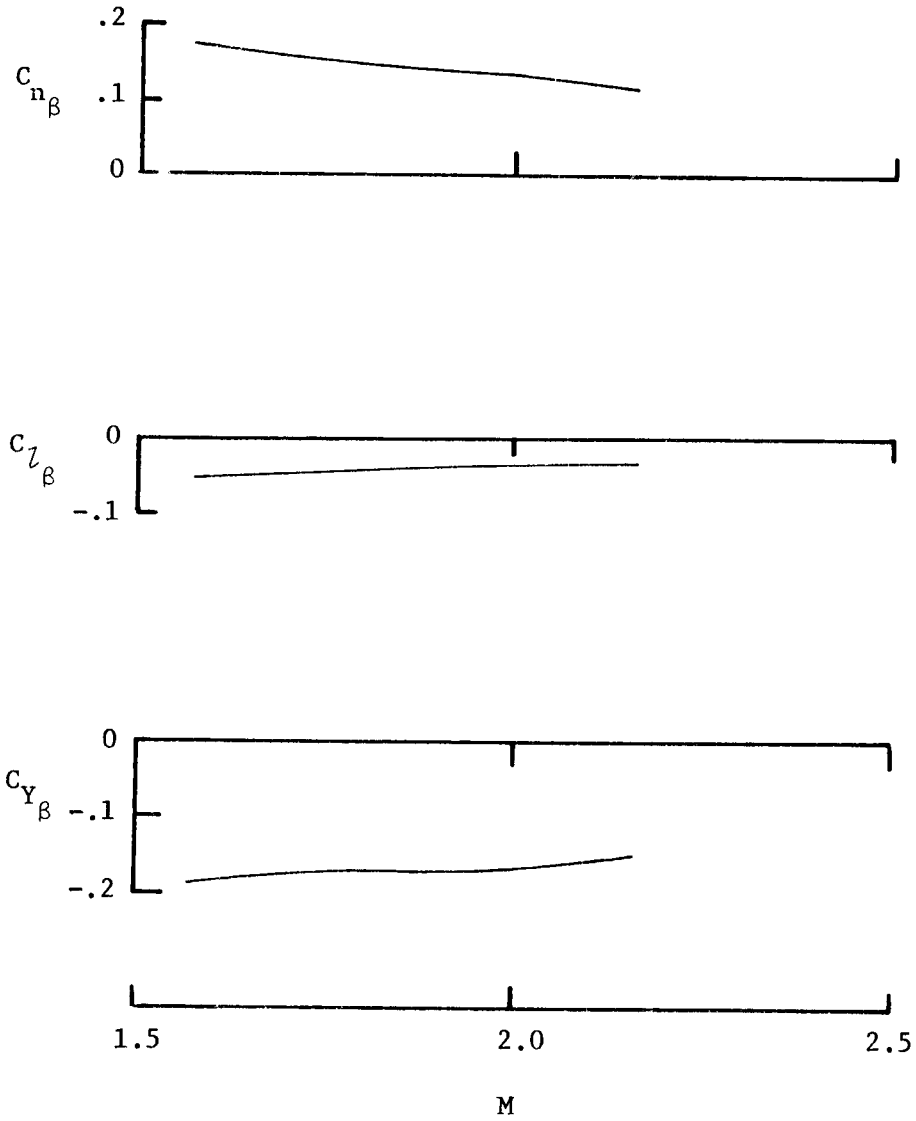


Figure 65. - Variation of sideslip derivatives with Mach number; $\alpha=0^\circ$.

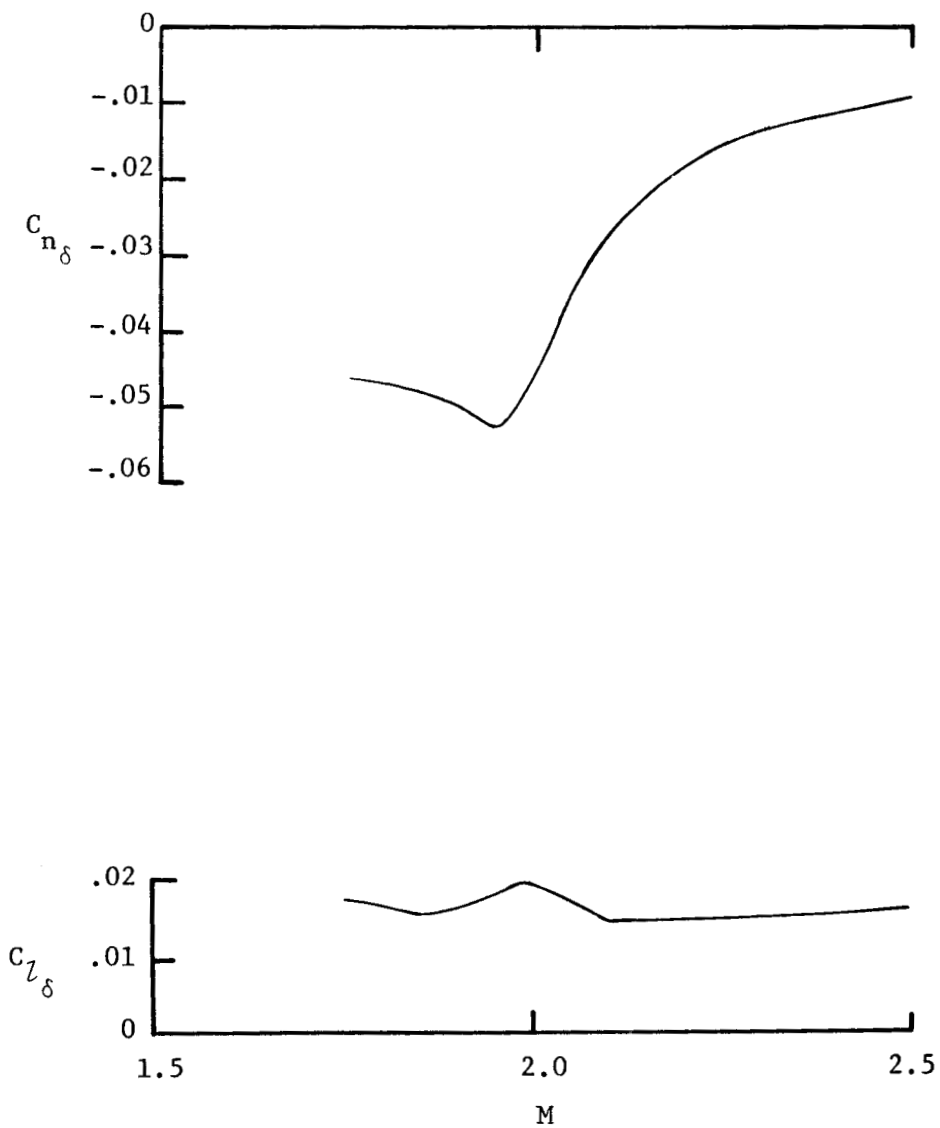


Figure 66. - Directional and lateral control effectiveness; $\alpha \approx 0^\circ$.

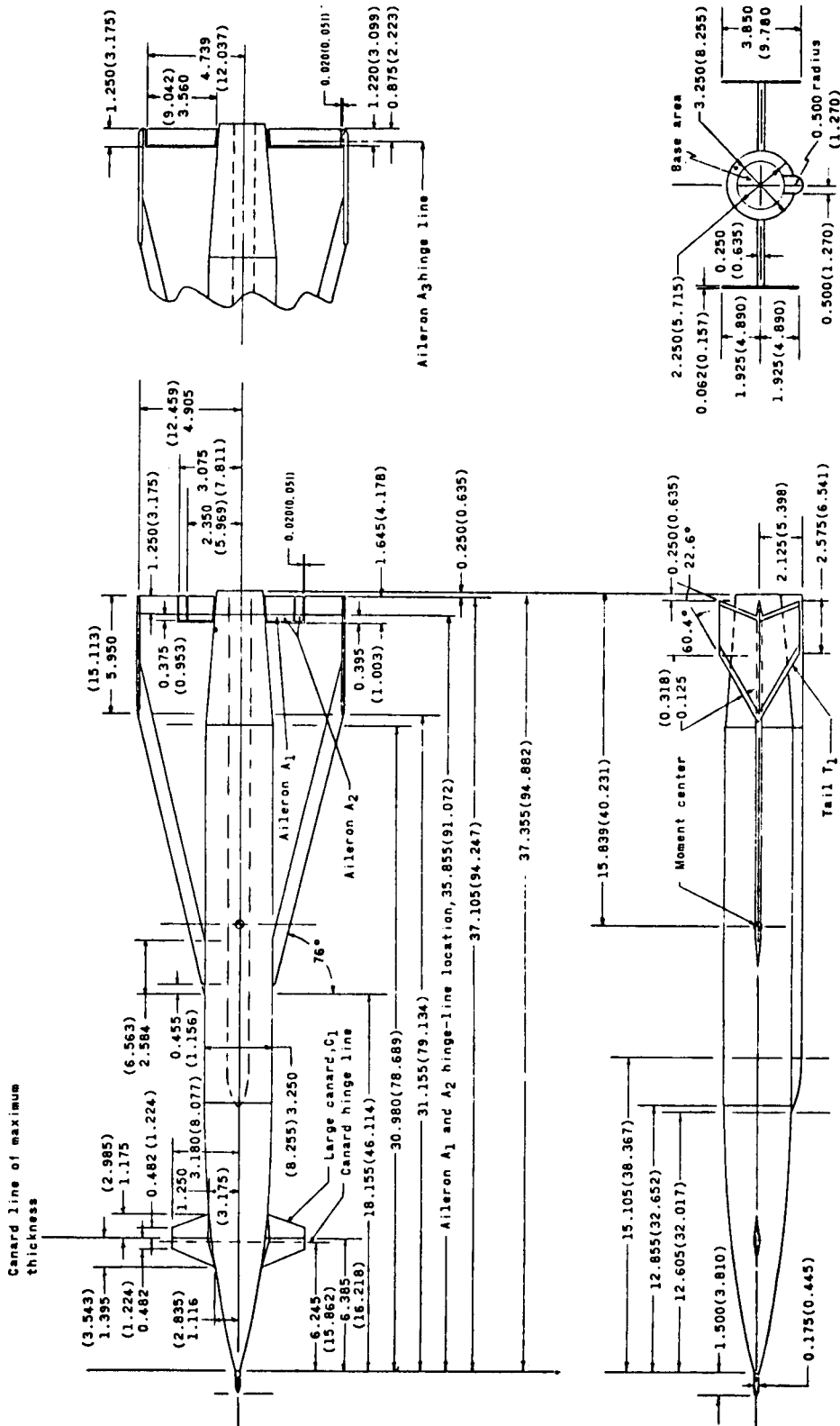
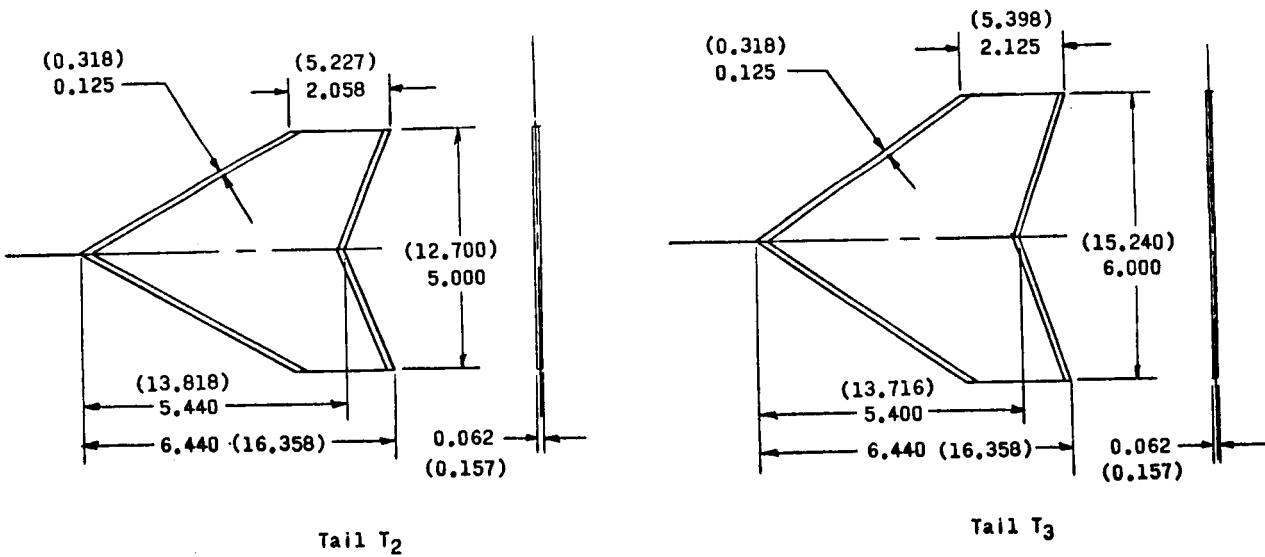
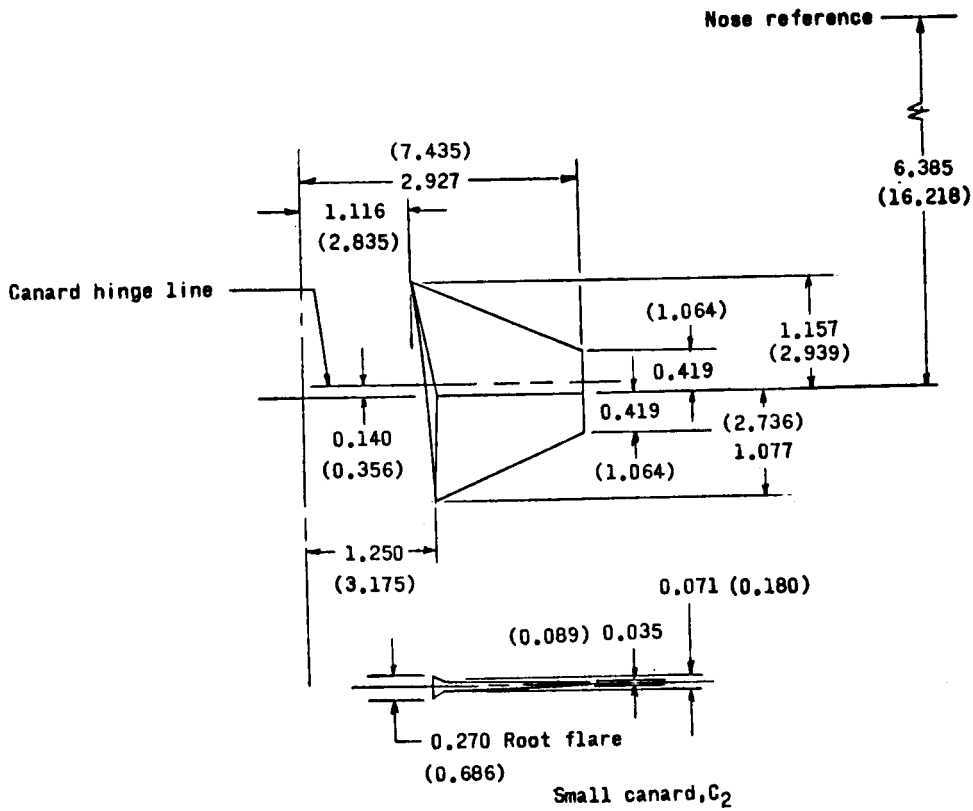


Figure 67. - Details of model. All dimensions are given first in inches and parenthetically in centimeters.



(b) Vertical tails and canard.

Figure 67. - Concluded

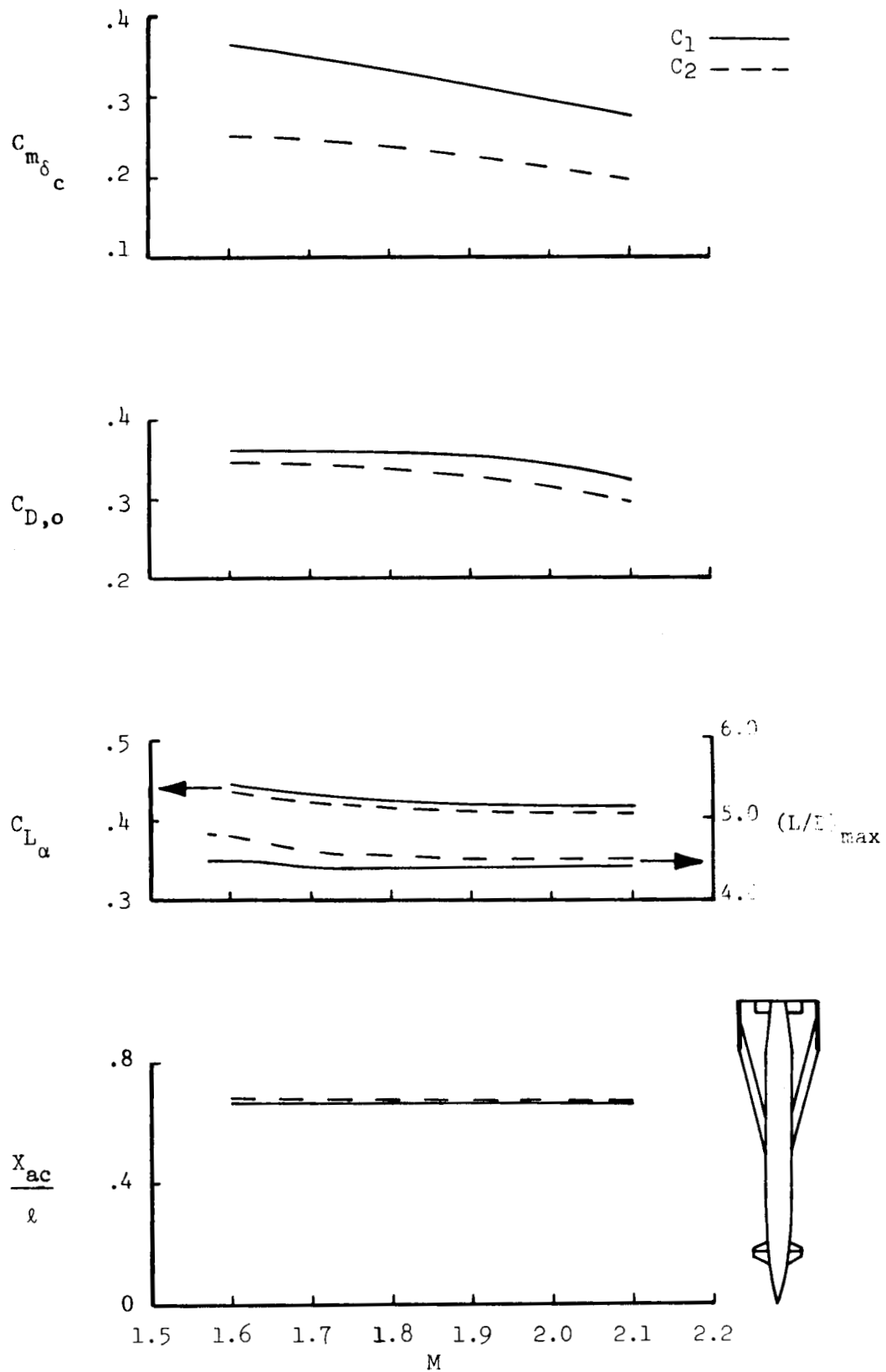


Figure 68. - Variation of longitudinal parameters with Mach number; $\alpha=0^\circ$.

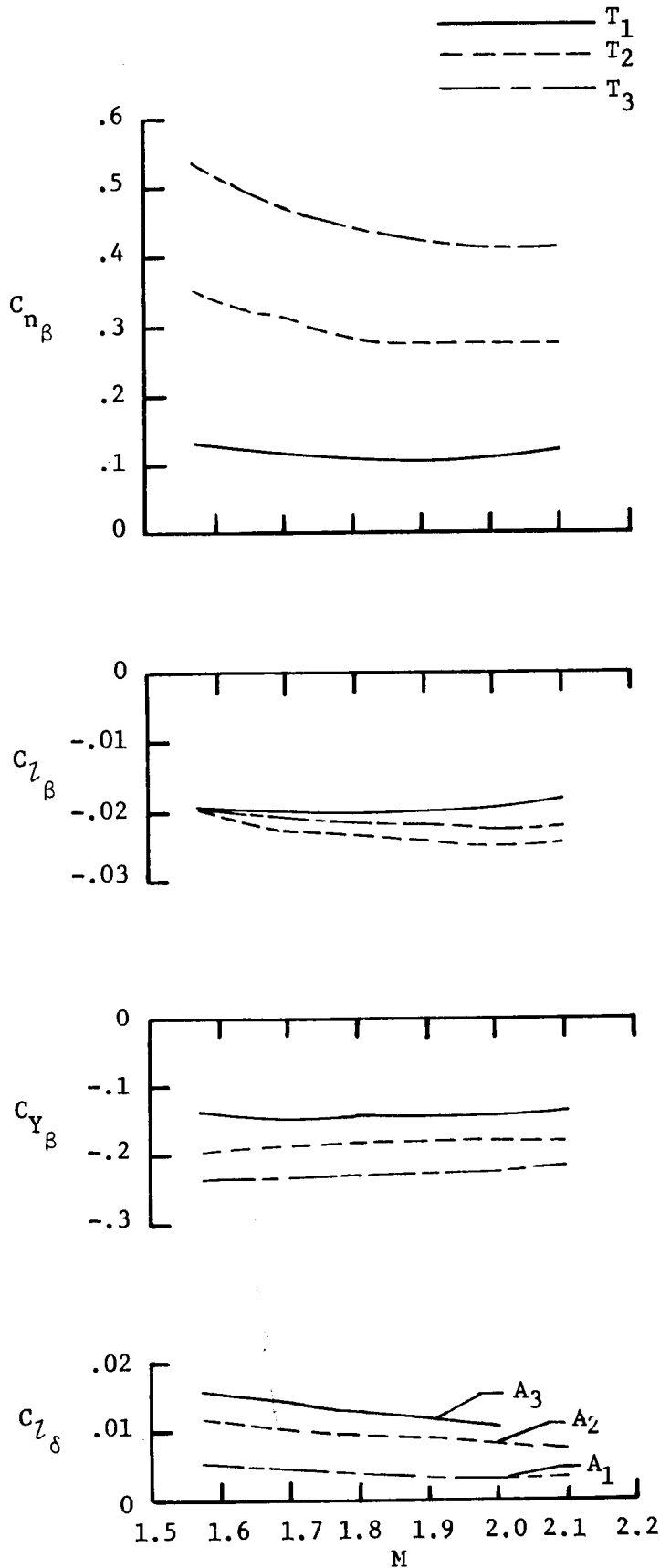
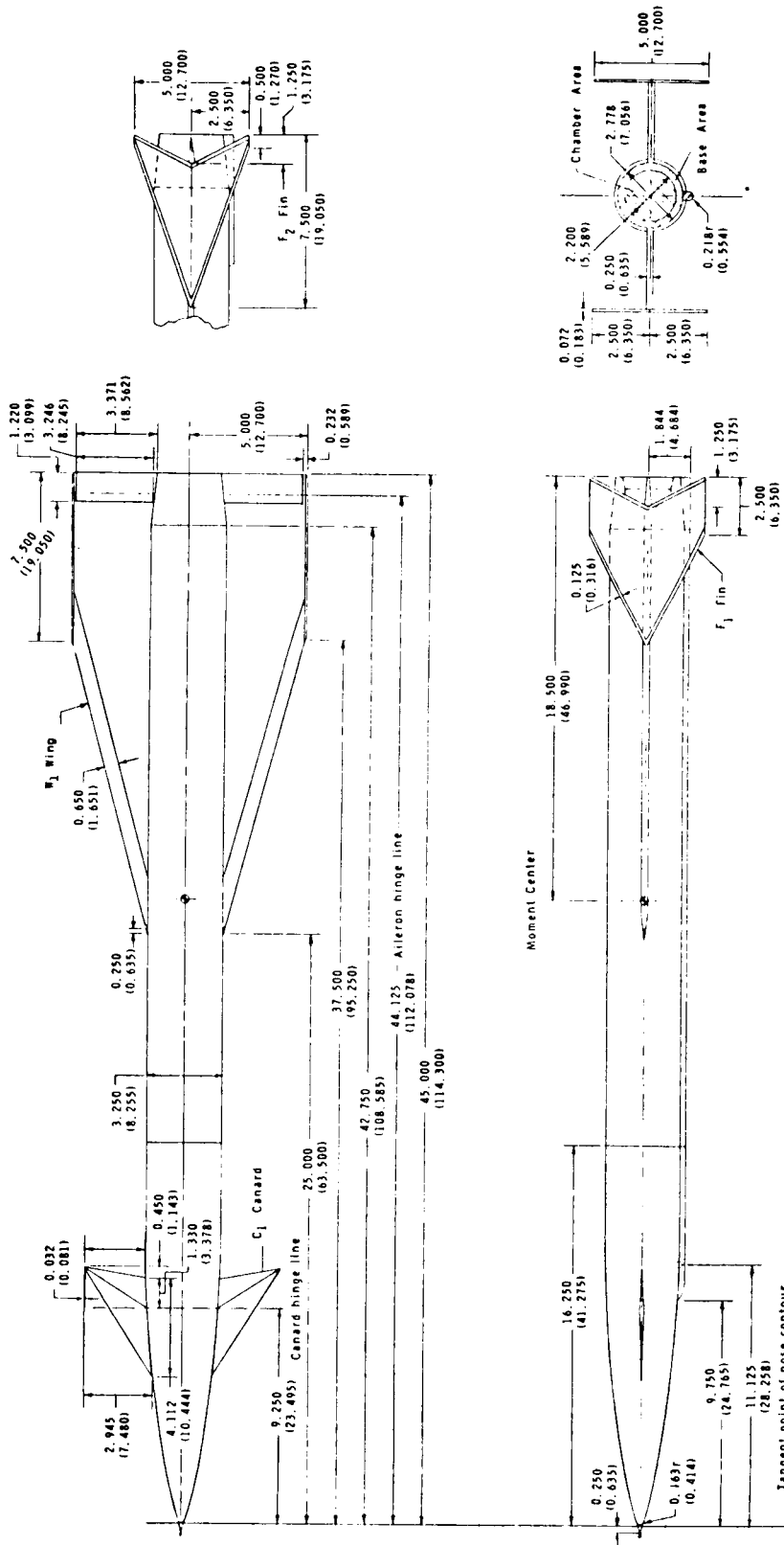
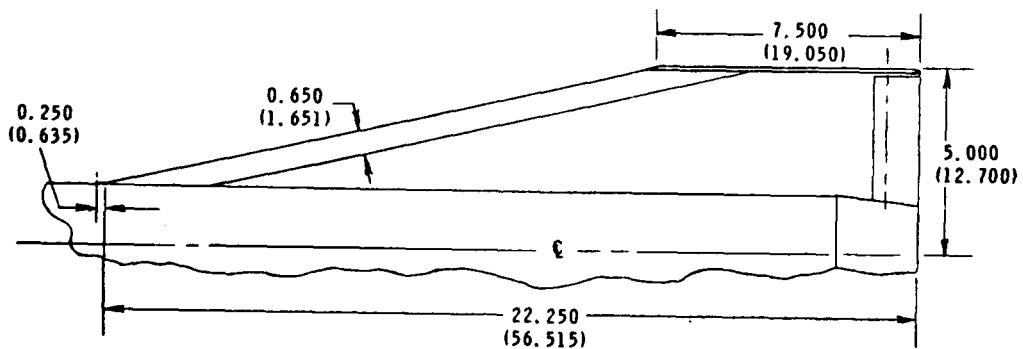


Figure 69. - Variation of sideslip derivatives and roll control effectiveness with Mach number; $\alpha=0^\circ$.



(a) Complete model.

Figure 70. - Model details. All dimensions are given in inches and parenthetically in centimeters.



W₂ Wing

Figure 70. - Concluded

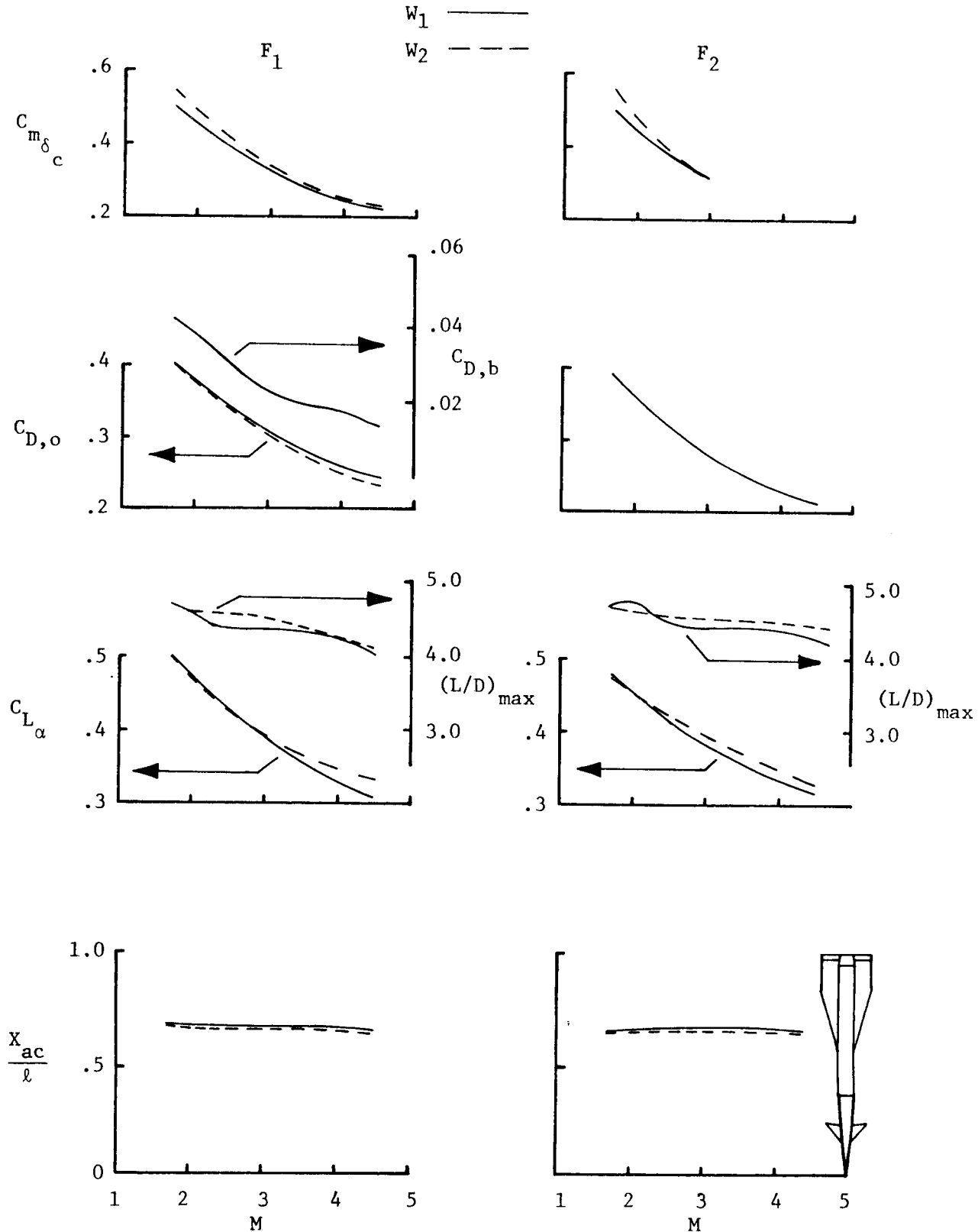


Figure 71. - Variation of longitudinal parameters with Mach number; $\alpha \approx 0^\circ$.

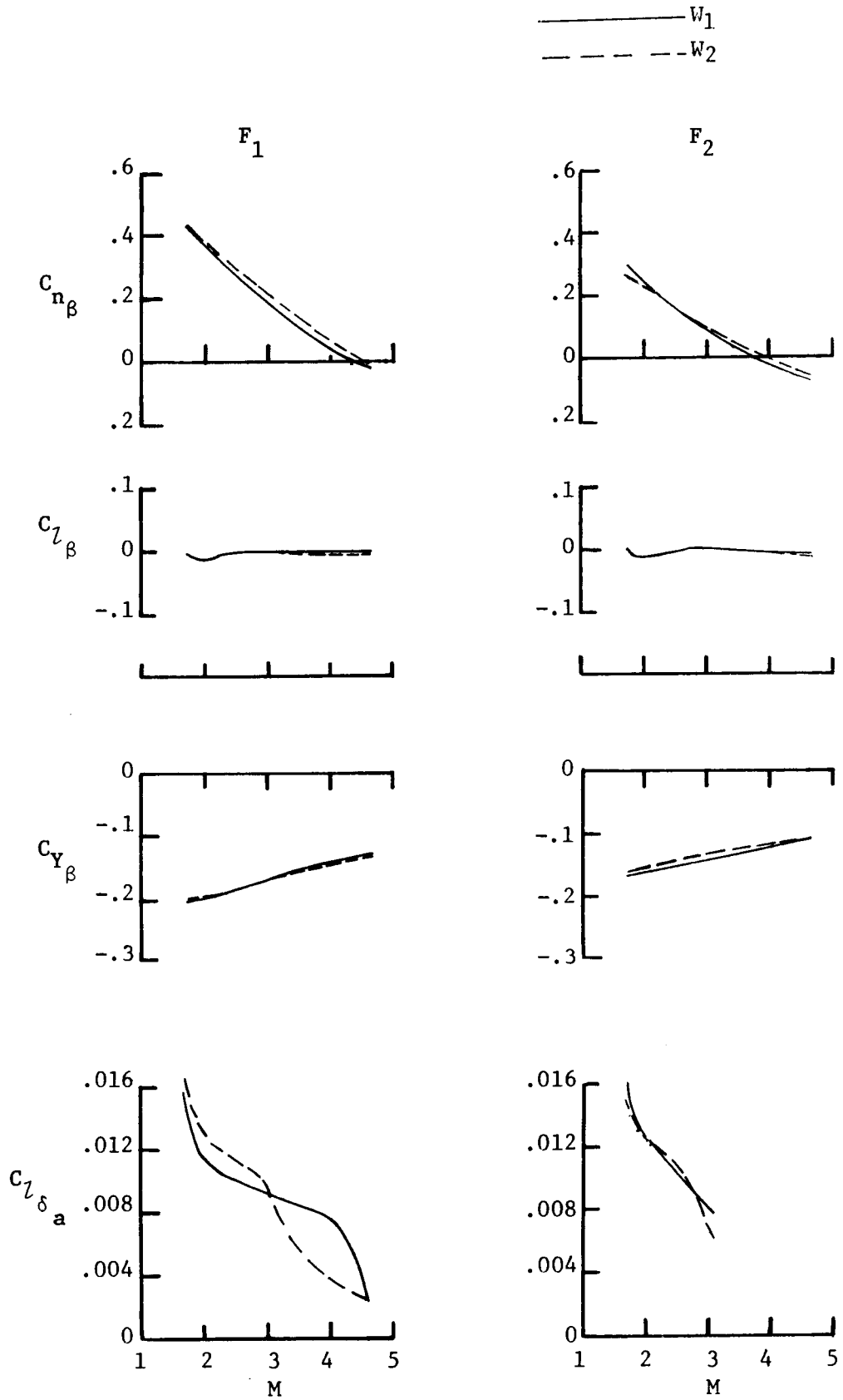


Figure 72. - Variation of sideslip derivatives and roll control effectiveness with Mach number; $\alpha=0^\circ$.

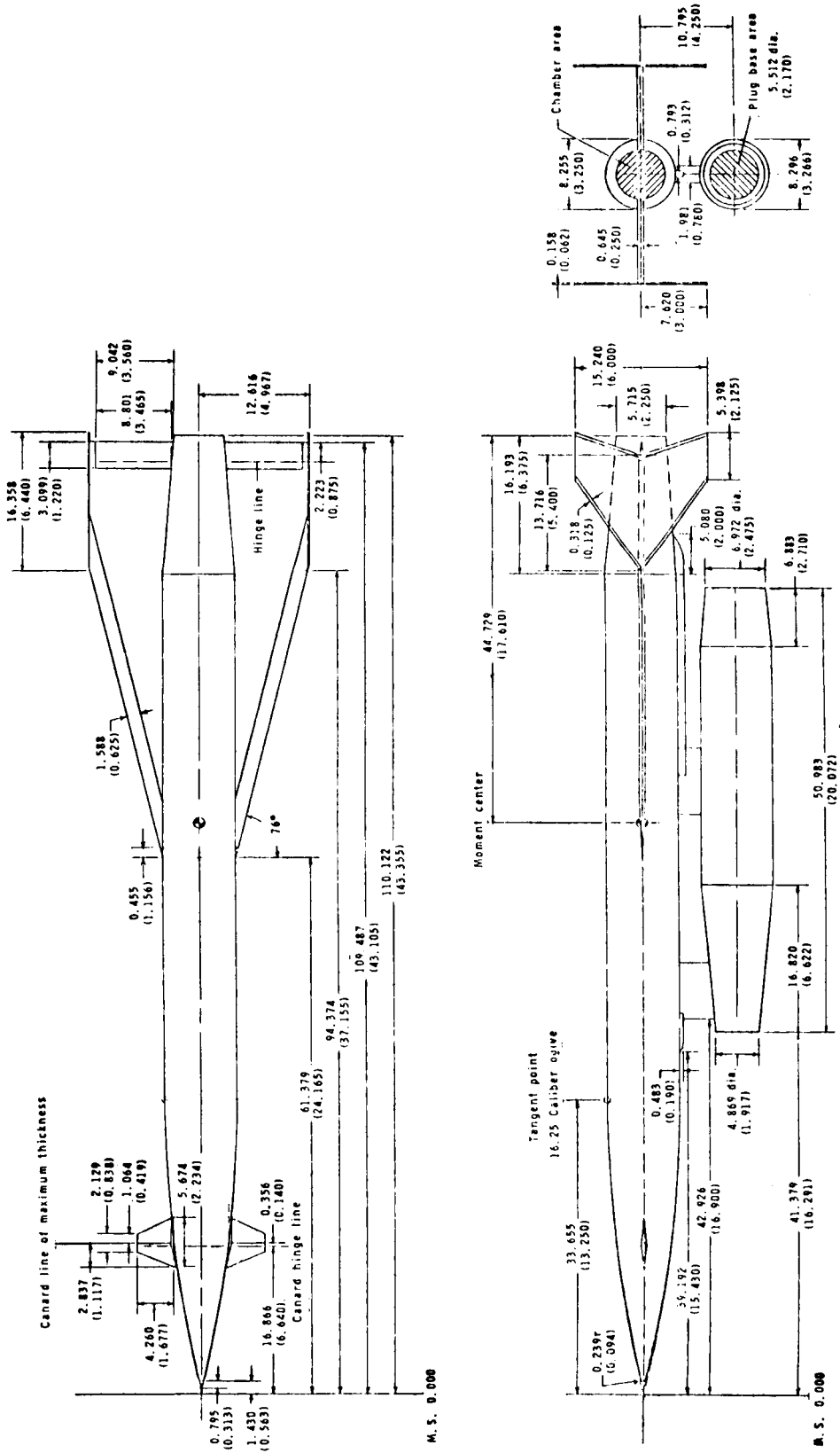


Figure 73. - Details of 1/4-scale model. All dimensions are given in centimeters and parenthetically in inches.

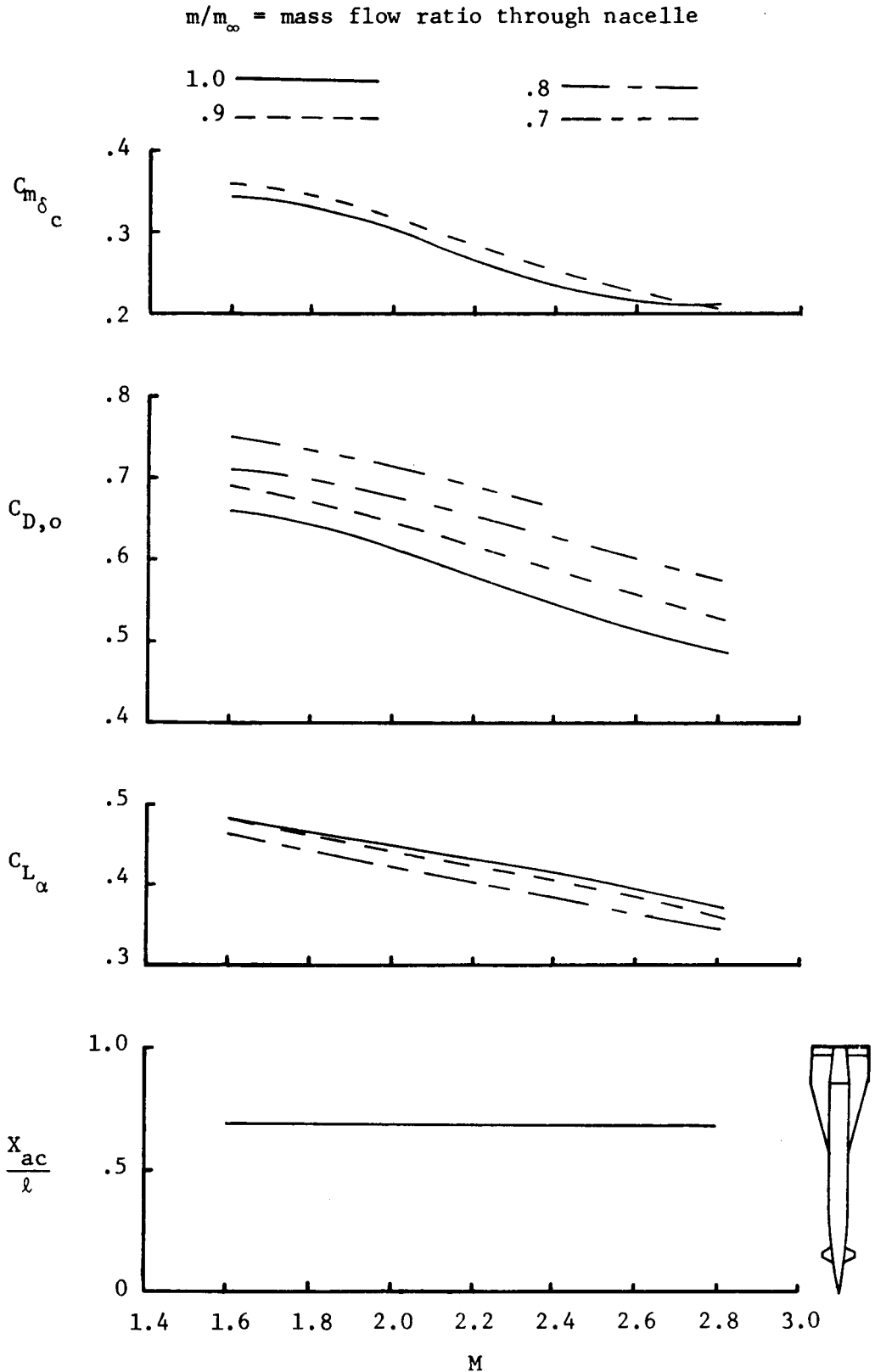


Figure 74. - Variation of longitudinal parameters with Mach numbers; $\alpha=0^\circ$.

m/m_∞ = mass flow ratio through nacelle

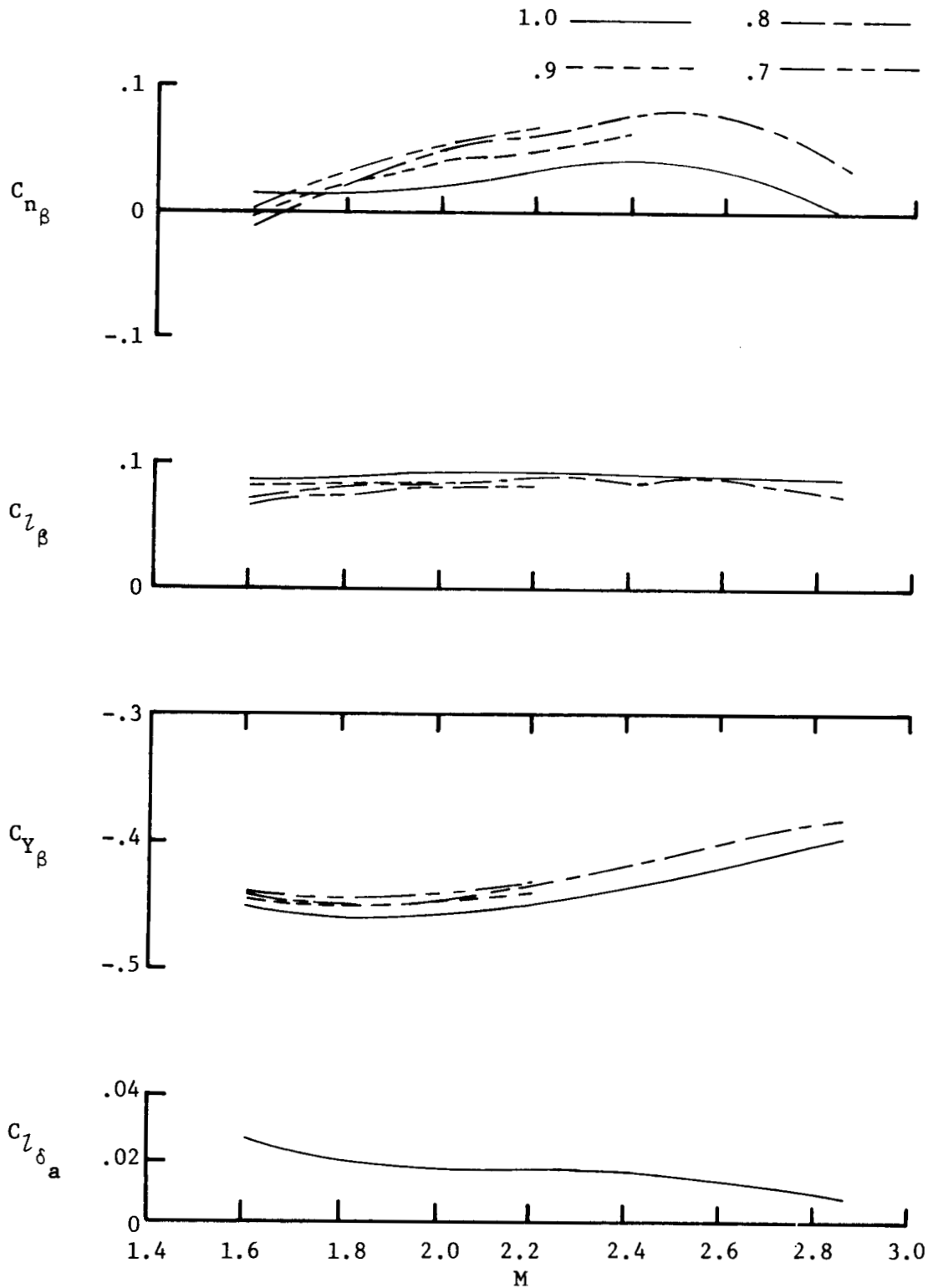


Figure 75. - Variation of sideslip derivatives and roll control effectiveness with Mach number; $\alpha \approx 0^\circ$.

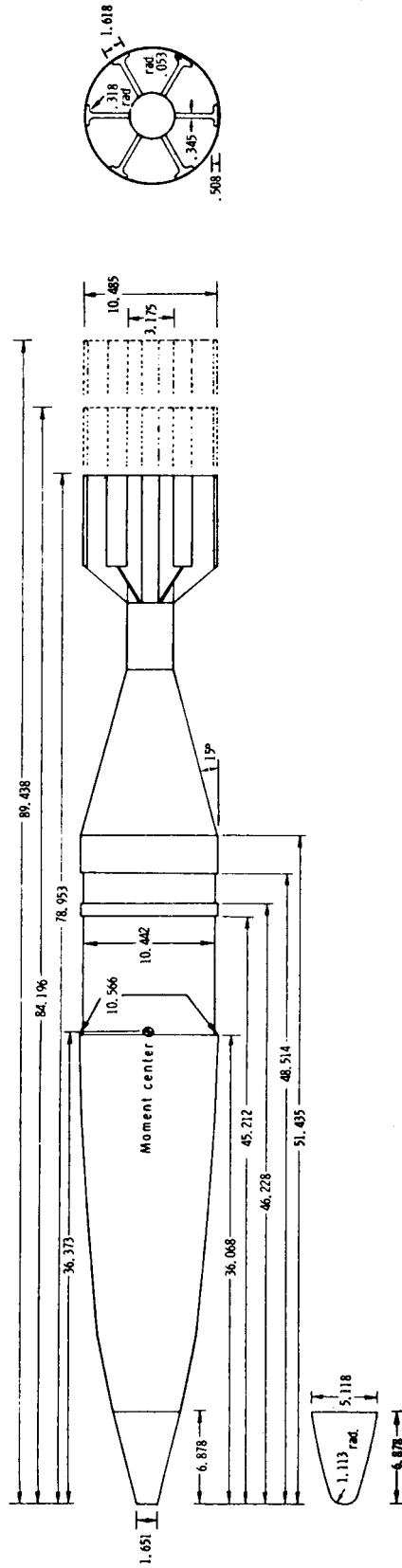


Figure 76. - Wind-tunnel model of a 105-mm projectile. (Model dimensions are in centimeters.)

Ref. TM X-2831

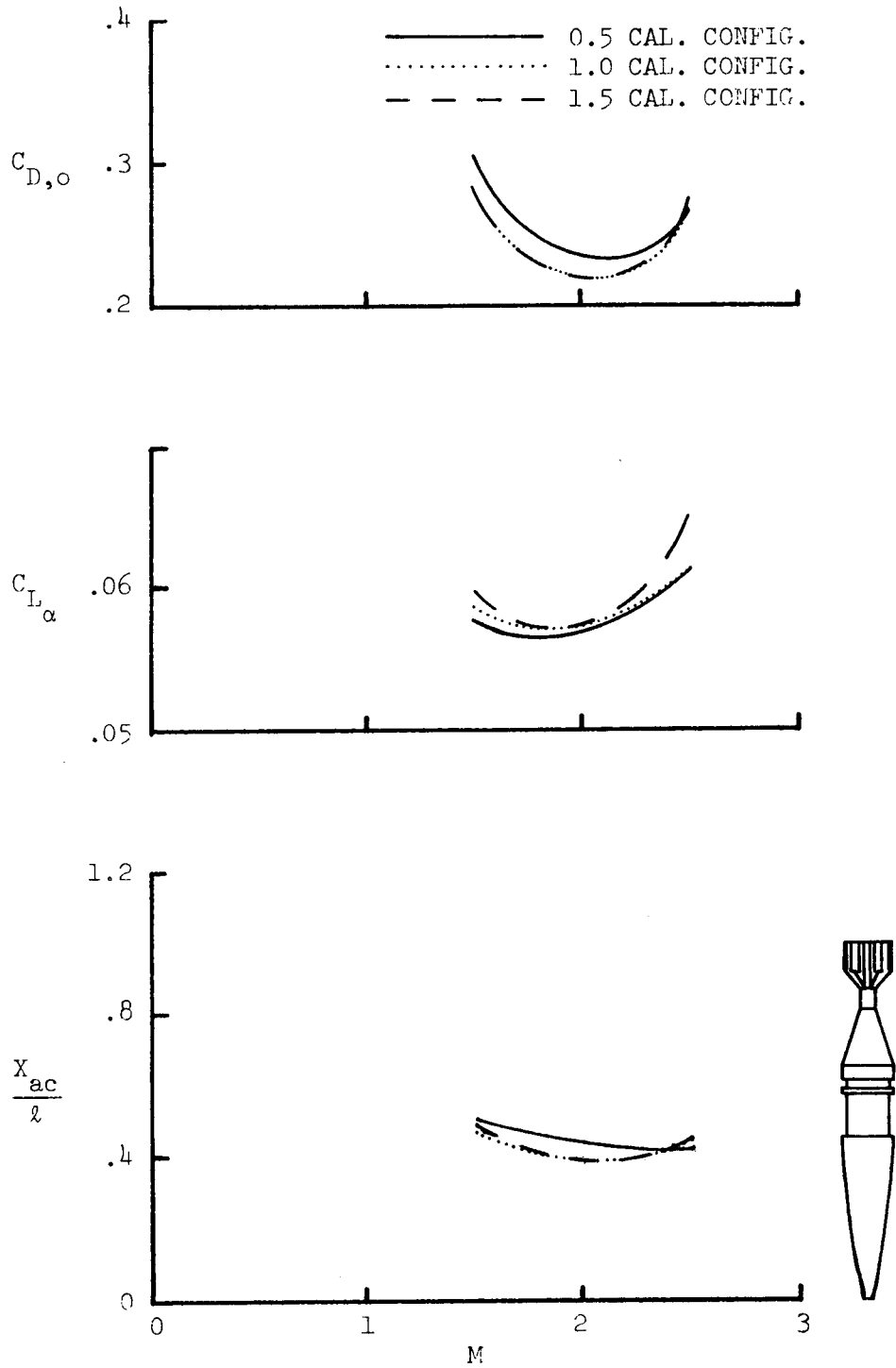


Figure 77. -- Variation of longitudinal parameters with Mach number; $\alpha=0^\circ$.

LIST OF DOCUMENTS SUMMARIZED

- NACA RM L58C19 INVESTIGATION OF CONTROL EFFECTIVENESS AND STABILITY CHARACTERISTICS OF A MODEL OF A LOW-WING MISSILE WITH INTERDIGITATED TAIL SURFACES AT MACH NUMBERS OF 2.29, 2.97, AND 3.51.
John G. Presnell, Jr., 1958.
- NASA TM X-187 STATIC AERODYNAMIC CHARACTERISTICS OF SEVERAL HYPERSONIC MISSILE-AND-CONTROL CONFIGURATIONS AT A MACH NUMBER OF 4.65.
James D. Church and Ida M. Kirkland, 1960.
- NASA TM X-348 EFFECTS OF AFTERBODY SHAPE ON THE AERODYNAMIC CHARACTERISTICS OF A FINENESS-RATIO-10 CONE-CYLINDER CONFIGURATION AT MACH NUMBERS FROM 1.57 TO 4.65 INCLUDING DESIGN PARAMETER CURVES FOR CIRCULAR AFTERBODY FLARES.
Ausley B. Carraway, Kenneth L. Turner, and Janette M. Crowder, 1960.
- NASA TM X-846 LONGITUDINAL STABILITY AND CONTROL CHARACTERISTICS OF AN AIR-TO-AIR MISSILE CONFIGURATION AT MACH NUMBERS OF 2.30 AND 4.60 AND ANGLES OF ATTACK FROM -45° TO 90° .
Royce L. McKinney, 1963.
- NASA TM X-1025 SUPERSONIC AERODYNAMIC CHARACTERISTICS OF A CRUCIFORM MISSILE CONFIGURATION WITH LOW-ASPECT-RATIO WINGS AND IN-LINE TAIL CONTROLS.
Dennis E. Fuller and William A. Corlett, 1964.
- NASA TM X-1112 AERODYNAMIC CHARACTERISTICS AT MACH 1.60, 2.00, AND 2.50 OF A CRUCIFORM MISSILE CONFIGURATION WITH IN-LINE TAIL CONTROLS.
William A. Corlett and Dennis E. Fuller, 1965.
- NASA TM X-1184 AERODYNAMIC CHARACTERISTICS AT MACH NUMBERS FROM 0.40 TO 2.86 OF A MISSILE MODEL HAVING ALL-MOVABLE WINGS AND INTERDIGITATED TAILS.
Gerald V. Foster and William A. Corlett, 1965.
- NASA TM X-1304 AERODYNAMIC CHARACTERISTICS OF A 0.187-SCALE MODEL OF A TARGET MISSILE AT MACH 1.80 TO 2.16.
William A. Corlett, 1966.

- NASA TM X-1309 AERODYNAMIC CHARACTERISTICS OF A MANEUVERABLE MISSILE WITH CRUCIFORM WINGS AND IN-LINE CANARD SURFACES AT MACH NUMBERS FROM 0.50 TO 4.63.
William A. Corlett, 1966.
- NASA TM X-1332 AERODYNAMIC CHARACTERISTICS AT MACH NUMBERS OF 3.95 AND 4.63 FOR A MISSILE MODEL HAVING ALL-MOVABLE WINGS AND INTERDIGITATED TAILS.
M. Leroy Spearman and William A. Corlett, 1967.
- NASA TM X-1352 AERODYNAMIC CHARACTERISTICS AT MACH NUMBERS FROM 1.50 TO 4.63 OF A MANEUVERABLE MISSILE WITH IN-LINE CRUCIFORM WINGS AND CANARD SURFACES.
M. Leroy Spearman and William A. Corlett, 1967.
- NASA TM X-1416 AERODYNAMIC CHARACTERISTICS OF A WINGED CRUCIFORM MISSILE CONFIGURATION WITH AFT TAIL CONTROLS AT MACH NUMBERS FROM 1.60 TO 4.63.
M. Leroy Spearman and William A. Corlett, 1967.
- NASA TM X-1491 SUPERSONIC AERODYNAMIC CHARACTERISTICS OF A MODEL OF AN AIR-TO-GROUND MISSILE.
Clyde Hayes, 1968.
- NASA TM X-1492 AERODYNAMIC CHARACTERISTICS AT MACH 2.50 OF A CRUCIFORM MISSILE CONFIGURATION WITH IN-LINE INLETS, WINGS, AND TAIL SURFACES.
Dennis E. Fuller and Celia S. Richardson, 1968.
- NASA TM SX-1531 AERODYNAMIC CHARACTERISTICS OF A TARGET DRONE VEHICLE AT MACH NUMBERS FROM 1.57 TO 2.10.
A. B. Blair, Jr., and Roger H. Fournier, 1968.
- NASA TM X-1538 STABILITY AND CONTROL CHARACTERISTICS AT MACH 1.57 TO 2.16 OF A TARGET DRONE MODEL WITH AN UNDERSLUNG INLET.
A. B. Blair, Jr., and Melvin M. Carmel, 1968.
- NASA TM X-1751 AERODYNAMIC CHARACTERISTICS OF A MODIFIED MISSILE MODEL WITH TRAPEZOIDAL WINGS AND AFT TAIL CONTROLS AT MACH NUMBERS OF 2.50 TO 4.63.
William A. Corlett, 1969.
- NASA TM X-1834 AERODYNAMIC CHARACTERISTICS OF A CRUCIFORM-WING MISSILE MODEL WITH A SYSTEMATIC VARIATION OF CANARD AND TAIL LOCATIONS AT MACH 1.60 TO 4.63.
William A. Corlett, 1969.
- NASA TM X-1839 EFFECTS OF WING PLANFORM ON THE STATIC AERODYNAMICS OF A CRUCIFORM WING-BODY MISSILE FOR MACH NUMBERS UP TO 4.63.
M. Leroy Spearman and Charles D. Trescot, Jr., 1969.

- NASA TM SX-1961 EFFECTS OF ADDITIONAL REVISIONS ON THE AERODYNAMIC CHARACTERISTICS OF A TARGET DRONE VEHICLE AT MACH NUMBERS FROM 1.70 TO 4.63.
A. B. Blair, Jr., and Dorothy H. Tudor, 1970.
- NASA TM X-2289 EFFECTS OF NOSE BLUNTNESS ON THE STATIC AERODYNAMIC CHARACTERISTICS OF A CRUCIFORM-WING MISSILE AT MACH NUMBERS 1.50 TO 2.86.
Roger H. Fournier and M. Leroy Spearman, 1971.
- NASA TM SX-2299 AERODYNAMIC CHARACTERISTICS AT MACH NUMBERS FROM 1.60 TO 2.86 OF A TARGET-DRONE VEHICLE WITH AN UNDERSLUNG ENGINE NACELLE.
A. B. Blair, Jr., 1971.
- NASA TM X-2367 LONGITUDINAL AERODYNAMIC CHARACTERISTICS AT MACH 1.50 TO 4.63 OF A MISSILE MODEL EMPLOYING VARIOUS CANARDS AND A TRAILING-EDGE FLAP CONTROL.
Charles D. Trescot, Jr., 1971.
- NASA TM X-2491 EFFECTS OF STRAP-ON BOOSTERS ON THE AERODYNAMIC CHARACTERISTICS OF A SIMULATED LAUNCH VEHICLE AT MACH NUMBERS FROM 1.50 TO 2.86.
M. Leroy Spearman and Roger H. Fournier, 1972.
- NASA TM X-2774 EFFECTS OF FIN PLANFORM ON THE AERODYNAMIC CHARACTERISTICS OF A WINGLESS MISSILE WITH AFT CRUCIFORM CONTROLS AT MACH 1.60, 2.36, AND 2.86.
Charles D. Trescot, Jr., Gerald V. Foster, and C. Donald Babb, 1973.
- NASA TM X-2780 AERODYNAMIC CHARACTERISTICS AT MACH 0.60 TO 4.63 OF TWO CRUCIFORM MISSILE MODELS, ONE HAVING TRAPEZOIDAL WINGS WITH CANARD CONTROLS AND THE OTHER HAVING DELTA WINGS WITH TAIL CONTROLS.
William A. Corlett and Dorothy T. Howell, 1973.
- NASA TM X-2831 EFFECT OF NOSE SHAPE AND TAIL LENGTH ON SUPERSONIC STABILITY CHARACTERISTICS OF A PROJECTILE.
Wallace C. Sawyer and Ida K. Collins, 1973.
- NASA TM X-3070 STABILITY AND CONTROL CHARACTERISTICS AT MACH NUMBERS FROM 0.20 TO 4.63 OF A CRUCIFORM AIR-TO-AIR MISSILE WITH TRIANGULAR CANARD CONTROLS AND A TRAPEZOIDAL WING.
Ernest B. Graves and Roger H. Fournier, 1974.
- NASA TM X-71984 STABILITY AND CONTROL CHARACTERISTICS OF A MONOPLANE MISSILE WITH LARGE DELTA WINGS AND VARIOUS TAIL CONTROLS AT MACH 1.90 TO 2.86.
Lloyd S. Jernell, 1974.

NASA TN D-7069 AERODYNAMIC CHARACTERISTICS OF A SWEEP-WING CRUISE
MISSILE AT MACH NUMBERS FROM 0.50 TO 2.86.
M. Leroy Spearman and Ida K. Collins, 1972.